

PB 294735

REPORT NO.
UCB/EERC-78/22
OCTOBER 1978

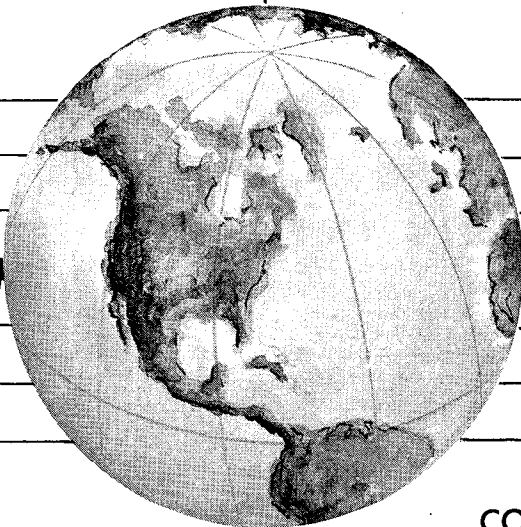
EARTHQUAKE ENGINEERING RESEARCH CENTER

OPTIMAL DESIGN OF AN EARTHQUAKE ISOLATION SYSTEM

by

M. A. BHATTI
K. S. PISTER
E. POLAK

A report on research sponsored by
the National Science Foundation



COLLEGE OF ENGINEERING

UNIVERSITY OF CALIFORNIA • Berkeley, California

REPRODUCED BY
**NATIONAL TECHNICAL
INFORMATION SERVICE**
U.S. DEPARTMENT OF COMMERCE

For sale by the National Technical Information Service, U. S. Department of Commerce, Springfield, Virginia 22161.

See back of report for up to date listing of EERC reports.

OPTIMAL DESIGN OF AN EARTHQUAKE ISOLATION SYSTEM

by

M.A. Bhatti

K.S. Pister

and

E. Polak

Prepared under the sponsorship of
National Science Foundation
Grant ENV76-04264

Report No. UCB/EERC-78/22
Earthquake Engineering Research Center
College of Engineering
University of California
Berkeley, California 94720

October 1978

ABSTRACT

Optimal design of an earthquake isolation system, consisting of natural rubber bearings and special nonlinear energy absorbing devices, is presented. An algorithm for efficient analysis of structural response, based upon the Newmark and Runge-Kutta methods with optional Newton-Raphson iteration, is given. The optimal design problem, incorporating this simulation algorithm, is formulated as a mathematical programming problem with time-dependent constraints and is solved using a feasible directions algorithm. Several numerical examples are presented, in which it is demonstrated that a properly designed isolation system can substantially reduce structural damage for a class of potential earthquakes.



ACKNOWLEDGEMENTS

The experimental program investigating the use of energy absorbing devices to mitigate earthquake-induced structural damage constitutes the source of the optimal design problems reported here. This program is under the direction of Professor J.M. Kelly, whose many helpful discussions and comments concerning the present work are gratefully acknowledged.

The research was conducted under National Science Foundation Grant ENV76-04264. The authors are grateful for this support.

Careful typing by Ms. Shirley Edwards is gratefully acknowledged.



TABLE OF CONTENTS

	<u>Page</u>
ABSTRACT	i
ACKNOWLEDGEMENTS	ii
1. INTRODUCTION	1
1.1 Program Objective and Limitations	2
1.2 Report Outline	4
2. AN EARTHQUAKE ISOLATION SYSTEM	5
2.1 Steel Test Frame	5
2.2 Natural Rubber Bearings	5
2.3 Torsional Energy Absorbing Devices	6
3. STRUCTURAL ANALYSIS	7
3.1 Mathematical Model for Hysteretic Behavior of the Energy Absorbing Devices	7
3.2 Equations of Motion for the System	9
3.3 Numerical Solution of the Differential Equations of Motion	11
3.4 Sensitivity Analysis	22
4. OPTIMIZATION	24
4.1 Optimal Design Problem	24
4.2 Nonlinear Programming Problem	25
4.3 Method of Feasible Directions	27
4.4 Computational Considerations	39
5. APPLICATIONS	42
5.1 Structural System	42
5.2 Equations of Motion	45



	<u>Page</u>
5.3 Design Parameters	45
5.4 Optimal Design Problems	46
5.5 Sensitivity of Optimal Design to Different Earthquake Ground Motions	55
6. CONCLUDING REMARKS	57
REFERENCES	59
NOTATION	61
FIGURES	63



1. INTRODUCTION

Earthquake ground motion introduces accelerations at the base of a structure, producing forces and deformations in the structure. If there is some type of isolation system between the base of the structure and the ground, the adverse effect of the accelerations on the structure may be reduced. Based upon this simple idea, researchers have suggested a number of different types of isolation systems. Two basic approaches have been followed: One is to support the structure on mechanical devices such as rollers, self-centering rocking mechanisms, rubber bearings etc.; the major drawbacks of these devices are large lateral base deflections and undesirable motion under wind and other small excitations. The second approach is the so called "soft story" concept in which the first-story columns are designed so that the structure remains elastic under small excitations, but yields and absorbs a considerable amount of energy under strong earthquakes. Large lateral deflections are a problem in this case, resulting in damage to the first-story columns during a strong earthquake. Behavior of the main building of the Olive View Hospital in the 1971 San Fernando Earthquake is a classic example of this [1].

More recently another type of earthquake isolation system using natural rubber bearings and mild steel energy absorbing devices has been proposed [2]. The structure is supported on natural rubber bearings which are very rigid vertically but have a low lateral stiffness. To prevent excessive lateral deformation under small earthquakes as well as dissipate energy under strong earthquakes, special devices are attached at the foundation level and at any other desired floor

level. The devices, made of ductile steel, rely on the hysteretic behavior of steel subjected to torsional deformation. A half-scale model of a steel framed structure employing these energy absorbing devices attached at the bottom floor girder was tested on an earthquake simulator by Kelly et. al. The results of these tests, reported in [2,3,4 and 5], show that for small earthquakes the structure behaved as if attached to a rigid foundation, strongly amplifying the ground motion, while for strong earthquakes, the devices yielded and absorbed large amounts of energy amounting to as much as the equivalent of 30% - 35% of critical viscous damping. A number of different devices with different elastic and post-yield stiffnesses were used. The results show that different degrees of isolation were provided by each device. The question naturally arises, what is the "best" choice of these energy absorbing devices for a particular structure?

The present research is motivated by this question. The problem of choosing the best device parameters is formulated as an optimization problem with time dependent constraints. A second important aspect of the present study is the application of nonlinear programming techniques to solve the optimal design problem resulting from the use of energy absorbing devices.

1.1 Program Objective and Limitations

The objective of the present research program is to study the problem of optimal design of an earthquake isolation system of the type described utilizing nonlinear programming techniques, specifically, the Method of Feasible Directions.

The first step is to develop methods for efficient analysis and re-analysis of the structural system, which is assumed to remain elastic

during the earthquake, the only nonlinearity occurring in the behavior of the energy absorbing devices. The optimization process requires time-history analysis of structural response at each design iteration. This is a very time-consuming operation for a general nonlinear structural system, and it requires exploitation of the "localized" nonlinear nature of the present problem to obtain a satisfactory computational algorithm. The present study is deterministic in the sense that an actual ground motion record is used as input. In the absence of any suitable method for characterization of earthquakes for nonlinear systems, the probabilistic nature of the design problem is taken into account by carrying out a series of analyses for different earthquake inputs and comparing the structural response under these earthquakes for the isolation system designed from the single record. This procedure gives at least an indirect indication of the sensitivity of the optimal design to the selection of input earthquake ground motion.

The method of feasible directions used to find the optimal design is a very general method capable of handling a variety of design problems. Modifications of the basic algorithm are required to make it computationally efficient for the special class of design problems associated with earthquake-resistant design.

The objectives of the present research are thus summarized as follows:

- (i) to develop an efficient algorithm for the analysis of structures with localized nonlinear energy absorbing devices subjected to earthquakes.
- (ii) to formulate the problem of design of an earthquake isolation system as an optimal design problem.

(iii) to apply the method of feasible directions to achieve the optimal design, making use of the special nature of the earthquake problem to achieve computational efficiency.

1.2 Report Outline

A short description of the test structure and the isolation system used in the earthquake simulator tests conducted at the University of California, Berkeley, is given in Section 2. In Section 3, the mathematical model used to describe the hysteretic behavior of the energy absorbing devices is described. Equations of motion for the system are obtained and an efficient algorithm based upon the Newmark and Runge-Kutta methods with optional Newton-Raphson iteration is presented. Comments are made about sensitivity analysis results, i.e. computation of the rate of change of response quantities with respect to the design parameters required by the optimization algorithm. A general optimal design problem is then formulated in Section 4, which also presents a feasible direction algorithm to solve it. Comments about the computational aspects of the algorithm are included. Section 5 describes application of the general techniques presented in Sections 3 and 4 to the optimal design of an isolation system for the steel test frame described in Section 2. The report is completed by some concluding remarks in Section 6.

2. AN EARTHQUAKE ISOLATION SYSTEM

A half-scale model of a three-story steel framed-structure with an isolation system consisting of rubber bearings and energy absorbing devices was tested on an earthquake simulator. This Section gives a brief description of the test frame and the isolation system used. Further details of design and fabrication are given in [2,4,5,6].

2.1 Steel Test Frame

The test structure consisted of two identical, three-story, single-bay steel frames, interconnected by floor diaphragm systems which were essentially rigid in their planes as shown in Fig. 1. The model weighed 39.5 kips, was 20 ft high and was 12 ft by 6 ft in plan. The columns and beams were W5 x 12 and W6 x 12 rolled sections, respectively, and were welded together by typical moment resistant connections. A heavy W10 x 49 girder was used at the base to ensure that the rubber bearings would have little tendency to undergo bending deformations. Concrete blocks weighing 8 kips were added to each floor to simulate the dead weight of the building. The model was supported on rubber bearings and energy absorbing devices were attached to the base floor through a horizontal link, as shown in Fig. 2.

2.2 Natural Rubber Bearings

The natural rubber bearings used in the test are shown in Figs. 3 and 4. Each layer of a multilayer bearing was hand-fabricated from sheets of rubber vulcanization-bonded to aluminum foil. The aluminum foil was in turn bonded to the mild steel interleaves using adhesive tape over two-thirds of the surface area and epoxy resin, for greater shear strength, over the remaining one-third area.

The vertical stiffness characteristics of the rubber bearings are shown in Fig. 5. After an initial soft cycle, the bearings showed little hysteresis. The vertical stiffness under the working load is of the order of 150 kips/in.

Horizontal stiffness characteristics are shown in Fig. 6. The initial tangent stiffness at zero deflection is 320 lb/in., reducing to about 250 lb/in. at 2.5 in. deflection. The hysteresis loops represent approximately 10% critical damping.

2.3 Torsional Energy Absorbing Devices

A typical energy absorbing device is shown in Fig. 7. The key element in the device is the mild steel torsion bar of rectangular cross-section to which four clamps are welded. The outer clamping arms are used to attach the device to structural and foundation elements, with the inner arms linked to the active structural element. When this element is displaced, it pushes the inner arms introducing torsion in the mild steel bar.

In this steel frame test devices were attached to the base floor in such a way that they applied a horizontal force to the model structure. The devices were tested under sinusoidal and random loadings to establish that they are capable of withstanding many cycles of large plastic deformation without appreciable deterioration in their energy absorption capacity. In this regard see Fig. 8. Under small excitations the devices are elastic and the system behaves as a rigid foundation system, while under strong excitations the devices yield and produce large hysteresis loops, thus absorbing a considerable amount of energy.

3. STRUCTURAL ANALYSIS

A procedure for efficient analysis of a structural system containing earthquake isolation devices is the first step in developing an optimal design methodology. This section introduces a mathematical model to describe the hysteretic behavior of the energy absorbing devices. Equations of motion for a multistory frame containing energy absorbing devices are then derived and an efficient algorithm for their numerical integration using substructuring is given.

3.1 Mathematical Model for Hysteretic Behavior of the Energy Absorbing Devices

A number of models have been employed to specify the force-deformation relationship for inelastic structural elements under cyclic loading. Two of the most common are the bilinear and the Ramberg-Osgood models. The bilinear model exhibits sharp transition from elastic to inelastic states; kinematic or isotropic hardening rules are used for unloading and reloading. The model fails to represent actual material behavior under cyclic loading and is computationally quite inefficient because it requires one to keep track of all stiffness transition points.

The Ramberg-Osgood model, coupled with Masing's rule for unloading and reloading gives a continuous transition from elastic to inelastic states. Computationally, this is a very difficult model to use because of different equations for different parts of the loop. Matzen and McNiven [7] have pointed out that the model as presented originally is not suitable for random earthquake-type excitations. At least thirteen new rules have been added to make it applicable to this case, making the model even harder to use.

Recently a series of newly-proposed models for cyclic behavior of structural elements has been described [8]. These models are given in the form of differential equations and are sufficiently general to include strain hardening, stiffness degradation, etc. A single equation governs initial loading, unloading and reloading (facilitating computation) and it behaves well in the case of arbitrary excitations.

The particular rate-independent model to be used for the energy absorbing devices in this study is given by the following equations:

$$\dot{F}(t) = K_0 \left[\dot{U}(t) - |\dot{U}(t)| \left(\frac{F(t)}{F_0} - s \right)^n \right] \quad (3.1.1)$$

$$s(t) = \alpha \left[\frac{U(t)}{U_0} - \frac{F(t)}{F_0} \right] \quad (3.1.2)$$

where

$F(t)$ = horizontal force in the energy absorber

$U(t)$ = displacement of the energy absorber

$\dot{U}(t)$ = velocity of the energy absorber

K_0 = F_0/U_0

F_0 = yield force

U_0 = yield displacement

α = a constant which controls the slope after yielding,

$$K_y \approx K_0 \frac{\alpha}{1+\alpha} .$$

n = a material parameter, taken as an odd integer which controls the sharpness of transition from the elastic to the inelastic region. As $n \rightarrow \infty$ the model approaches a bilinear model.

The parameters F_0 , U_0 , α and n are chosen such that predicted response from the model closely matches experimental response. Typical

loops generated by this model under displacements varying sinusoidally in time are shown in Fig. 9.

3.2 Equations of Motion for the System

The structural system considered here, consists of an assemblage of discrete beam and column elements as shown in Fig. 10. The frame may have any number of stories and bays. Axial deformations in both beams and columns are neglected; thus, we have only one lateral and $M+1$ rotational degrees of freedom per story, where M is the number of bays. The nonlinear energy absorbing elements can be attached to any story. Story masses are assumed to be lumped at the floor levels and no rotational inertia is associated with the rotational degrees of freedom. The structure is assumed to remain elastic during an earthquake; thus, the nonlinearity is only associated with the energy absorbers. The equations of motion of the system can be written as follows:

$$\tilde{\underline{M}} \ddot{\underline{U}} + \tilde{\underline{C}} \dot{\underline{U}} + \tilde{\underline{K}}^E \underline{U} + \tilde{\underline{F}} = - \tilde{\underline{M}} \underline{r} \ddot{U}_g(t) \quad (3.2.1)$$

where

$\underline{U}^T(t) = (U_1^r, \dots, U_{N(M+1)}^r; U_1^l, \dots, U_1^n, \dots)$ is the nodal point displacement vector, $\underline{U} \in \mathbb{R}^{N(M+2)}$.

$\dot{\underline{U}}(t)$ = velocity vector

$\ddot{\underline{U}}(t)$ = acceleration vector

$\tilde{\underline{M}}$ = diagonal mass matrix, $\tilde{\underline{M}} \in \mathbb{R}^{N(M+2)} \times \mathbb{R}^{N(M+2)}$

$\tilde{\underline{C}}$ = damping matrix, $\tilde{\underline{C}} \in \mathbb{R}^{N(M+2)} \times \mathbb{R}^{N(M+2)}$

$\tilde{\underline{K}}^E$ = stiffness matrix of the structure excluding the energy absorbing elements, $\tilde{\underline{K}}^E \in \mathbb{R}^{N(M+2)} \times \mathbb{R}^{N(M+2)}$

$$\begin{aligned} \underline{\tilde{F}} &= \text{vector of forces in the energy absorbing elements,} \\ \underline{\tilde{F}} &\in \mathbb{R}^{N(M+2)} \end{aligned}$$

$$\underline{r} = (0, \dots; 1, \dots; 1, \dots, 1)^T, \quad \underline{r} \in \mathbb{R}^{N(M+2)}$$

$$\ddot{U}_g(t) = \text{ground acceleration time history.}$$

In order to eliminate rotational degrees of freedom from the system, the matrices $\underline{\tilde{M}}$, $\underline{\tilde{C}}$ and $\underline{\tilde{K}}^E$ are partitioned corresponding to the rotational and translational degrees of freedom. The system of equations then has the form

$$\begin{aligned} \begin{bmatrix} 0 & 0 \\ \hline 0 & \underline{M} \end{bmatrix} \begin{bmatrix} \ddot{U}_{-\theta} \\ \hline \ddot{U}_{-} \end{bmatrix} + \begin{bmatrix} 0 & 0 \\ \hline 0 & \underline{C} \end{bmatrix} \begin{bmatrix} \dot{U}_{-\theta} \\ \hline \dot{U}_{-} \end{bmatrix} + \begin{bmatrix} \underline{K}_{-\theta\theta}^E & \underline{K}_{-\theta t}^E \\ \hline [\underline{K}_{-\theta t}^E]^T & \underline{K}_{tt}^E \end{bmatrix} \begin{bmatrix} U_{-\theta} \\ \hline U_{-} \end{bmatrix} \\ + \begin{bmatrix} 0 \\ \hline \underline{F}_{-} \end{bmatrix} = - \begin{bmatrix} 0 & 0 \\ \hline 0 & \underline{M} \end{bmatrix} \begin{bmatrix} 0 \\ \hline \underline{e} \end{bmatrix} \ddot{U}_g(t) \end{aligned}$$

where

$$\underline{e}^T = (1, 1, 1, \dots), \quad \underline{e} \in \mathbb{R}^N$$

\underline{U} , $\dot{\underline{U}}$, $\ddot{\underline{U}} \in \mathbb{R}^N$ represent, respectively, translational displacement, velocity and acceleration vectors.

$\underline{U}_{-\theta}$, $\dot{\underline{U}}_{-\theta}$, $\ddot{\underline{U}}_{-\theta} \in \mathbb{R}^{N(M+1)}$ represent state vectors corresponding to rotational degrees of freedom

The first sub-matrix equation gives

$$\underline{U}_{-\theta} = - \begin{bmatrix} \underline{K}_{-\theta\theta}^E \end{bmatrix}^{-1} \underline{K}_{-\theta t}^E \underline{U}_{-}.$$

The second equation gives

$$\begin{aligned} \underline{M} \ddot{\underline{U}}_{-} + \underline{C} \dot{\underline{U}}_{-} + \underline{K}_{tt}^E \underline{U}_{-} + \begin{bmatrix} \underline{K}_{-\theta t}^E \end{bmatrix}^T \underline{U}_{-\theta} \\ + \underline{F}_{-} = - \underline{M} \underline{e} \ddot{U}_g. \end{aligned}$$

Substituting for U_θ from the first into the second equation yields

$$\underline{M} \ddot{\underline{U}} + \underline{C} \dot{\underline{U}} + \underline{K}^E \underline{U} + \underline{F} = - \underline{M} \underline{e} \ddot{U}_g(t)$$

where

$$\underline{K}^E = \underline{K}_{-tt}^E - \begin{bmatrix} \underline{K}_{-t\theta}^E \\ \underline{K}_{-\theta t}^E \end{bmatrix}^T \begin{bmatrix} \underline{K}_{-t\theta}^E \\ \underline{K}_{-\theta t}^E \end{bmatrix}^{-1} \underline{K}_{-\theta\theta}^E.$$

Define

$$\underline{P}(t) = - \underline{M} \underline{e} \ddot{U}_g(t).$$

Then, the equations of motion in terms of lateral degrees of freedom are

$$\underline{M} \ddot{\underline{U}}(t) + \underline{C} \dot{\underline{U}}(t) + \underline{K}^E \underline{U}(t) + \underline{F}(t) = \underline{P}(t). \quad (3.2.2)$$

$$\underline{M}, \underline{C}, \underline{K}^E \in \mathbb{R}^N \times \mathbb{R}^N$$

$$\underline{U}(t), \dot{\underline{U}}(t), \ddot{\underline{U}}(t) \in \mathbb{R}^N.$$

3.3 Numerical Solution of the Differential Equations of Motion

The equations of motion (3.2.2) are solved numerically by discretizing them in time, with the exact solution $\underline{U}(t)$, $\dot{\underline{U}}(t)$ and $\ddot{\underline{U}}(t)$ approximated by \underline{U}_t , $\dot{\underline{U}}_t$ and $\ddot{\underline{U}}_t$, respectively. The step-by-step integration procedures start with the known initial conditions and march forward in time giving the solution at discrete time intervals. The process for a nonlinear system has two distinct phases. The first phase is the linearization phase, in which the equations are linearized about the current state by retaining only the first order terms of the Taylor series expansion. Estimates of the solution at the next step are then obtained by using these linearized equations. The second phase is the state determination phase, in which the internal forces in equilibrium with the new state of motion are calculated. If the

discrepancy between these internal forces and the external applied loads is within some tolerance level, the solution is accepted and the process repeated for the next step. Otherwise, a Newton-Raphson type iteration is used until the unbalanced forces are within acceptable limits.

In this study the estimates of the solution are obtained using Newmark's method and the internal forces in the energy absorbers are computed using a fourth-order Runge-Kutta scheme. The details of the process are given below.

The equations of motion (3.2.2) at time $\tau = t + \Delta t$ can be written as

$$\underline{M} \ddot{\underline{U}}_{\tau} + \underline{C} \dot{\underline{U}}_{\tau} + \underline{K}^E \underline{U}_{\tau} + \underline{F}_{\tau} = \underline{P}_{\tau} \quad (3.3.1)$$

Define the increments in acceleration, velocity, displacement and force in the energy absorbers occurring in the time increment Δt by

$$\begin{aligned} \Delta \ddot{\underline{U}}_{-t} &= \ddot{\underline{U}}_{\tau} - \ddot{\underline{U}}_{-t} \\ \Delta \dot{\underline{U}}_{-t} &= \dot{\underline{U}}_{\tau} - \dot{\underline{U}}_{-t} \\ \Delta \underline{U}_{-t} &= \underline{U}_{\tau} - \underline{U}_{-t} \\ \Delta \underline{F}_{-t} &= \underline{F}_{\tau} - \underline{F}_{-t} \\ &= \left. \frac{\partial \underline{F}}{\partial \underline{U}} \right|_t \Delta \underline{U}_{-t} \\ &= \underline{K}_{-t}^N \Delta \underline{U}_{-t} \end{aligned} \quad (3.3.2)$$

Substituting these expressions in Eq. (3.3.1) produces the incremental form of the equations of motion

$$\underline{M} \Delta \ddot{\underline{U}}_t + \underline{C} \Delta \dot{\underline{U}}_t + (\underline{K}^E + \underline{K}_t^N) \Delta \underline{U}_t = \underline{P}_t^* \quad (3.3.3)$$

where

$$\underline{P}_t^* = \underline{P}_T - \left[\underline{M} \ddot{\underline{U}}_t + \underline{C} \dot{\underline{U}}_t + \underline{K}^E \underline{U}_t + \underline{F}_t \right]$$

Computation of \underline{K}_t^N

\underline{K}_t^N is a diagonal matrix whose i th diagonal element is $\left. \frac{\partial F_i}{\partial U_i} \right|_t$. Since $\underline{F}(t)$ represents the force in the energy absorbers, only those elements on the diagonal, which correspond to a degree of freedom at which an energy absorbing element is attached, will be non-zero.

The force in the energy absorbing element at the i th degree of freedom is obtained from Eqs. (3.1.1) and (3.1.2):

$$\begin{aligned} \dot{F}_i(t) &= K_0 \left(\dot{U}_i(t) - |\dot{U}_i(t)| \left(\frac{F_i(t)}{F_0} - S_i(t) \right)^n \right) \\ S_i(t) &= \alpha \left(\frac{U_i(t)}{U_0} - \frac{F_i(t)}{F_0} \right) \end{aligned}$$

or

$$\begin{aligned} \dot{F}_i(t) &= K_0 \dot{U}_i(t) \left(1 - \text{sign} \left(\frac{F_i(t)}{F_0} - S_i(t) \right)^n \right) \\ S_i(t) &= \alpha \left(\frac{U_i(t)}{U_0} - \frac{F_i(t)}{F_0} \right) \end{aligned}$$

where

$$\begin{aligned} \text{sign} &= 1 \text{ if } U_i(t) > 0 \\ &= -1 \text{ if } U_i(t) < 0. \end{aligned}$$

Thus

$$\frac{\dot{F}_i(t)}{\dot{U}_i(t)} = K_0 \left\{ 1 - \text{sign} \left(\frac{F_i(t)}{F_0} - S_i(t) \right)^n \right\}$$

and

$$\left. \frac{\partial F_i}{\partial U_i} \right|_t = K_0 \left\{ 1 - \text{sign} \left(\frac{F_i(t)}{F_0} - S_i(t) \right)^n \right\} \quad (3.3.4)$$

with

$$S_i(t) = \alpha \left(\frac{U_i(t)}{U_0} - \frac{F_i(t)}{F_0} \right)$$

Newmark's Method

An implicit, single-step, two parameter family of integration operators described by Newmark [9] is used for the numerical integration of the equations of motion. The method assumes that the increments in velocity and acceleration are related to the increment in displacement and the state of motion at time t , as follows:

$$\Delta \dot{U}_t = \frac{\gamma}{\beta \Delta t} \Delta U_t - \frac{\gamma}{\beta} \dot{U}_t - \Delta t \left(\frac{\gamma}{2\beta} - 1 \right) \ddot{U}_t \quad (3.3.5)$$

$$\Delta \ddot{U}_t = \frac{1}{\beta (\Delta t)^2} \Delta U_t - \frac{1}{\beta \Delta t} \dot{U}_t - \frac{1}{2\beta} \ddot{U}_t \quad (3.3.6)$$

where

Δt = time step of integration

γ, β are the two integration parameters.

A "constant average acceleration" operator is obtained with

$\beta = 1/4$ and $\gamma = 1/2$, which is unconditionally stable for linear problems.

A "linear acceleration" operator is obtained with $\beta = 1/6$ and

$\gamma = 1/2$.

Substituting Eqs. (3.3.5) and (3.3.6) into the incremental equations of motion (3.3.3) and simplifying gives

$$\underline{K}_t^* \Delta \underline{U}_t = \underline{R}_t^* \quad (3.3.7)$$

where

$$\begin{aligned} \underline{K}_t^* &= \frac{1}{\beta \Delta t} \underline{M} + \frac{\gamma}{\beta \Delta t} \underline{C} + \underline{K}^E + \underline{K}_t^N \\ \underline{R}_t^* &= \underline{P}_t^* + \underline{M} \left[\frac{1}{\beta \Delta t} \dot{\underline{U}}_t + \frac{1}{2\beta} \ddot{\underline{U}}_t \right] \\ &\quad + \underline{C} \left[\frac{\gamma}{\beta} \dot{\underline{U}}_t + \Delta t \left(\frac{\gamma}{2\beta} - 1 \right) \ddot{\underline{U}}_t \right] \end{aligned}$$

Solution of $\underline{K}_t^* \Delta \underline{U}_t = \underline{R}_t^*$

The most expensive part of the integration process is the solution of the above set of linear equations. Fortunately, because of the localized nonlinearity of the problem, it is not necessary to form and decompose the whole matrix \underline{K}_t^* at each step. The substructuring technique is used to separate effectively the nonlinear part from the linear part of the problem as follows:

Partition the displacement vector such that displacements corresponding to the energy absorbers are separated from the remaining displacements

$$\Delta \underline{U}_t = \begin{bmatrix} \Delta \underline{U}_t^E \\ \hline \Delta \underline{U}_t^N \end{bmatrix}$$

$\Delta \underline{U}_t^N$ = incremental displacements corresponding to energy absorbing elements.

$\Delta \underline{U}_t^E$ = incremental displacements corresponding to the rest of the system

Partition the matrices \underline{K}_t^* and \underline{R}_t^* accordingly, as follows:

$$\begin{bmatrix} \underline{K}_{EE} & \underline{K}_{EN} \\ \hline \underline{K}_{NE} & \underline{K}_{NN} \end{bmatrix} \begin{bmatrix} \Delta \underline{U}_t^E \\ \hline \Delta \underline{U}_t^N \end{bmatrix} = \begin{bmatrix} \underline{R}_t^E \\ \hline \underline{R}_t^N \end{bmatrix} \quad (3.3.8)$$

The first equation gives

$$\underline{K}_{-EE} \underline{\Delta U}^E + \underline{K}_{-EN} \underline{\Delta U}^N = \underline{R}^E$$

or

$$\underline{\Delta U}^E = \underline{K}_{-EE}^{-1} \left[\underline{R}^E - \underline{K}_{-EN} \underline{\Delta U}^N \right]. \quad (3.3.9)$$

The second submatrix equation in Eq. (3.3.8) gives

$$\underline{K}_{-NE} \underline{\Delta U}^E + \underline{K}_{-NN} \underline{\Delta U}^N = \underline{R}^N. \quad (3.3.10)$$

Substitute Eq. (3.3.9) into Eq. (3.3.10)

$$\underline{K}_{-NE} \underline{K}_{-EE}^{-1} \left[\underline{R}^E - \underline{K}_{-EN} \underline{\Delta U}^N \right] + \underline{K}_{-NN} \underline{\Delta U}^N = \underline{R}^N.$$

Define

$$\underline{Q} = - \underline{K}_{-EE}^{-1} \underline{K}_{-EN}$$

$$\underline{Q}^T = - \underline{K}_{-NE} \underline{K}_{-EE}^{-1}.$$

Thus

$$\left[\underline{K}_{-NE} \underline{Q} + \underline{K}_{-NN} \right] \underline{\Delta U}^N = \underline{R}^N + \underline{Q}^T \underline{R}^E.$$

or

$$\underline{\Delta U}^N = \left[\underline{K}_{-NE} \underline{Q} + \underline{K}_{-NN} \right]^{-1} \left[\underline{R}^N + \underline{Q}^T \underline{R}^E \right] \quad (3.3.11)$$

Once the $\underline{\Delta U}^N$ are known, $\underline{\Delta U}^E$ are calculated from Eq. (3.3.9).

The computational steps can be summarized in the following algorithm.

Algorithm

In the beginning of the integration loop

- (i) form $\underline{K}_{-EE}, \underline{K}_{-EN}, \underline{K}_{-NE} = \underline{K}_{-EN}^T$,
- (ii) triangularize \underline{K}_{-EE} ,

(iii) obtain \underline{Q} by forward reduction and back substitution from

$$\underline{K}_{-EE} \underline{Q} = - \underline{K}_{-EN},$$

(iv) form \underline{Q}^T and the product $\underline{K}_{-NE} \underline{Q}$.

At each time step of integration

(i) form \underline{K}_{-NN} at the current step,

(ii) form load vectors \underline{R}^E and \underline{R}^N ,

(iii) Solve $\left[\underline{K}_{-NE} \underline{Q} + \underline{K}_{-NN} \right] \Delta \underline{U}^N = \underline{R}^N + \underline{Q}^T \underline{R}^E$
for $\Delta \underline{U}^N$,

(iv) obtain $\Delta \underline{U}^E$ by forward reduction and back-substitution from

$$\underline{K}_{-EE} \Delta \underline{U}^E = \underline{R}^E - \underline{K}_{-EN} \Delta \underline{U}^N$$

Computation of Forces in the Energy Absorbing Elements

After increments in the displacements and velocities are obtained, the next step is to compute the internal resisting forces in equilibrium with this new state of motion. Since the structure is assumed to remain elastic, the internal forces in the structural elements are obtained simply by multiplying the current displacements with the appropriate stiffnesses of these elements. Computation of forces in the energy absorbers, however, is not that simple, because of lack of an algebraic expression for their force-deformation behavior, which instead, is described by a set of first order differential equations. These equations are integrated numerically to compute internal forces in the energy absorbers. An explicit fourth-order Runge-Kutta scheme, with the option of using a smaller time step than the one used in Newmark's method, is used in this study. An explicit scheme is favored over an implicit scheme because of the

added complexity of an implicit scheme, which would involve an additional iteration cycle. The details of the process are given below.

To integrate force-deformation equations of energy absorbers from time t to time $\tau = t + \Delta t$, some assumptions regarding the variation of acceleration, velocity and displacement during the time interval (t, τ) are needed. Since the Newmark linear acceleration method has been demonstrated to be quite effective for solving non-linear structural dynamics problems [10], it seems reasonable to assume linear variation in the acceleration during the time interval. This will imply quadratic variation of velocity and cubic variation of displacement. These variations are shown in Fig. 11.

The force in the energy absorber at the i th floor is given by Eqs. (3.1.1) and (3.1.2):

$$\dot{F}_i(x) = K_0 \left\{ \dot{U}_i(x) - |\dot{U}_i(x)| \left(\frac{F_i(x)}{F_0} - S_i \right)^n \right\}$$

$$S_i(x) = \alpha \left(\frac{U_i(x)}{U_0} - \frac{F_i(x)}{F_0} \right).$$

or

$$\dot{F}_i(x) = K_0 \left[\dot{U}_i(x) - |\dot{U}_i(x)| \left\{ (\alpha+1) \frac{F_i(x)}{F_0} - \alpha \frac{U_i(x)}{U_0} \right\}^n \right]$$

$$x \in [0, \Delta t] \quad (3.3.12)$$

Equation (3.3.12) is integrated by employing a fourth order Runge-Kutta method with time step Δx , where $\Delta x \leq \Delta t$, and the initial condition

$$F_i(0) = F_i(t),$$

$$\dot{F}_i(x) = f \left(F_i(x), x \right)$$

$$= K_0 \left[\dot{U}_i(x) - |\dot{U}_i(x)| \left\{ (\alpha+1) \frac{F_i(x)}{F_0} - \alpha \frac{U_i(x)}{U_0} \right\}^n \right].$$

The following calculations are made to advance the solution

from x_K to $x_{K+1} = x_K + \Delta x$

$$\begin{aligned} K_1 &= \Delta x f \left(F_i(x_K), x_K \right) \\ &= \Delta x K_0 \left[\dot{U}_i(x_K) - |\dot{U}_i(x_K)| \left\{ (\alpha+1) \frac{F_i(x_K)}{F_0} - \alpha \frac{U_i(x_K)}{U_0} \right\}^n \right] \end{aligned}$$

where

$$\begin{aligned} \dot{U}_i(x_K) &= \dot{U}_i(t) + \ddot{U}_i(t) x_K + \frac{\Delta \ddot{U}_i}{\Delta x} \frac{x_K^2}{2} \\ U_i(x_K) &= U_i(t) + \dot{U}_i(t) x_K + \ddot{U}_i(t) \frac{x_K^2}{2} + \frac{\Delta \ddot{U}_i}{\Delta x} \frac{x_K^3}{6} . \end{aligned}$$

$$\begin{aligned} K_2 &= \Delta x f \left(F_i(x_K) + \frac{1}{2} K_1, x_K + \frac{1}{2} \Delta x \right) \\ &= K_0 \Delta x \left[\dot{U}_i \left(x_K + \frac{1}{2} \Delta x \right) - |\dot{U}_i \left(x_K + \frac{1}{2} \Delta x \right)| \right. \\ &\quad \left. (\alpha+1) \frac{F_i(x_K) + \frac{1}{2} K_1}{F_0} - \alpha \frac{U_i \left(x_K + \frac{\Delta x}{2} \right)}{U_0} \right]^n \end{aligned}$$

where

$$\begin{aligned} \dot{U}_i \left(x_K + \frac{1}{2} \Delta x \right) &= \dot{U}_i(t) + \ddot{U}_i(t) \left(x_K + \frac{1}{2} \Delta x \right) \\ &\quad + \frac{\Delta \ddot{U}_i}{\Delta x} \frac{1}{2} \left(x_K + \frac{1}{2} \Delta x \right)^2 \\ U_i \left(x_K + \frac{1}{2} \Delta x \right) &= U_i(t) + \dot{U}_i(t) \left(x_K + \frac{1}{2} \Delta x \right) \\ &\quad + \ddot{U}_i(t) \frac{1}{2} \left(x_K + \frac{1}{2} \Delta x \right)^2 + \frac{\Delta \ddot{U}_i}{\Delta x} \frac{1}{6} \left(x_K + \frac{1}{2} \Delta x \right)^3 \end{aligned}$$

$$K_3 = \Delta x f \left(F_i(x_K) + \frac{1}{2} K_2, x_K + \frac{1}{2} \Delta x \right)$$

$$= K_0 \Delta x \left[\dot{U}_i(x_K + \frac{1}{2} \Delta x) - \left| \dot{U}_i(x_K + \frac{1}{2} \Delta x) \right| \left\{ (\alpha+1) \frac{F_i(x_K) + \frac{1}{2} K_2}{F_0} - \alpha \frac{U_i(x_K + \frac{1}{2} \Delta x)}{U_0} \right\}^n \right]$$

$$K_4 = \Delta x f(F_i(x_K) + K_3, x_K + \Delta x)$$

$$= K_0 \Delta x \left[\dot{U}_i(x_K + \Delta x) - \left| \dot{U}_i(x_K + \Delta x) \right| \left\{ (\alpha+1) \frac{F_i(x_K) + K_3}{F_0} - \alpha \frac{U_i(x_K + \Delta x)}{U_0} \right\}^n \right]$$

where

$$\dot{U}_i(x_K + \Delta x) = \dot{U}_i(t) + \ddot{U}_i(t) (x_K + \Delta x) + \frac{\Delta \ddot{U}_i}{\Delta x} \frac{1}{2} (x_K + \Delta x)^2$$

$$U_i(x_K + \Delta x) = U_i(t) + \dot{U}_i(t) (x_K + \Delta x) + \ddot{U}_i(t) \frac{1}{2} (x_K + \Delta x)^2 + \frac{\Delta \ddot{U}_i}{\Delta x} \frac{1}{6} (x_K + \Delta x)^3$$

$$F_i(x_{K+1}) = F_i(x_K) + \frac{1}{6} (K_1 + 2K_2 + 2K_3 + K_4).$$

Algorithm for Integration of Equations of Motion

Now the algorithm for numerical integration of the equations of motion (3.2.2) can be presented.

A: INITIAL CALCULATIONS

DATA: Integration parameters β, γ

time steps Δt and $\Delta x, .$

Convergence tolerance parameter TOL.

structural property matrices $\underline{M}, \underline{K}^E$ and \underline{C}

energy absorber properties F_0, U_0, α and n .

STEP 1: Compute the constants

$$a_1 = \frac{1}{\beta(\Delta t)^2} \quad a_2 = \frac{1}{\beta\Delta t} \quad a_3 = \frac{1}{2\beta}$$

$$a_4 = \frac{\gamma}{\beta\Delta t} \quad a_5 = \frac{\gamma}{\beta} \quad a_6 = \Delta t \left(\frac{\gamma}{2\beta} - 1 \right) .$$

STEP 2: Initialize the state of motion, i.e. specify \underline{U}_0 , $\dot{\underline{U}}_0$ and $\ddot{\underline{U}}_0$.

STEP 3: Partition the stiffness matrix as explained in Eq. (3.3.8), triangularize \underline{K}_{EE} and form \underline{Q} .

B. FOR EACH TIME STEP

STEP 4: Form \underline{K}_t^* and \underline{R}_t^*

$$\underline{K}_t^* = a_1 \underline{M} + a_4 \underline{C} + \underline{K}^E + \underline{K}_t^N$$

$$\underline{R}_t^* = \underline{P}_t^* + \underline{M} \left[a_2 \dot{\underline{U}}_t + a_3 \ddot{\underline{U}}_t \right] + \underline{C} \left[a_5 \dot{\underline{U}}_t + a_6 \ddot{\underline{U}}_t \right]$$

$$\text{where } \underline{P}_t^* = \underline{P}_\tau - \left[\underline{M} \ddot{\underline{U}}_t + \underline{C} \dot{\underline{U}}_t + \underline{K}^E \underline{U}_t + \underline{F}_t \right]$$

$$\underline{P}_\tau = - \underline{M} \underline{e} \ddot{U}_g(\tau)$$

STEP 5: Solve

$$\underline{K}_t^* \Delta \underline{U}_t = \underline{R}_t^*$$

for $\Delta \underline{U}_t$, using the algorithm given previously.

STEP 6: Update the state of motion at $\tau = t + \Delta t$

$$\ddot{\underline{U}}_\tau = \ddot{\underline{U}}_t + a_1 \Delta \underline{U}_t - a_2 \dot{\underline{U}}_t - a_3 \ddot{\underline{U}}_t$$

$$\dot{\underline{U}}_\tau = \dot{\underline{U}}_t + a_4 \Delta \underline{U}_t - a_5 \dot{\underline{U}}_t - a_6 \ddot{\underline{U}}_t$$

$$\underline{U}_\tau = \underline{U}_t + \Delta \underline{U}_t .$$

STEP 7: Compute \underline{F}_τ , the forces in the energy absorbing devices using the fourth-order Runge-Kutta method.

STEP 8: Compute the unbalanced force at time τ

$$\hat{\underline{f}} = \underline{P}_\tau - \left[\underline{M} \ddot{\underline{U}}_\tau + \underline{C} \dot{\underline{U}}_\tau + \underline{K}^E \underline{U}_\tau + \underline{F}_\tau \right].$$

STEP 9: Compute $\|\hat{\underline{f}}\|_2$, the Euclidean norm of $\hat{\underline{f}}$. If $\|\hat{\underline{f}}\|_2 \leq \text{TOL}$, no iteration is needed in this step. Go to step 4 for the next step calculations, else proceed to step 10.

C: ITERATION WITHIN A TIME STEP

STEP 10: Compute $\underline{K}_\tau^* = a_1 \underline{M} + a_4 \underline{C} + \underline{K}^E + \underline{K}_\tau^N$.

STEP 11: Solve $\underline{K}_\tau^* \delta \underline{U}_\tau = \hat{\underline{f}}$ for $\delta \underline{U}_\tau$.

STEP 12: Update the state of motion

$$\text{new } \ddot{\underline{U}}_\tau = \ddot{\underline{U}}_\tau + a_1 \delta \underline{U}_\tau$$

$$\text{new } \dot{\underline{U}}_\tau = \dot{\underline{U}}_\tau + a_4 \delta \underline{U}_\tau$$

$$\text{new } \underline{U}_\tau = \underline{U}_\tau + \delta \underline{U}_\tau.$$

STEP 13: Compute the unbalance as in step 8. See if convergence criterion of step 9 is satisfied. If yes, go to step 4 for next time step. Else go to step 10.

3.4 Sensitivity Analysis

The method of feasible directions for optimization requires gradients of the constraint functions, which in turn require gradients of the response quantities with respect to the system parameters. The computation of these gradients, so-called sensitivity analysis, is important in itself because the information produced can be used directly for design trade-off studies.

One way of computing such sensitivity matrices is to integrate numerically the sensitivity equations obtained by differentiating the system equations of motion with respect to the system parameters. In the present case because of the complicated nature of the hysteretic model of the energy absorbers, the analytical expressions for sensitivity equations are very complex. Numerical integration of these equations with the same time step as that used for the system equations poses additional difficulties.

Because of these difficulties, a straight-forward approach using finite difference approximations is used. Partial derivatives are given by expressions of the type

$$\frac{\partial f(b)}{\partial b} \sim \frac{f(b+\Delta b) - f(b)}{\Delta b}$$

where

$f(\cdot)$ is any response function and

b is an element of the parameter vector.

Some errors are introduced by the above approximation, but by proper selection of the step size they can be controlled.

4. OPTIMIZATION

In this section a class of optimal design problems is formulated for the multistory frame with energy absorbing devices. The design problem is then transcribed into a canonical form of nonlinear programming problem. A feasible directions algorithm to solve this problem is discussed and some comments made about the computational aspects of the method.

4.1 Optimal Design Problem

The main objective of an earthquake isolation system is to reduce detrimental effects of earthquake ground motion on the structure. Thus, one may formulate an optimal design problem as selection of the controlling parameters (e.g. yield force, yield displacement, etc., of the energy absorber) of the isolation system in such a way as to minimize some measure of the structural response of the system. In this section, the problem is first considered in an abstract manner, since the techniques described are applicable to a broad class of such problems. Specific design problems will then be treated in the next section.

A class of optimal design problems can be written in the form

$$\min_{\underline{z}} \max_{t \in T} [F(\underline{R}(\underline{z}, t))]$$

such that

$$\begin{aligned} \max_{t \in T} \quad \underline{G}(\underline{R}(\underline{z}, t)) &\leq \underline{\delta}_1 \\ \underline{H}(\underline{z}) &\geq \underline{\delta}_2 \end{aligned} \quad (4.1.1)$$

where

$$T = [t_0, t_f], \text{ specified time interval}$$

The following notation has been used:

- $F : \mathbb{R}^Q \times \mathbb{R} \rightarrow \mathbb{R} \times \mathbb{R}$: is some function of structural response which is to be minimized.
- Q : number of structural response functions.
- $\underline{z} \in \mathbb{R}^P$: is the design parameter vector.
- P : total number of design parameters.
- $\underline{R} : \mathbb{R}^P \times \mathbb{R} \rightarrow \mathbb{R}^Q \times \mathbb{R}$: is some function of structural response.
- $\underline{G} : \mathbb{R}^P \times \mathbb{R} \rightarrow \mathbb{R}^M \times \mathbb{R}$: are the time dependent inequality constraints (functional constraints)
- M : number of functional inequality constraints.
- $\underline{H} : \mathbb{R}^P \rightarrow \mathbb{R}^L$: are conventional inequality constraints.
- $\delta_{-1} \in \mathbb{R}^M, \delta_{-2} \in \mathbb{R}^L$: are prescribed constraint bounds.

As an example, consider the problem of minimizing the maximum acceleration at the top floor of a multistory frame, with an energy absorber at the bottom floor, such that the bottom floor displacement is less than a certain allowable value. The design parameters could be chosen to be the yield force and yield displacement of the energy absorber, with the requirement that both design parameters be positive. Similarly the function F is taken as the square of the top floor acceleration while the function G is the square of the bottom floor displacement. The function H represents positivity constraints on the design parameters, as noted above.

4.2 Nonlinear Programming Problem

The design problem formulated in the previous section is not directly suitable for the application of nonlinear programming

techniques; an appropriate canonical form can be expressed as [11, 12, 13, 14]

$$\min_{\underline{z}} \{f^0(\underline{z})\} \quad (4.2.1)$$

such that

$$f^j(\underline{z}) = \max_{t \in T} \phi^j(\underline{z}, t) \leq 0 \quad j = 1, \dots, M$$

$T \in \mathbb{R}$ is a compact interval.

$$g^j(\underline{z}) \leq 0 \quad j = 1, \dots, L$$

where

$\underline{z} \in \mathbb{R}^P$ is the design parameter vector.

$f^0 : \mathbb{R}^P \rightarrow \mathbb{R}$ is the cost or objective function.

$f^j : \mathbb{R}^P \rightarrow \mathbb{R} \quad j = 1, \dots, M$ are functional constraints.

$g^j : \mathbb{R}^P \rightarrow \mathbb{R} \quad j = 1, \dots, L$ are conventional inequality constraints.

The optimal design problem (4.1.1) can be transcribed to the canonical form (4.2.1) by augmenting the parameter vector \underline{z} by a dummy cost parameter z^{P+1} . The dummy cost parameter is an upper bound to the objective function to be minimized, i.e.

$$\max_{t \in T} [F(\underline{R}(\underline{z}, t))] \leq z^{P+1}$$

Thus, the minimization of z^{P+1} implies the minimization of the actual objective function. The design problem can then be written as:

$$\min_{\underline{z}} z^{P+1}$$

such that

$$\begin{aligned}
 \max_{t \in T} [F(\underline{R}(\underline{z}, t))] - z^{P+1} &\leq 0 \\
 \max_{t \in T} [G(\underline{R}(\underline{z}, t))] - \underline{\delta}_1 &\leq 0 \\
 -\underline{H}(\underline{z}) + \underline{\delta}_2 &\leq 0,
 \end{aligned} \tag{4.2.2}$$

which is in the canonical form with

$$\begin{aligned}
 f^0(\underline{z}) &= z^{P+1} \\
 f^1(\underline{z}) &= \max_{t \in T} [F(\underline{R}(\underline{z}, t)) - z^{P+1}] \\
 f^j(\underline{z}) &= \max_{t \in T} [G^j(\underline{R}(\underline{z}, t)) - \delta_1^j] \quad j = 2, 3, \dots, M \\
 g^j(\underline{z}) &= -H^j(\underline{z}) + \delta_2^j \quad j = 1, \dots, L.
 \end{aligned}$$

4.3 Method of Feasible Directions

An algorithm of the feasible direction type for solving the nonlinear programming problem (4.2.1) is presented in this section. The basic algorithm is due to Polak and Trahan [15]. Only a short description of the algorithm will be given here; readers interested in more details and the convergence proof are referred to the original paper.

Before presenting the algorithm, some definitions and assumptions are required. As noted earlier, the nonlinear programming problem (NLP) is defined as:

$$\min_{\underline{z}} \left\{ f^0(\underline{z}) \mid f^j(\underline{z}) \leq 0, \quad j \in J_m \quad ; \quad g^j(\underline{z}) \leq 0, \quad j \in J_\ell \right\}$$

where

$$f^j(\underline{z}) = \max_{t \in T} \phi^j(\underline{z}, t) \tag{4.3.1}$$

$$T = [t_0, t_f]$$

$$J_m = \{1, 2, \dots, M\}$$

$$J_\ell = \{1, 2, \dots, L\}$$

$f^0: \mathbb{R}^P \rightarrow \mathbb{R}$, $g^j: \mathbb{R}^P \rightarrow \mathbb{R}$, $j \in J_\ell$ are assumed to be continuously differentiable.

$\phi^j: \mathbb{R}^P \times \mathbb{R} \rightarrow \mathbb{R} \times \mathbb{R}$, $j \in J_m$ are continuously differentiable in the first variable and continuous in the second.

Define the feasible set,

$$F = \left\{ \underline{z} \in \mathbb{R}^P \mid f^j(\underline{z}) \leq 0, j \in J_m ; g^j(\underline{z}) \leq 0, j \in J_\ell \right\}$$

The interval T is discretized into $q+1$ points and is denoted by T_q

Define

$$\tilde{\psi}_q(\underline{z}) = \max \left\{ \phi^j(\underline{z}, t), j \in J_m, t \in T_q; g^j(\underline{z}), j \in J_\ell \right\}$$

$$\psi_q(\underline{z}) = \max \left\{ 0, \tilde{\psi}_q(\underline{z}) \right\}$$

Note that, if $\underline{z} \in F$, then $\psi_q(\underline{z}) = 0$.

Define the " ϵ -active constraint" points

$$\tilde{T}_{q,\epsilon}^j(\underline{z}) = \left\{ t \in T_q \mid \phi^j(\underline{z}, t) - \psi_q(\underline{z}) \geq -\epsilon \right\}, j \in J_m.$$

Now define the "intervals"

$$I_{q,\epsilon,k}^j(\underline{z}) \subset \tilde{T}_{q,\epsilon}^j(\underline{z}) \quad k = 1, 2, \dots, k_{q,\epsilon}^j(\underline{z}), j \in J_m,$$

recursively, as follows.

To define the first interval, $I_{q,\epsilon,1}^j(\underline{z})$, let t_1 be the smallest number in $\tilde{T}_{q,\epsilon}^j(\underline{z})$ and let n_1 be the largest integer such that

$$\left(t_1 + n_1 \Delta t\right) \in \tilde{T}_{q,\varepsilon}^j(\underline{z}), \text{ but } \left(t_1 + (n_1 + 1) \Delta t\right) \notin \tilde{T}_{q,\varepsilon}^j(\underline{z})$$

where

$$\Delta t = (t_f - t_0)/q.$$

Then

$$I_{q,\varepsilon,1}^j = \left\{ t_1, t_1 + \Delta t, t_1 + 2 \Delta t, \dots, t_1 + n_1 \Delta t \right\}.$$

Next suppose that $I_{q,\varepsilon,k}^j(\underline{z})$ have been defined for $k = 1, 2, \dots, k_1$, then

$I_{q,\varepsilon,(k_1+1)}^j(\underline{z})$ are defined as follows. Let $t_{k_1+1} \in \tilde{T}_{q,\varepsilon}^j(\underline{z})$ be the smallest number such that

$$t_{k_1+1} \notin \bigcup_{k=1}^{k_1} I_{q,\varepsilon,k}^j(\underline{z}),$$

and let n_{k_1+1} be the largest integer such that

$$\left(t_{k_1+1} + n_{k_1+1} \Delta t\right) \in \tilde{T}_{q,\varepsilon}^j(\underline{z}) \text{ but } \left(t_{k_1+1} + (n_{k_1+1} + 1) \Delta t\right) \notin \tilde{T}_{q,\varepsilon}^j(\underline{z})$$

Then define

$$I_{q,\varepsilon,(k_1+1)}^j(\underline{z}) = \left\{ t_{k_1+1}, t_{k_1+1} + \Delta t, t_{k_1+1} + 2 \Delta t, \dots, t_{k_1+1} + n_{k_1+1} \Delta t \right\},$$

and define

$$K_{q,\varepsilon}^j(\underline{z}) = \left\{ 1, 2, \dots, k_{q,\varepsilon}^j(\underline{z}) \right\}.$$

Note that

$$\tilde{T}_{q,\varepsilon}^j(\underline{z}) = \bigcup_{k \in K_{q,\varepsilon}^j(\underline{z})} I_{q,\varepsilon,k}^j(\underline{z}).$$

Next, define the "local maximum points"

$$t_{q,\varepsilon,k}^j(\underline{z}) \text{ of } I_{q,\varepsilon,k}^j, \quad k \in K_{q,\varepsilon}^j(\underline{z})$$

as follows.

$$t_{q,\varepsilon,k}^j(\underline{z}) = \left\{ t^* \in I_{q,\varepsilon,k}^j \mid \phi^j(\underline{z}, t^*) \geq \phi^j(\underline{z}, t), \quad t \in I_{q,\varepsilon,k}^j \right\}, \quad j \in J_m$$

and the local maximum ε -active constraint points set is defined

$$\text{as } T_{q,\varepsilon}^j(\underline{z}) = \bigcup_{k \in K_{q,\varepsilon}^j(\underline{z})} t_{q,\varepsilon,k}^j(\underline{z})$$

The " ε -active constraint index" sets are defined as

$$J_{\varepsilon,q}^\phi(\underline{z}) = \left\{ (j,t) \mid \phi^j(\underline{z}, t) - \psi_q(\underline{z}) \geq -\varepsilon, \quad j \in J_m, \quad t \in T_{q,\varepsilon}^j(\underline{z}) \right\}$$

$$J_\varepsilon^g(\underline{z}) = \left\{ j \mid g^j(\underline{z}) - \psi_g(\underline{z}) \geq -\varepsilon, \quad j \in J_\ell \right\}$$

The optimality function for the NLP is defined by

$$\theta_{\varepsilon,q}; \quad \mathbb{R}^P \rightarrow \mathbb{R},$$

where for any

$$\varepsilon \geq 0, \quad \gamma \geq 1, \quad q > 0$$

$$\theta_{\varepsilon,q}(\underline{z}) = \min_{\underline{h} \in \mathbb{R}^P} \left[\frac{1}{2} \|\underline{h}\|^2 + \max \left\{ \langle \nabla f^0, \underline{h} \rangle - \gamma \psi_q(\underline{z}); \right. \right. \\ \left. \left. \langle \nabla g^j(\underline{z}), \underline{h} \rangle, \quad j \in J_\varepsilon^g(\underline{z}); \right. \right. \\ \left. \left. \langle \nabla_z \phi^j(\underline{z}, t), \underline{h} \rangle, \quad (j,t) \in J_{\varepsilon,q}^\phi(\underline{z}) \right\} \right] \quad (4.3.2)$$

and in the dual form

$$\theta_{\varepsilon,q}(\underline{z}) = \max_{\mu \geq 0} \left[-\frac{1}{2} \left\| \sum_{j \in J_\varepsilon^g(\underline{z})} \mu_g^j \nabla_g^j(\underline{z}) + \sum_{(j,t) \in J_{\varepsilon,q}^\phi(\underline{z})} \mu_\phi^j \nabla_z \phi^j(\underline{z}, t) \right. \right. \\ \left. \left. + \mu^0 \|\nabla f^0(\underline{z})\|^2 + \gamma \mu^0 \psi_q(\underline{z}) \mid \sum_{j \in J_\varepsilon^g(\underline{z})} \mu_g^j + \sum_{j \in J_{\varepsilon,q}^\phi(\underline{z})} \mu_\phi^j + \mu^0 = 1 \right. \right] \\ \dots (4.3.3)$$

$$- \underline{h}_{\varepsilon, q}(\underline{z}) = \sum_{j \in J_{\varepsilon}^g(\underline{z})} \mu_g^j \nabla_g^j(\underline{z}) + \sum_{(j, t) \in J_{\varepsilon, q}^{\phi}(\underline{z})} \mu_{\phi}^j \nabla_z \phi^j(\underline{z}, t) + \mu^0 \nabla f^0(\underline{z}), \quad (4.3.4)$$

where

$\| \cdot \|$ denotes the Euclidean norm in \mathbb{R}^P and is defined by

$$\| \underline{x} \| = \sqrt{\langle \underline{x}, \underline{x} \rangle}$$

$\langle \cdot, \cdot \rangle$ denotes the scalar product in \mathbb{R}^P and is defined by

$$\langle \underline{x}, \underline{y} \rangle = \sum_{i=1}^P x_i y_i.$$

$\nabla f(\underline{z})$ denotes the gradient of the function $f : \mathbb{R}^P \rightarrow \mathbb{R}$ at \underline{z} . The gradient vector is treated as a column vector.

THEOREM

If $\hat{\underline{z}}$ is optimal for NLP (4.3.1), then $\theta_{0, q}(\hat{\underline{z}}) = 0$.

An implementable form of the feasible directions algorithm can now be presented.

ALGORITHM

DATA: $\alpha \in (0, 1)$, $\beta \in (0, 1)$, $\gamma \geq 1$

$\delta \in (0, 1]$, $\varepsilon_0 > 0$

$\mu_1 > 0$, $\mu_2 > 0$, $M > 0$

$q_0 > 0$, $q_{\max} \geq q_0$, $z_0 \in \mathbb{R}^P$.

STEP 0: Set $i = 0$, $q = q_0$

STEP 1: Set $\varepsilon = \varepsilon_0$

STEP 2: Compute $(\theta_{\varepsilon, q}(\underline{z}_i), \underline{h}_{\varepsilon, q}(\underline{z}_i))$ by solving (4.3.3) and (4.3.4)

STEP 3: If $\theta_{\varepsilon, q}(\underline{z}_i) \leq -2\varepsilon\delta$, go to step 6; Else set $\varepsilon = \varepsilon/2$ and go to step 4.

STEP 4: If $\varepsilon < \varepsilon_0 \frac{\mu_1}{q}$ and $\psi_q(\underline{z}_i) < \frac{\mu_2}{q}$, Set $q = 2q$ and go to step 5; Else go to step 2.

STEP 5: If $q > q_{\max}$, STOP; Else go to step 1.

STEP 6: Compute the smallest integer $k(\underline{z}_i)$ in $\lambda(\underline{z}_i) \in (0, \hat{M}]$ with $\lambda(\underline{z}_i) = \beta^k(\underline{z}_i)$ and $\hat{M} = \max \left\{ 1, \frac{M}{\|h_{\varepsilon, q}(\underline{z}_i)\|_{\infty}} \right\}$ such that

(i) if $\underline{z}_i \in F^c$ (the complement of F in \mathbb{R}^P)

$$\psi_q\left(\underline{z}_i + \lambda(\underline{z}_i) h_{\varepsilon, q}(\underline{z}_i)\right) - \psi_q(\underline{z}_i) \leq -\alpha \lambda(\underline{z}_i) \delta \varepsilon,$$

(ii) if $\underline{z}_i \in F$

$$f^0\left(\underline{z}_i + \lambda(\underline{z}_i) h_{\varepsilon, q}(\underline{z}_i)\right) - f^0(\underline{z}_i) \leq -\alpha \lambda(\underline{z}_i) \delta \varepsilon$$

$$g^j\left(\underline{z}_i + \lambda(\underline{z}_i) h_{\varepsilon, q}(\underline{z}_i)\right) \leq 0 \quad j \in J_{\ell}$$

$$\phi^j\left(\underline{z}_i + \lambda(\underline{z}_i) h_{\varepsilon, q}(\underline{z}_i), t\right) \leq 0 \quad j \in J_m$$

$$t \in T_q.$$

STEP 7: Set $\underline{z}_{i+1} = \underline{z}_i + \lambda(\underline{z}_i) h_{\varepsilon, q}(\underline{z}_i)$. Set $i = i+1$ and go to step 2.

REMARK

The algorithm as presented above does not require an initial feasible point. If $\underline{z}_0 \notin F$, then $\psi_q(\underline{z}_0)$ is non-zero and the algorithm constructs a sequence of points which forces the design into the feasible domain. This aspect of the algorithm is very advantageous in the case of complicated problems where the choice of an initial feasible point is not obvious, e.g., in earthquake resistant design if the relative drift of a particular story in a framed structure is to be

limited to a certain value, it is not easy to find an initial design that will satisfy that requirement. Of course, the algorithm is more efficient if one can find an initial feasible point.

EXPLANATION OF THE ALGORITHM

The algorithm has two distinct phases. First, a feasible direction is computed by solving equations (4.3.3) and (4.3.4), then a step is taken in this direction in such a way that the objective function is reduced and none of the constraints is violated.

Direction finding subproblem

As noted, a feasible direction is found by first solving the problem

$$\theta_{\epsilon, q}(\underline{z}) = \max_{\underline{\mu} \geq 0} \left[-\frac{1}{2} \left\| \sum_{j \in J_{\epsilon}^g}(\underline{z}) \mu_g^j \nabla g^j(\underline{z}) + \sum_{(j,t) \in J_{\epsilon, q}^{\phi}(\underline{z})} \mu_{\phi}^j \nabla_z \phi^j(\underline{z}, t) + \mu_0 \nabla f^0(\underline{z}) \right\|^2 + \gamma \mu_0 \psi_q(\underline{z}) \right] \left[\sum_{j \in J_{\epsilon}^g}(\underline{z}) \mu_g^j + \sum_{(j,t) \in J_{\epsilon, q}^{\phi}(\underline{z})} \mu_{\phi}^j + \mu_0 = 1 \right] \quad (4.3.3)$$

and then computing the direction from

$$-\underline{h}_{\epsilon, q}(\underline{z}) = \sum_{j \in J_{\epsilon}^g}(\underline{z}) \mu_g^j \nabla g^j(\underline{z}) + \sum_{(j,t) \in J_{\epsilon, q}^{\phi}(\underline{z})} \mu_{\phi}^j \nabla_z \phi^j(\underline{z}, t) + \mu_0 \nabla f^0(\underline{z}) \quad (4.3.4)$$

Equation (4.3.3) can be transcribed into a standard quadratic programming problem as follows. Let $k_g(\underline{z})$ be the total number of points in $J_{\epsilon}^g(\underline{z})$ and $k_{\phi}(\underline{z})$ be the total number of points in $J_{\epsilon, q}^{\phi}(\underline{z})$.

Define the vector

$$\underline{\mu} \in \mathbb{R}^{1 + k_g(\underline{z}) + k_{\phi}(\underline{z})}$$

as follows:

$$\underline{\mu}^T = \left[\mu_0, \mu_g^1, \mu_g^2, \dots, \mu_g^{k_g}, \mu_\phi^1, \dots, \mu_\phi^{k_\phi} \right].$$

Define the matrix

$$\underline{A} \in \mathbb{R}^{1 + k_g(\underline{z}) + k_\phi(\underline{z}) \times \mathbb{R}^P}$$

as

$$\underline{A} = \begin{bmatrix} [\nabla f^0(\underline{z})]^T \\ [\nabla g^1(\underline{z})]^T \\ \vdots \\ [\nabla g^{k_g}(\underline{z})]^T \\ [\nabla_z \phi^1(\underline{z}, t_{q,\epsilon,1}^1)]^T \\ \vdots \\ [\nabla_z \phi^{k_\phi}(\underline{z}, t_{q,\epsilon,k_\phi}^k)]^T \end{bmatrix}.$$

Then Eq. (4.3.3) can be written as

$$\max_{\underline{\mu} \geq 0} \left\{ -\frac{1}{2} (\underline{\mu}^T \underline{A}) (\underline{\mu}^T \underline{A})^T + \gamma \mu_0 \psi_q(\underline{z}) \mid \sum_{j=0}^{1+k_g+k_\phi} \mu^j = 1 \right\}$$

or

$$\min_{\underline{\mu} \geq 0} \left\{ \frac{1}{2} \underline{\mu}^T \underline{A} \underline{A}^T \underline{\mu} - \gamma \mu_0 \psi_g(\underline{z}) \mid \sum_{j=0}^{1+k_g+k_\phi} \mu^j = 1 \right\}. \quad (4.3.5)$$

Define a vector

$$\underline{D} \in \mathbb{R}^{1 + k_g(\underline{z}) + k_\phi(\underline{z})}$$

such that

$$\underline{D}^T = -\left[\gamma \psi_g(\underline{z}), 0, 0, \dots \right]$$

and a matrix

$$\underline{Q} \in \mathbb{R}^{1+k_g(\underline{z})+k_\phi(\underline{z})} \times \mathbb{R}^{1+k_g(\underline{z})+k_\phi(\underline{z})}$$

such that

$$\underline{Q} = \underline{A} \underline{A}^T.$$

Then Eq. (4.3.5) can be written as

$$\min_{\underline{\mu} > 0} \left\{ \frac{1}{2} \underline{\mu}^T \underline{Q} \underline{\mu} + \underline{D}^T \underline{\mu} \mid \sum_{j=1}^{1+k_g(\underline{z})+k_\phi(\underline{z})} \mu^j = 1 \right\} \quad (4.3.6)$$

which is a standard quadratic programming problem. Once the μ 's are obtained, the direction is computed from

$$- \underline{h}_{-\varepsilon, q}(\underline{z}) = \underline{\mu}^T \underline{A} \quad (4.3.7)$$

Computational Considerations

The quadratic programming problem (QP) as formulated in Eq. (4.3.6) may be computationally ill-posed because of different magnitudes of the gradients of different functions. Proper scaling of these gradients is therefore essential to make the problem computationally efficient. In the present version the following scaling was used.

Define

$$\begin{aligned} s_g^j &= \|\nabla g^j(\underline{z})\|_\infty, \quad j \in J_\varepsilon^g(\underline{z}); \\ s_\phi^j &= \|\nabla_z \phi^j(\underline{z}, t)\|_\infty, \quad (j, t) \in J_{\varepsilon, q}^\phi(\underline{z}); \\ s_0 &= \|\nabla f^0(\underline{z})\|_\infty \end{aligned} \quad (4.3.8)$$

where

$\|\cdot\|_\infty$ is the maximum norm in \mathbb{R}^P defined by

$$\|\underline{x}\|_\infty = \max_{i \in \mathbb{R}^P} |x_i|$$

Define

$$\tilde{s} = \max \left\{ s_0 ; s_g^j , j \in J_\varepsilon^g(\underline{z}) ; s_\phi^j , j \in J_{\varepsilon,q}^\phi(\underline{z}) \right\}.$$

Define a vector

$$\underline{R} \in \mathbb{R}^{1 + k_g(\underline{z}) + k_\phi(\underline{z})}$$

as

$$\underline{R} = \begin{bmatrix} \tilde{s}/s_0 \\ \eta \tilde{s}/s_g^1 \\ \eta \tilde{s}/s_g^2 \\ \vdots \\ \eta \tilde{s}/s_g^{k_g(\underline{z})} \\ \eta \tilde{s}/s_\phi^1 \\ \vdots \\ \eta \tilde{s}/s_\phi^{k_\phi(\underline{z})} \end{bmatrix} \quad (4.3.9)$$

where $\eta \in \mathbb{R}$ is a parameter which may be adjusted to force the direction vector toward or away from a constraint.

The \underline{A} matrix is scaled as

$$\underline{A} = \begin{bmatrix} \left[\nabla f^0(\underline{z}) \right]^T / s_0 \\ \left[\nabla g^1(\underline{z}) \right]^T / s_g^1 \\ \vdots \\ \left[\nabla g^{k_g(\underline{z})}(\underline{z}) \right]^T / s_g^{k_g(\underline{z})} \\ \left[\nabla_z \phi^1(\underline{z}, t_{q,\varepsilon}^1) \right]^T / s_\phi^1 \\ \vdots \\ \left[\nabla_z \phi^{k_\phi(\underline{z})}(\underline{z}, t_{q,\varepsilon,k_\phi(\underline{z})}) \right]^T / s_\phi^{k_\phi(\underline{z})} \end{bmatrix} \quad (4.3.10)$$

$$\underline{Q} = \underline{A} \underline{A}^T .$$

Then, the scaled version of QP can be written as

$$\min_{\underline{\mu} \geq 0} \left\{ + \frac{1}{2} \underline{\mu}^T \underline{Q} \underline{\mu} + \underline{D}^T \underline{\mu} \mid \underline{R}^T \underline{\mu} = 1 \right\} \quad (4.3.11)$$

The direction vector is still obtained from Eq. (4.3.7).

Step Length Computation

After a feasible direction is obtained, the next step is to compute the step length in that direction. If the current design is inside the feasible domain, the step length should be chosen in such a way that there is a maximum reduction in the objective function, while still maintaining feasibility. When the current design is outside the feasible domain, the objective is to take a step such that the new design is as close to the feasible domain as possible. The step size calculations begin by minimizing the objective function along the feasible direction and then checking whether any of the constraints is violated. If any one of the constraints is violated, the step length is reduced until the new design satisfies all of the constraints. A number of methods are available for this unidirectional search, the most popular among them being Fibonacci search, Newton's method, quadratic or cubic fit, etc. [11,16]. For general non-convex problems, these methods tend to be very expensive. Since computation of the exact minimum along the feasible direction is not absolutely necessary, an approximate line search technique, known as the Armijo step size rule, is often used [11,17]. The method performs only an approximate line search and is quite efficient for general non-convex problems. The method is as follows.

Given the constants $\alpha, \delta, \varepsilon, \beta, M$, current design vector \underline{z}_i , $\underline{h}_{\varepsilon, q}(\underline{z}_i)$ and $\psi_{\varepsilon, q}(\underline{z}_i)$, compute the smallest integer $k(\underline{z}_i)$ in $\lambda(\underline{z}_i) \in (0, \hat{M}]$ with $\lambda(\underline{z}_i) = \beta^k(\underline{z}_i)$ and

$$\hat{M} = \max \left\{ 1, \frac{M}{\|\underline{h}_{\varepsilon, q}(\underline{z}_i)\|_{\infty}} \right\},$$

such that

(i) if $\psi_{\varepsilon, q}(\underline{z}_i) > 0$ (i.e. $\underline{z}_i \notin F$),

$$\text{then } \psi_{\varepsilon, q}(\underline{z}_i + \lambda(\underline{z}_i) \underline{h}_{\varepsilon, q}(\underline{z}_i)) - \psi_{\varepsilon, q}(\underline{z}_i) \leq -\alpha \lambda(\underline{z}_i) \delta \varepsilon;$$

(ii) if $\psi_{\varepsilon, q}(\underline{z}_i) = 0$, i.e. $\underline{z}_i \in F$,

$$\text{then } f^0(\underline{z}_i + \lambda(\underline{z}_i) \underline{h}_{\varepsilon, q}(\underline{z}_i)) - f^0(\underline{z}_i) \leq -\alpha \lambda(\underline{z}_i) \delta \varepsilon,$$

$$g^j(\underline{z}_i + \lambda(\underline{z}_i) \underline{h}_{\varepsilon, q}(\underline{z}_i)) \leq 0 \quad j \in J_{\ell},$$

$$\phi^j(\underline{z}_i + \lambda(\underline{z}_i) \underline{h}_{\varepsilon, q}(\underline{z}_i), t) \leq 0 \quad j \in J_m$$

$$t \in T_q$$

The algorithm to implement the above process is as follows

STEP 1: Set $\lambda = \beta$. Compute $\hat{M} = \max \left\{ 1, \frac{M}{\|\underline{h}_{\varepsilon, q}(\underline{z}_i)\|_{\infty}} \right\}$

Set FLAG = 0. Set n = 0.

STEP 2: Compute $\underline{z}_{-i+1}^n = \underline{z}_i + \lambda \underline{h}_{\varepsilon, q}(\underline{z}_i)$

STEP 3: If $\psi_{\varepsilon, q}(\underline{z}_i) > 0$, go to step 5, Else go to step 4.

STEP 4: Compute $f^0(\underline{z}_{-i+1}^n)$.

If $f^0(\underline{z}_{-i+1}^n) + \alpha \lambda \leq f^0(\underline{z}_i)$, go to step 5

Else go to step 7.

STEP 5: Compute $g^j(\underline{z}_{i+1}^n)$, $j \in J_\ell$
 and $\phi^j(\underline{z}_{i+1}^n, t)$, $j \in J_m$ $t \in T_g$
 If $g^j(\underline{z}_{i+1}^n) \leq 0$, $j \in J_\ell$ and $\phi^j(\underline{z}_{i+1}^n, t) \leq 0$
 $j \in J_m$, $t \in T_g$,
 go to step 6
 Else go to step 7

STEP 6: Set $\lambda = \lambda/\beta$
 If FLAG = - 1 go to step 8
 Else set FLAG = 1, $n = n + 1$ and go to step 2.

STEP 7: Set $\lambda = \lambda \times \beta$
 If FLAG = 1, go to step 8
 Else set FLAG = - 1, $n = n + 1$ and go to step 2.

STEP 8: Set $\lambda = \lambda^*$ and the new design vector is

$$\underline{z}_{i+1} = \underline{z}_i + \lambda^* \underline{h}_{\epsilon, q}(\underline{z}_i).$$

4.4 Computational Considerations

As is clear from the previous section, the feasible directions algorithm requires computation of constraint functions and gradients of "active" constraint functions at each iteration. The computation of conventional inequality constraints (functions 'g' in the previous section) and their gradients presents no great difficulty. The functional constraints (functions 'phi' in the previous section), however, are very expensive to compute because they require the computation of the time history of response of the structure, which for a nonlinear

system is not a trivial matter. The problem becomes even more complicated because the algorithm requires computation of the gradients of the functional constraints, which in turn, require sensitivity analysis, i.e., computation of gradients of the response quantities with respect to the design parameters. The structural response equations, in their state-space formulation, can be differentiated with respect to design parameters, using the chain rule, to obtain differential equations for sensitivity analysis [18,19]. Numerical integration of the sensitivity equations then gives the required gradients of the response quantities. For a nonlinear system of the type considered here the analytical form of the sensitivity equations becomes quite complicated, so that the direct finite difference scheme of computing these derivatives seems to be more appropriate. The finite difference scheme requires an additional p time history analyses, where p is the total number of design parameters. Thus, computation of functional constraints and their gradients requires $p + 1$ time history analyses of an "N" degree of freedom nonlinear system, clearly a major computational task. Therefore, any reduction in the number of times that these calculations are executed will significantly reduce the total computational cost.

In the actual implementation of the algorithm for the type of problem under consideration a number of things can be done to reduce the computational cost. The most obvious is to make the integration of response equations as efficient as possible. This is done by exploiting the localized nonlinear nature of the problem, using substructuring techniques. An efficient Newmark method with optional Newton-Raphson iteration is used to carry out numerical integration of the equations of motion. Provision is made in the program to do the

structural and/or sensitivity analysis only if the design parameters are changed "appreciably". Thus, if at a particular iteration, design parameters are changed very little, so that the maximum difference between the new and old design parameters is less than a certain prescribed value, the program does not compute the new time history analysis, instead, it uses the previous values.

A closer look at the algorithm shows that, when none of the functional constraints is active, gradients of the response quantities are not needed. In the program, therefore, constraint functions are first computed and then checked to determine if any of the constraints is active. If none of the constraints is active, the sensitivity analysis part is skipped, resulting in a significant saving in computation. Another source of considerable savings is the observation that gradients of response quantities are required only at those times included in the ϵ -active constraint set defined in the previous section. In earthquake problems structural response typically builds up slowly and then dies down, whence the ϵ -active times are for the most part much smaller than the total duration of the response time history. Therefore, when performing sensitivity analysis it is not necessary to compute the response time history beyond the maximum time included in the ϵ -active set. This feature has been incorporated into the program.

5. APPLICATIONS

The general techniques described in the previous sections have been applied to the three-story steel test frame described in Section 2. This section describes the formulation of the mathematical model for the test structure and presents numerical results for several design problems.

5.1 Structural System

The structural system chosen for numerical studies consists of a three-story, single bay steel frame as shown in Fig. 12. The bottom floor is supported on rubber bearings and an energy absorbing device attached to the frame at that level in such a way that the device exerts a horizontal force on the frame.

If axial deformations in beams and columns are neglected, the frame has 12 degrees of freedom as shown in Fig. 13. The 12 x 12 stiffness matrix (\tilde{K}^E , in Eq. (3.2.1)) for a single frame is shown in Table 1.

Since the masses are assumed to be lumped at the floor levels, the 12 x 12 stiffness matrix can be condensed to a 4 x 4 matrix with respect to lateral degrees of freedom only, as explained in Section 3. The condensed stiffness matrix for the frame (matrix K^E in Eq. (3.2.2)) is

$$\begin{bmatrix} 23.19 & -33.32 & 11.52 & -1.39 \\ & 72.20 & -48.25 & 9.37 \\ \text{SYMMETRIC} & & 61.22 & -24.49 \\ & & & 16.51 \end{bmatrix} .$$

TABLE 1

58.81	-58.81	0	0	-940.90	-940.90	-940.90	-940.90	0	0	0	0	0
	117.61	-58.81	0	940.90	940.90	0	0	-940.90	-940.90	0	0	0
		81.82	-23.01	0	0	940.90	940.90	437.53	437.53	-503.37	-503.37	-503.37
			23.01	0	0	0	0	503.37	503.37	503.37	503.37	503.37
				57658.3	8756.67	20072.5	20072.5	0	0	0	0	0
					57658.3	0	20072.5	0	0	0	0	0
						97803.3	8756.67	20072.5	0	0	0	0
							97803.3	0	20072.5	0	0	0
								87021.5	8756.67	14681.6	14681.6	0
									87021.5	0	14681.6	14681.6
										253748.0	112192.0	112192.0
												253748.0

[Units are kip-inches]

Thus, the lateral stiffness matrix of the complete structure, including the stiffness of rubber bearings at 1.2 kip/in is

$$\underline{K}^E = \begin{bmatrix} 46.38 & -66.64 & 23.04 & -2.78 \\ & 144.40 & -96.50 & 18.74 \\ \text{SYMMETRIC} & & 122.43 & -48.97 \\ & & & 34.21 \end{bmatrix}$$

The mass matrix of the structure corresponding to the lateral degrees of freedom is

$$\underline{M} = \begin{bmatrix} 0.02438 & & & \\ & 0.02438 & & \\ & & 0.02514 & \\ & & & 0.02832 \end{bmatrix}.$$

Rayleigh damping is assumed in constructing the damping matrix

$$\underline{C} = \alpha \underline{M} + \beta \underline{K}^E.$$

The coefficients α and β are computed from

$$\begin{bmatrix} \frac{1}{\omega_1} & \omega_1 \\ \frac{1}{\omega_2} & \omega_2 \end{bmatrix} \begin{Bmatrix} \alpha \\ \beta \end{Bmatrix} = \begin{Bmatrix} \xi_1 \\ \xi_2 \end{Bmatrix},$$

where ω_1 and ω_2 are first and second mode frequencies, and ξ_1 and ξ_2 are the respective critical damping ratios in these modes. The damping matrix for the present structure, assuming $\xi_1 = 3\%$ and $\xi_2 = 1\%$, is given below.

$$\underline{C} = \begin{bmatrix} .0279 & -.0332 & .0115 & -.0014 \\ & .0768 & -.0481 & .0093 \\ & & .0660 & -.0244 \\ \text{SYMMETRIC} & & & .0226 \end{bmatrix}.$$

5.2 Equations of Motion

The equations of motion expressed in terms of lateral degrees of freedom of the structure can be written as

$$\underline{M} \ddot{\underline{U}} + \underline{C} \dot{\underline{U}} + \underline{K}^E \underline{U} + \underline{F} = - \underline{M} \underline{e} \ddot{U}_g(t)$$

where \underline{M} , \underline{C} and \underline{K}^E are given in the previous section and

$$\underline{U}^T = [U_1, U_2, U_3, U_4]$$

$$\underline{F}^T = [0, 0, 0, F_4^N]$$

$$\underline{e}^T = [1, 1, 1, 1]$$

$$F_4^N = \text{force in the energy absorbing device, whose}$$

constitutive equations are

$$\dot{F}_4^N = K_0 \left[\dot{U}_4(t) - |\dot{U}_4(t)| \left(\frac{F_4^N(t)}{F_0} - S \right)^n \right]$$

$$S(t) = \alpha \left[\frac{U_4(t)}{U_0} - \frac{F_4(t)}{F_0} \right].$$

These equations are integrated using the numerical techniques given in Section 3.3.

5.3 Design Parameters

It is assumed here that the characteristics of the rubber bearings are fixed. Therefore, only the energy absorbing device will

be adjusted to obtain the optimal design. The two basic variables in the design of energy absorbers are the elastic stiffness and the post-yield stiffness. These variables are controlled by the parameters F_0 , U_0 and α in the hysteretic model of the energy absorbers. The elastic stiffness is approximately equal to F_0/U_0 and the post-yield stiffness is approximately equal to $\frac{F_0}{U_0} \left(\frac{\alpha}{1+\alpha} \right)$. Thus, the design variables are F_0 , U_0 and α . Another parameter which may influence the design is the exponent "n" in the hysteretic model, but it is not considered as a variable in the present study.

5.4 Optimal Design Problems

The purpose of an earthquake isolation system is to minimize some measure of the response of the structure. There are a number of response quantities which could be minimized, e.g., the maximum acceleration in the structure, maximum base shear, maximum story shear, maximum inter-story drift, etc. In order to get meaningful results, response constraints are also needed. Some of the constraints are dictated by the problem itself, e.g., the design parameters F_0 , U_0 and α are not allowed to attain negative values. Such constraints constitute what are known as conventional inequality constraints. Constraints on the response quantities are also needed; e.g., when accelerations in the frame are minimized, the displacements at the base must not be arbitrarily large. These restrictions give rise to functional inequality constraints. Thus, a number of design problems could be formulated depending upon the objective function and the type of constraints placed on the response. In what follows several design problems of interest are considered.

Design Problem 1

In this problem, the top story shear is minimized while maintaining the bottom floor displacement within a prescribed limit.

Mathematically, this problem can be expressed as

$$\min_{\underline{z}} \left[\max_{t \in T} \left\{ K_1 \left(U_1(\underline{z}, t) - U_2(\underline{z}, t) \right)^2 \right\} \right]$$

subject to

$$\max_{t \in T} \left(U_4(\underline{z}, t) \right)^2 \leq \delta^2$$

where

K_1 = top story lateral stiffness,

U_1 , U_2 and U_4 = top, second and bottom floor displacements, respectively,

T = $[t_0, t_f]$, the time interval of interest

δ = prescribed limit on U_4 ,

\underline{z}^T = $[z^1, z^2, z^3] = [F_0, U_0, \alpha]$.

As explained in Section 3.2, the problem can be transcribed into a mathematical programming problem, as follows.

The parameter vector \underline{z} is augmented by a dummy cost parameter z^4 and the above problem is then equivalent to the problem

$$\min_{\underline{z}} z^4$$

subject to

$$\max_{t \in T} \left\{ K_1 \left(U_1(\underline{z}, t) - U_2(\underline{z}, t) \right)^2 \right\} \leq z^4,$$

and

$$\max_{t \in T} \left[U_4(\underline{z}, t) \right]^2 \leq \delta^2$$

$$F_0, U_0, \alpha > 0.$$

In terms of the nonlinear programming problem in canonical form, Section 4.2, equation (4.2.1), the above problem is expressed as

$$f^0(\underline{z}) = z^4$$

$$\nabla f^0(\underline{z}) = [0, 0, 0, 1]^T$$

$$\phi^1(\underline{z}, t) = \frac{K_1}{z^4} \left[\left(U_1(\underline{z}, t) - U_2(\underline{z}, t) \right)^2 \right] - 1.0$$

$$\nabla_{\underline{z}} \phi^1(\underline{z}, t) = \begin{bmatrix} \frac{2K_1}{z^4} \left(U_1(\underline{z}, t) - U_2(\underline{z}, t) \right) \left(\frac{\partial U_1(\underline{z}, t)}{\partial z^1} - \frac{\partial U_2(\underline{z}, t)}{\partial z^1} \right) \\ \frac{2K_1}{z^4} \left(U_1(\underline{z}, t) - U_2(\underline{z}, t) \right) \left(\frac{\partial U_1(\underline{z}, t)}{\partial z^2} - \frac{\partial U_2(\underline{z}, t)}{\partial z^2} \right) \\ \frac{2K_1}{z^4} \left(U_1(\underline{z}, t) - U_2(\underline{z}, t) \right) \left(\frac{\partial U_1(\underline{z}, t)}{\partial z^3} - \frac{\partial U_2(\underline{z}, t)}{\partial z^3} \right) \\ - \frac{K_1}{(z^4)^2} \left(U_1(\underline{z}, t) - U_2(\underline{z}, t) \right)^2 \end{bmatrix}$$

$$\phi^2(\underline{z}, t) = \frac{1}{\delta^2} \left(U_4(\underline{z}, t) \right)^2 - 1.0$$

$$\nabla_{\underline{z}} \phi^2(\underline{z}, t) = \begin{bmatrix} \frac{2}{\delta^2} U_4(\underline{z}, t) & \frac{\partial U_4(\underline{z}, t)}{\partial z^1} \\ \frac{2}{\delta^2} U_4(\underline{z}, t) & \frac{\partial U_4(\underline{z}, t)}{\partial z^2} \\ \frac{2}{\delta^2} U_4(\underline{z}, t) & \frac{\partial U_4(\underline{z}, t)}{\partial z^3} \\ 0 & \end{bmatrix}$$

$$g_1(\underline{z}) = -0.2 z^1 + 1.0 \text{ E-5}$$

$$g_2(\underline{z}) = -10 z^2 + 1.0 \text{ E-5}$$

$$g_3(\underline{z}) = -20 z^3 + 1.0 \text{ E-5}$$

$$\nabla g(\underline{z}) = \begin{bmatrix} -0.2 & 0 & 0 \\ 0 & -10 & 0 \\ 0 & 0 & -20 \\ 0 & 0 & 0 \end{bmatrix}$$

The factors 0.2, 10 and 20 in the above expressions are used to obtain an initial scaling of all constraints to a value of 1.

RESULTS

A computer program based on algorithms presented in Sections 3 and 4 was used to solve the above design problem. The initial values of parameters were obtained from experimental data on the energy absorbing devices [2,4]. The following parameters were used:

$$F_0 = 5.0, \quad U_0 = 0.11, \quad \alpha = 0.064, \quad n = 1.$$

The upper limit on U_4 , i.e. δ was equal to 4 inches. The dummy cost parameter z^4 is the upper bound on the maximum shear in the top story. The initial value for z^4 was 2.22.

The Parkfield N65°E (1966) earthquake, with amplitude and time scaling as used in the experimental program [5] was used to excite the system. This accelerogram is shown in Fig. 14. The optimum parameters obtained are

$$F_0 = 3.5185 \quad U_0 = 0.07782 \quad \alpha = 0.07165 \quad n = 1$$

$$z^4 = 1.53094$$

Figure 15 shows the decrease in cost parameter as a function of iteration number. The percentage reduction in the dummy cost parameter is about 31%, which means that the relative story drift at the top story has been reduced by about this much. To see the effect of these new design parameters on overall structure response, the system was analysed with the new energy absorbing device parameters, and inter-story shear-time histories at all three floors were plotted along with the initial shear-time histories. These plots, which are shown in Figs. 18-20, show clearly that the local peak shears are reduced throughout the time history. The base displacement time histories is also plotted for initial and optimal parameters in Fig. 21. As expected the base displacements are increased with the optimal design parameters indicating that the optimal system is softer at the base than the original system. The elastic stiffness is reduced from 45.5 to 45.22 and the post yield stiffness is reduced from 10% to 6.6% of the elastic stiffness. Since the earthquake used was not strong enough to cause extensive nonlinearity in the energy absorbing device, the change in stiffness is not significant. It is expected (as shown

later by design example 2) that a strong earthquake would produce significant changes in these stiffnesses.

Hysteresis loops in the energy absorber are also plotted in Fig. 16, 17. The loops show that, except for a few large inelastic excursions, the energy absorbers remain in their elastic range and therefore there is no significant energy absorption in the energy absorbers.

Design Problem 2

This problem consists of minimizing the total shear at the bottom floor level subject to the condition that the maximum displacement in the bottom floor is less than a certain prescribed value, δ .

Mathematically we have

$$\min_{\underline{z}} \left[\max_{t \in T} \left\{ \left(K_1 (U_1(\underline{z}, t) - U_2(\underline{z}, t)) \right)^2 + \left(K_2 (U_2(\underline{z}, t) - U_3(\underline{z}, t)) \right)^2 + \left(K_3 (U_3(\underline{z}, t) - U_4(\underline{z}, t)) \right)^2 \right\} \right]$$

subject to

$$\max_{t \in T} (U_4(\underline{z}, t))^2 \leq \delta^2,$$

$$F_0, U_0, \alpha > 0$$

$$T = [t_0, t_f]$$

$$\underline{z}^T = [z^1, z^2, z^3] = [F_0, U_0, \alpha]$$

K_1, K_2, K_3 = the story stiffnesses (top down),

U_1, U_2, U_3, U_4 = displacement response histories at the floor levels (top down).

δ = prescribed limit on the bottom floor displacement, selected to be 4 inches in the present problem.

The equivalent nonlinear programming problem, is

$$\min_{\underline{z}} z^4$$

subject to

$$\max_{t \in T} \left[\left\{ K_1 (U_1(\underline{z}, t) - U_2(\underline{z}, t)) \right\}^2 + \left\{ K_2 (U_2(\underline{z}, t) - U_3(\underline{z}, t)) \right\}^2 + \left\{ K_3 (U_3(\underline{z}, t) - U_4(\underline{z}, t)) \right\}^2 \right] \leq z^4$$

$$\max_{t \in T} [U_4(\underline{z}, t)]^2 \leq \delta^2$$

$$F_0, U_0, \alpha > 0.$$

In terms of the canonical form of NLP given by (4.2.1) we have

$$f^0(\underline{z}) = z^4$$

$$\nabla f^0(\underline{z}) = [0, 0, 0, 1]^T$$

$$\phi^1(\underline{z}, t) = \frac{1}{z^4} \left[\left\{ K_1 (U_1(\underline{z}, t) - U_2(\underline{z}, t)) \right\}^2 + \left\{ K_2 (U_2(\underline{z}, t) - U_3(\underline{z}, t)) \right\}^2 + \left\{ K_3 (U_3(\underline{z}, t) - U_4(\underline{z}, t)) \right\}^2 \right] - 1.0$$

$$\begin{aligned}
\nabla_{\underline{z}} \phi^1(\underline{z}, t) = \frac{2}{z^4} & \left[\begin{aligned}
& K_1^2 (U_1(\underline{z}, t) - U_2(\underline{z}, t)) \left(\frac{\partial U_1(\underline{z}, t)}{\partial z^1} - \frac{\partial U_2(\underline{z}, t)}{\partial z^1} \right) \\
& + K_2^2 (U_2(\underline{z}, t) - U_3(\underline{z}, t)) \left(\frac{\partial U_2(\underline{z}, t)}{\partial z^1} - \frac{\partial U_3(\underline{z}, t)}{\partial z^1} \right) \\
& + K_3^2 (U_3(\underline{z}, t) - U_4(\underline{z}, t)) \left(\frac{\partial U_3(\underline{z}, t)}{\partial z^1} - \frac{\partial U_4(\underline{z}, t)}{\partial z^1} \right) \\
& K_1^2 (U_1(\underline{z}, t) - U_2(\underline{z}, t)) \left(\frac{\partial U_1(\underline{z}, t)}{\partial z^2} - \frac{\partial U_2(\underline{z}, t)}{\partial z^2} \right) \\
& + K_2^2 (U_2(\underline{z}, t) - U_3(\underline{z}, t)) \left(\frac{\partial U_2(\underline{z}, t)}{\partial z^2} - \frac{\partial U_3(\underline{z}, t)}{\partial z^2} \right) \\
& + K_3^2 (U_3(\underline{z}, t) - U_4(\underline{z}, t)) \left(\frac{\partial U_3(\underline{z}, t)}{\partial z^2} - \frac{\partial U_4(\underline{z}, t)}{\partial z^2} \right) \\
& K_1^2 (U_1(\underline{z}, t) - U_2(\underline{z}, t)) \left(\frac{\partial U_1(\underline{z}, t)}{\partial z^3} - \frac{\partial U_2(\underline{z}, t)}{\partial z^3} \right) \\
& + K_2^2 (U_2(\underline{z}, t) - U_3(\underline{z}, t)) \left(\frac{\partial U_2(\underline{z}, t)}{\partial z^3} - \frac{\partial U_3(\underline{z}, t)}{\partial z^3} \right) \\
& + K_3^2 (U_3(\underline{z}, t) - U_4(\underline{z}, t)) \left(\frac{\partial U_3(\underline{z}, t)}{\partial z^3} - \frac{\partial U_4(\underline{z}, t)}{\partial z^3} \right) \\
& - \frac{1}{2z^4} \left[\left\{ K_1 (U_1(\underline{z}, t) - U_2(\underline{z}, t)) \right\}^2 \right. \\
& + \left\{ K_2 (U_2(\underline{z}, t) - U_3(\underline{z}, t)) \right\}^2 \\
& \left. + \left\{ K_3 (U_3(\underline{z}, t) - U_4(\underline{z}, t)) \right\}^2 \right]
\end{aligned} \right]
\end{aligned}$$

$$\phi^2(\underline{z}, t) = \frac{1}{\delta^2} (U_4(\underline{z}, t))^2 - 1.0$$

$$\nabla_{\underline{z}} \phi^2(\underline{z}, t) = \begin{bmatrix} \frac{2}{\delta^2} U_4(\underline{z}, t) & \frac{\partial U_4(\underline{z}, t)}{\partial z^1} \\ \frac{2}{\delta^2} U_4(\underline{z}, t) & \frac{\partial U_4(\underline{z}, t)}{\partial z^2} \\ \frac{2}{\delta^2} U_4(\underline{z}, t) & \frac{\partial U_4(\underline{z}, t)}{\partial z^3} \\ 0 \end{bmatrix}$$

$$g_1(\underline{z}) = -0.2 z^1 + 1.0 E-5$$

$$g_2(\underline{z}) = -10 z^2 + 1.0 E-5$$

$$g_3(\underline{z}) = -20 z^3 + 1.0 E-5$$

$$\nabla g(\underline{z}) = \begin{bmatrix} -0.2 & 0 & 0 \\ 0 & -10 & 0 \\ 0 & 0 & -20 \\ 0 & 0 & 0 \end{bmatrix}$$

RESULTS

El Centro 1940 NS ground motion, with modified time scale and amplitude, as used in the experimental investigation [5], was used for this problem. The ground acceleration time history is shown in Fig. 22. This motion is very strong as compared with the Parkfield motion used for problem 1; therefore, considerable inelastic deformations can be expected in the energy absorbers. The initial values of the parameters are the same as those used for the first problem, i.e.

$$F_0 = 5.0, \quad U_0 = 0.11, \quad \alpha = 0.064, \quad n = 1.$$

The dummy cost parameter, z^4 , which is an upper bound on the total shear at the bottom floor level was 35.0.

The optimal parameters obtained are

$$F_0 = 4.2773 \quad U_0 = 1.7529 \quad \alpha = 0.005768 \quad z^4 = 9.1509.$$

Figure 23 shows the plot of the cost parameter vs the iteration number. Story shears, bottom floor displacement and hysteresis loops in the energy absorbers are plotted in Fig. 24-29, for both initial and optimal parameters. The plots of story shears clearly show the effectiveness of the optimal isolation system, which reduces the story shears by as much as half of the values with the initial parameters. Again the bottom floor displacements are increased, although they remain within the allowable limit of 4 inches. Likewise a comparison of the initial and optimal design hysteresis loops in the energy absorbers indicates the effectiveness of a "softer" system.

5.5 Sensitivity of the Optimal Design to Different Earthquake Ground Motions

As is clear from the preceding development, only one earthquake ground motion is used in the optimal design process. Since earthquakes are random in nature, it is unlikely that the same earthquake ground motion will be repeated at some future time. Therefore, it becomes necessary to see the effectiveness of the optimal design process for different earthquakes. To get meaningful results, these additional earthquakes should have characteristics similar to the one used in the design process. This requirement prohibits the use of actual past earthquake records, inasmuch as for a given site there is typically an insufficient number of past records. An alternative is the use of artificially generated earthquakes of the same class.

For the present study a family of five earthquakes having characteristics similar to the El Centro 1940 NS earthquake was generated using the computer program PSEQGN developed by P. Ruiz and J. Penzien [20] and later modified by M. Murakami [21]. The earthquake accelerograms were generated by passing nonstationary shot noise through two second-order linear filters and applying a base line correction. Each accelerogram was of thirty seconds duration with four seconds of parabolic built up, eleven seconds of constant intensity followed by fifteen seconds of exponential decay. The maximum acceleration in each record was about 0.30g. The structure was analyzed twice, with initial and optimal parameters obtained from problem 2, subjected to these five earthquakes. Story shears and bottom floor displacements are compared for the initial and the optimal parameters. The five accelerograms, along with structural response quantities for initial and optimal designs, appear in Figs. 30-34. In all the cases response is considerably reduced in the optimal system, while the base displacement is increased, although remaining within the specified constraint of four inches.

6. CONCLUDING REMARKS

Two of the main objectives of the present research were to study the effectiveness of the feasible directions method for optimal design problems with time dependent constraints and to arrive at an improved earthquake isolation system.

The feasible directions algorithm seems to be quite effective for the types of problems considered. The effectiveness of the algorithm depends, among other things, on a number of parameters which control the convergence and other numerical aspects. Some experience with these parameters is needed before arriving at the most suitable set of parameters for a particular problem. An interactive system, where the user can change these parameters during the optimization process seems to be a more efficient way of handling this situation. At the time of this research no such facilities were available, therefore this aspect has not yet been explored. Access to an interactive system is expected shortly and the work on implementing this algorithm interactively is underway.

The optimal design obtained shows that a softer isolation system, subjected to displacement constraints, is the better design. As pointed out in the Introduction, the softer systems have excessive lateral deflections under small earthquakes and wind excitations. Thus, in order to arrive at a more practical design some additional requirements, limiting the response under small earthquakes, are needed. This aspect is currently being investigated by introducing two levels of constraints, an upper limit on response under large earthquakes and a lower limit on response under small earthquakes. An additional

advantage of this kind of methodology would be that, instead of considering only two earthquakes, a family could be considered, and an optimal design would be achieved for the entire class of records considered.

REFERENCES

1. Mahin, S.A., Bertero, V.V., Chopra, A.K. and Collins, R.G., "Response of the Olive View Hospital Main Building during the San Fernando Earthquake," EERC 76-22, Earthquake Engineering Research Center, U.C. Berkeley, October 1976.
2. Kelly, J.M., Eidingen, J.M. and Derham, C.J., "A Practical Soft Story Earthquake Isolation System," UCB/EERC-77/27, Earthquake Engineering Research Center, U.C. Berkeley, November 1977.
3. Kelly, J.M. and Tsztoo, D.F., "Earthquake Simulation Testing of a Stepping Frame with Energy-Absorbing Devices," UCB/EERC-77/17, Earthquake Engineering Research Center, U.C. Berkeley, August 1977.
4. Kelly, J.M. and Tsztoo, D.F., "The Development of Energy Absorbing Devices for Aseismic Base Isolation System," UCB/EERC-78/01, Earthquake Engineering Research Center, U.C. Berkeley, January 1978.
5. Eidingen, J.M. and Kelly, J.M., "Experimental Results of an Earthquake Isolation System using Natural Rubber Bearings," UCB/EERC-78/03, Earthquake Engineering Research Center, U.C. Berkeley, February 1978.
6. Clough, R.W. and Tang, D.T., "Earthquake Simulator Study of a Steel Frame Structure, Vol. 1: Experimental Results," EERC 75-6, Earthquake Engineering Research Center, U.C. Berkeley, April 1975.
7. Matzen, V.C. and McNiven, H.D., "Investigation of the Inelastic Characteristics of a Single Story Steel Structure using System Identification and Shaking Table Experiments," EERC 76-20, Earthquake Engineering Research Center, U.C. Berkeley, August 1976.
8. Ozdemir, H., "Nonlinear Transient Dynamic Analysis of Yielding Structures," Ph.D Dissertation, Division of Structural Engineering and Structural Mechanics Department of Civil Engineering, U.C. Berkeley, 1976.
9. Newmark, N.M., "A Method of Computation for Structural Dynamics," Journal of the Engineering Mechanics Division, ASCE, Vol. 85, No. EM3, pp. 67-94, 1959.
10. Mondkar, D.P. and Powell, G.H., "Static and Dynamic Analysis of Nonlinear Structures," EERC 75-10, Earthquake Engineering Research Center, U.C. Berkeley, March 1975.
11. Polak, E., Computational Methods in Optimization Academic Press, New York, New York. 1971.
12. Polak, E. and Mayne, D.Q., "An Algorithm for Optimization Problems with Functional Inequality Constraints," IEEE Transaction on Automatic Control, Vol. AC-21, No. 2, April 1976.

13. Ray, D., Pister, K.S. and Chopra, A.K., "Optimum Design of Earthquake-Resistant Shear Buildings," EERC 74-3, Earthquake Engineering Research Center, U.C. Berkeley, January 1974.
14. Walker, N.D. and Pister, K.S., "Study of a Method of Feasible Directions for Optimal Elastic Design of Framed Structures Subjected to Earthquake Loading," EERC 75-39, Earthquake Engineering Research Center, U.C. Berkeley, December 1975.
15. Trahan, R. and Polak, E., "An Improved Algorithm for Optimization Problems with Functional Inequality Constraints," To be published.
16. Luenberger, D.G., Introduction to Linear and Nonlinear Programming. Addison-Wesley, 1973.
17. Armijo, L., "Minimization of Function Having Continuous Partial Derivatives," Pacific Jr. Math. 16, pp. 1-3, 1966.
18. Ray, D., "Sensitivity Analysis for Hysteretic Dynamic Systems: Application to Earthquake Engineering," EERC 74-5, Earthquake Engineering Research Center, U.C. Berkeley, April 1974.
19. Ray, D., Pister, K.S. and Polak, E., "Sensitivity Analysis for Hysteretic Dynamic Systems: Theory and Applications," EERC 76-12, Earthquake Engineering Research Center, U.C. Berkeley, February 1976.
20. Ruiz, P. and Penzien, J., "PSEQGN - Artificial Generation of Earthquake Accelerograms," A Computer Program Distributed by NISEE/Computer Applications, U.C. Berkeley, March 1969.
21. Murakami, M. and Penzien, J., "Nonlinear Response Spectra for Probabilistic Seismic Design and Damage Assessment of Reinforced Concrete Structures," EERC 75-38, Earthquake Engineering Research Center, U.C. Berkeley, November 1975.

NOTATION

\mathbb{R}^n Denotes the euclidean space of ordered n-tuples of real numbers. When an n-tuplet is a vector in \mathbb{R}^n , it is always treated as a column vector.

$\langle \dots \rangle$ Scalar product in \mathbb{R}^n defined by $\langle x, y \rangle = \sum_{i=1}^n x_i y_i$.

$\|\cdot\|_2$ Euclidean norm defined by $\|x\|_2 = \sqrt{x^T x}$

$\|\cdot\|_\infty$ Maximum norm in \mathbb{R}^n , defined by $\|x\|_\infty = \max_{i \in \mathbb{R}^n} |x_i|$

z Underscore signifies that z is a vector or a matrix

z^T Transpose of z

z⁻¹ Inverse of matrix z

|x| Absolute value of x

$A \subset B$ A is contained in B

$A \cup B$ Union of A and B

$\{x|p\}$ Set of points x having property p.

$x \in A$ x belongs to A.

$x \notin A$ x does not belong to A.

(a,b) Open interval

[a,b] Closed interval

(a,b] Semi-open or Semi-closed interval.

- $f(\cdot)$ or f Denotes a function, with the dot standing for the undesignated variable; $f(z)$ denotes the value of $f(\cdot)$ at point z . Domain A and range B of function $f(\cdot)$ is indicated by $f: A \rightarrow B$.
- $\nabla f(\underline{z})$ Denotes the gradient of f at z . The gradient is treated as a column vector. If f is a function of more than one variable, the variable with respect to which the gradient is evaluated is shown as a subscript to the gradient symbol, e.g. $\nabla_z f(z,t)$ indicates gradient with respect to z of a function of z , and t .
- $\min \{f(\underline{z}) \mid \underline{z} \in C\}$ Minimum of $f(\underline{z})$ over $\underline{z} \in C$
- $\dot{U}(t)$ The dot over the functions represents the derivative with respect to time. i.e. $\dot{U}(t) = dU(t)/dt$.

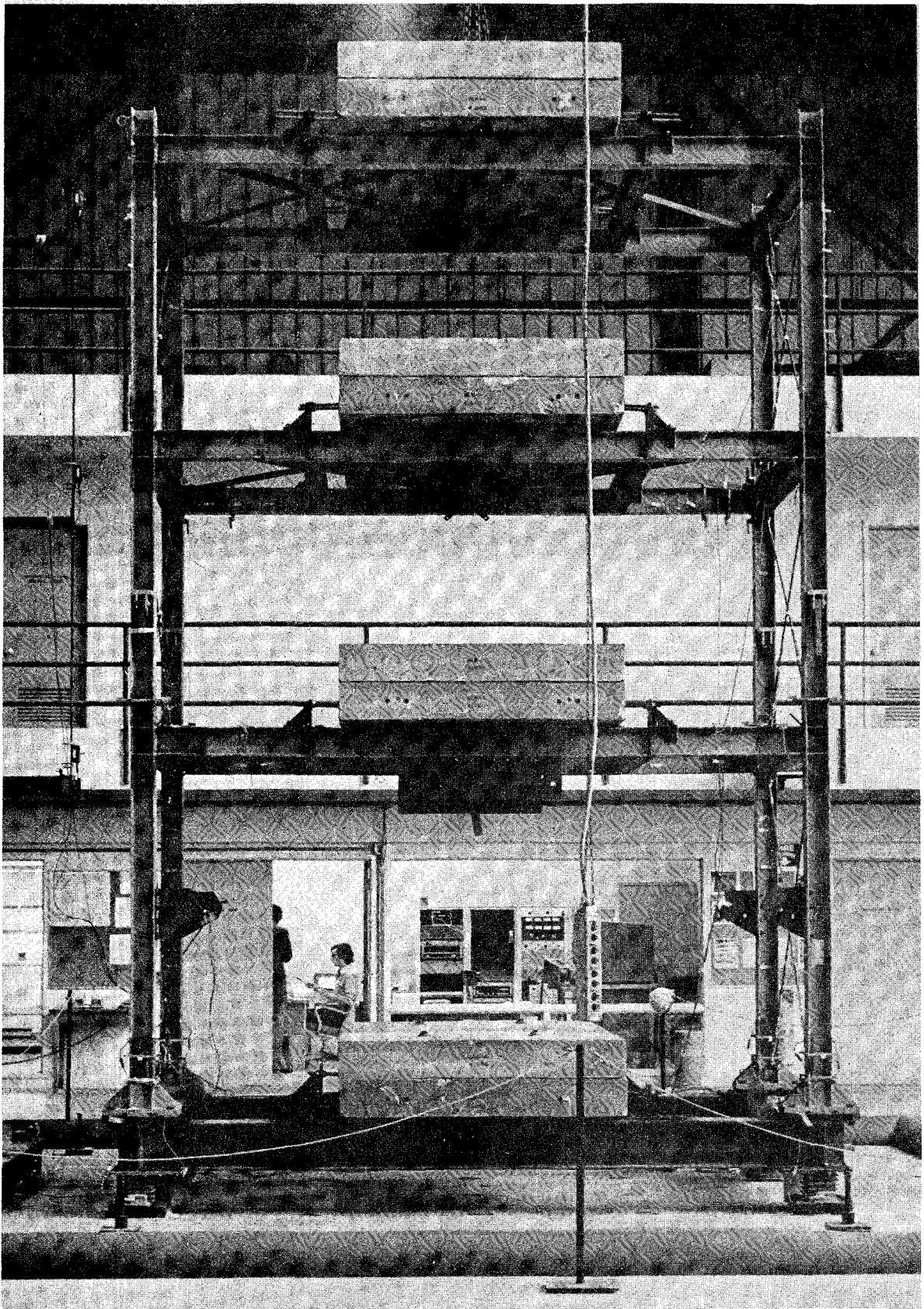


FIGURE 1 MODEL STRUCTURE

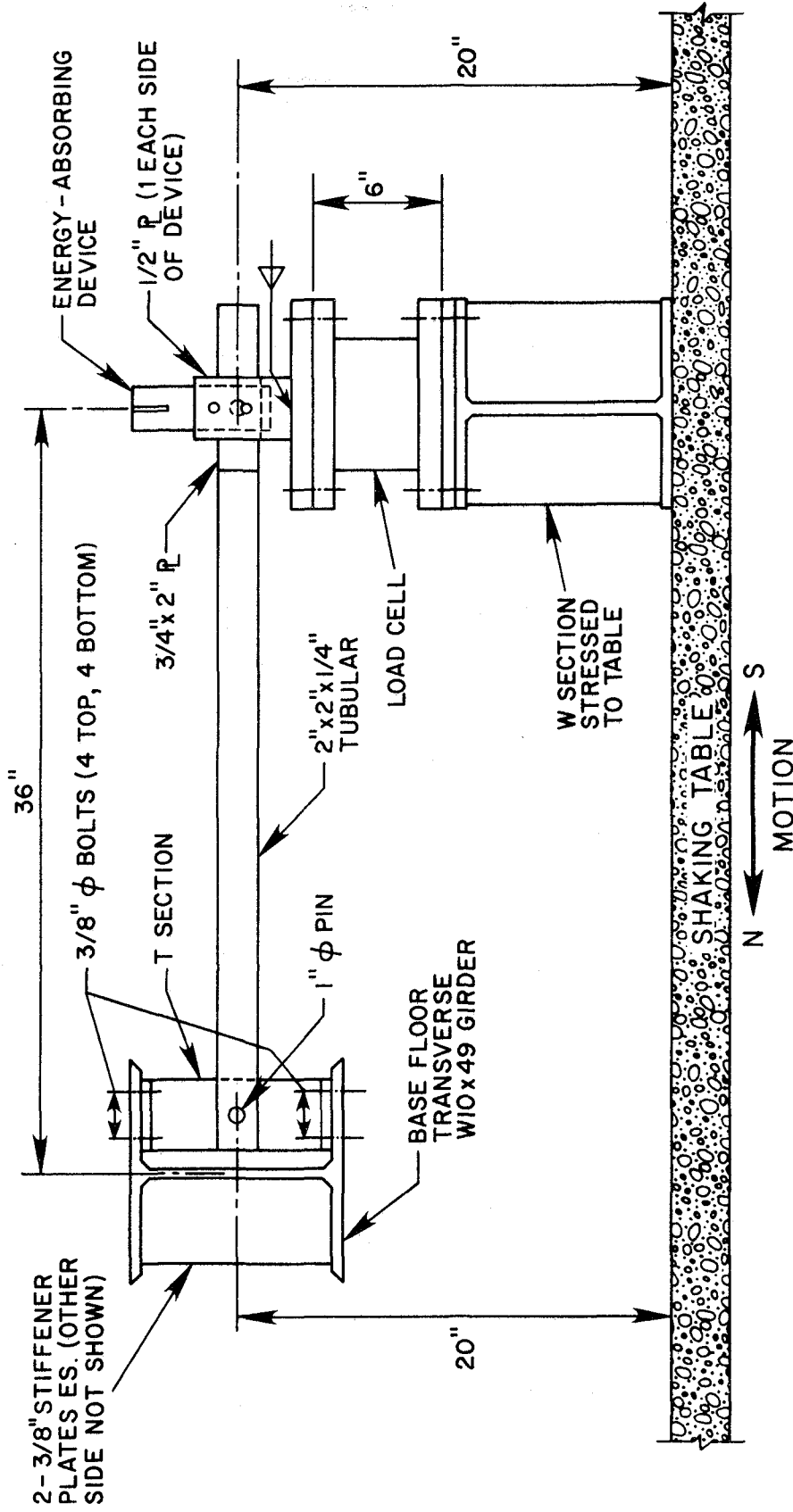


FIGURE 2 ENERGY-ABSORBING DEVICE CONNECTION - DETAIL

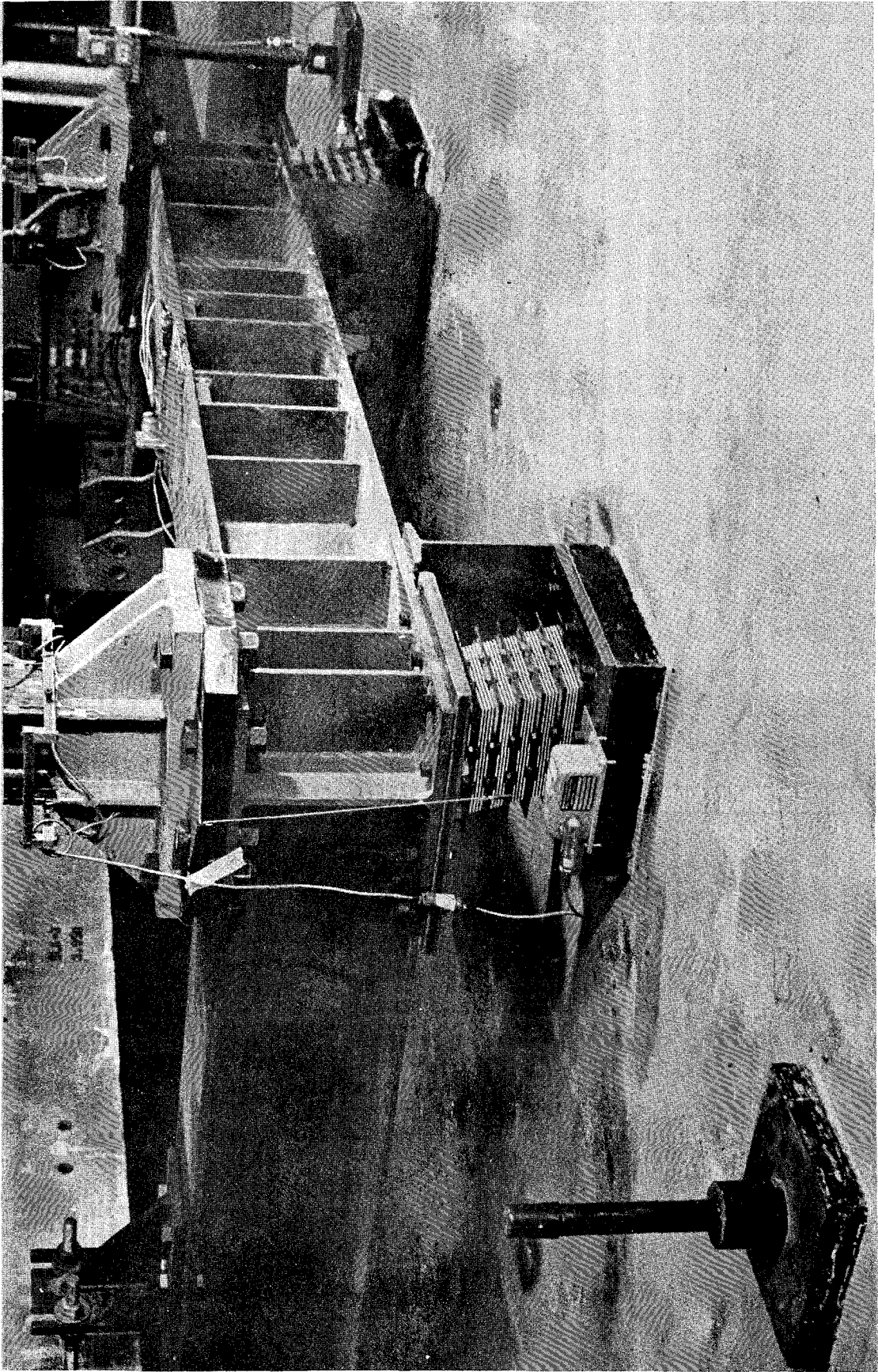


FIGURE 3 SHEAR DEFLECTION OF RUBBER BEARINGS

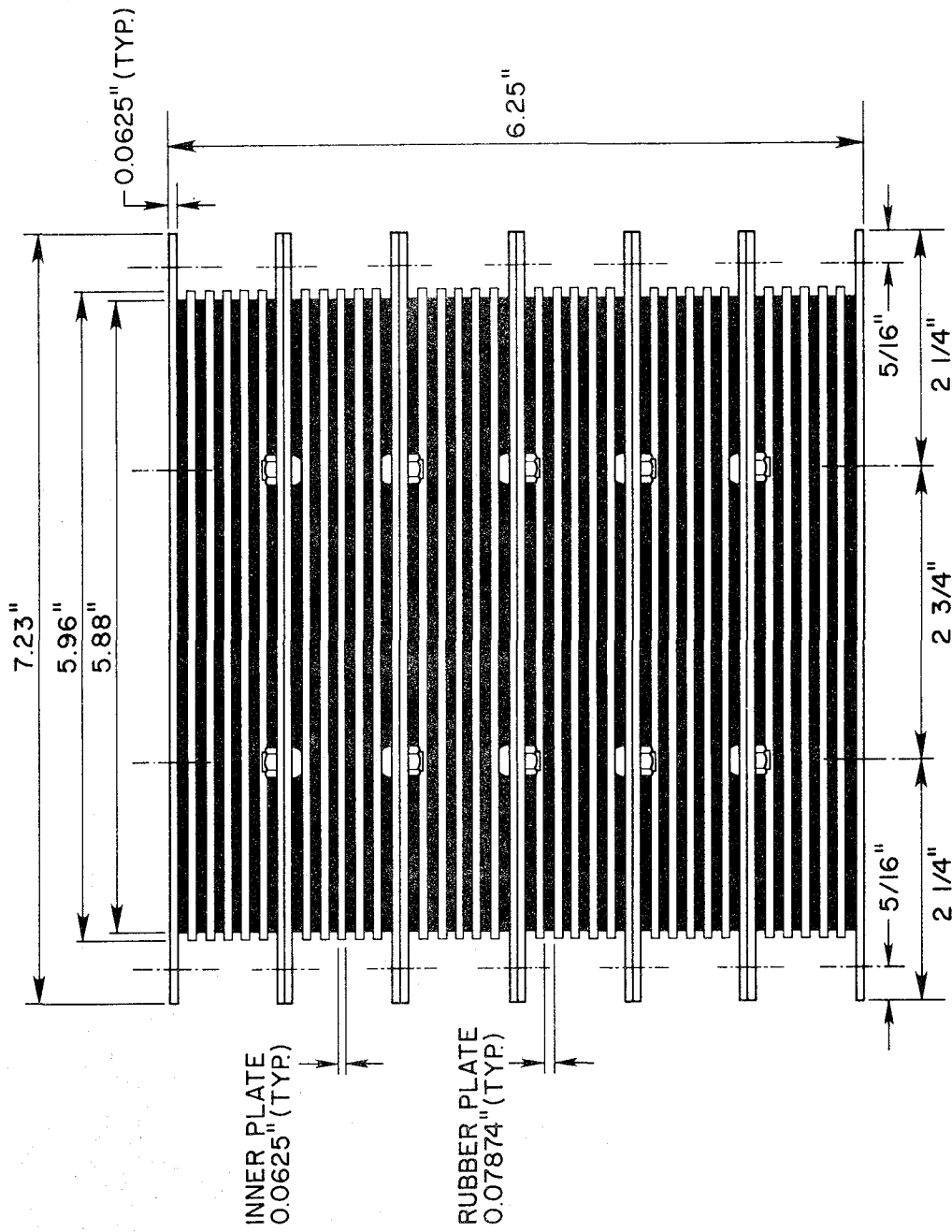


FIGURE 4 DIMENSIONS OF NATURAL RUBBER BEARINGS

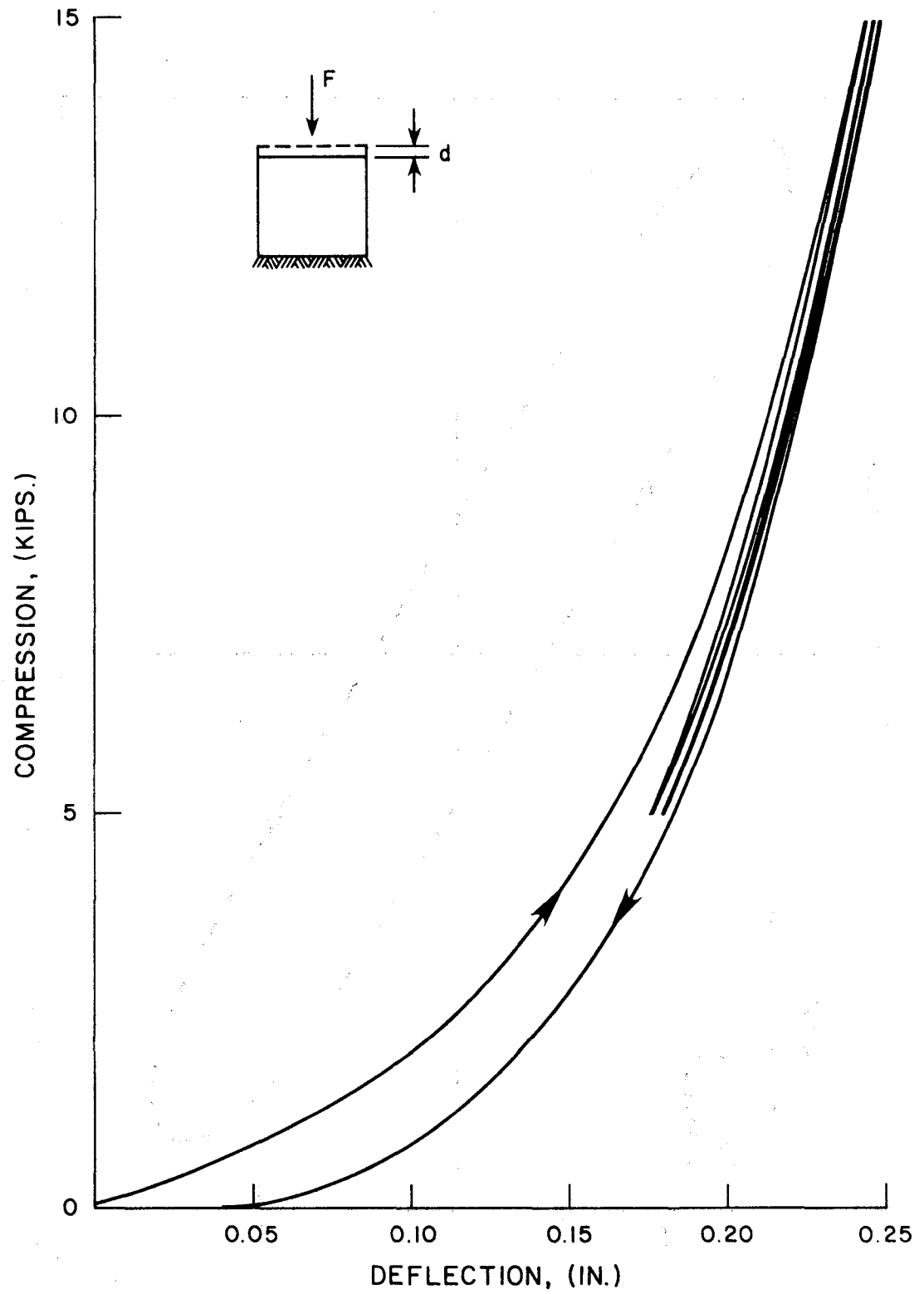


FIGURE 5 VERTICAL STIFFNESS OF BEARINGS

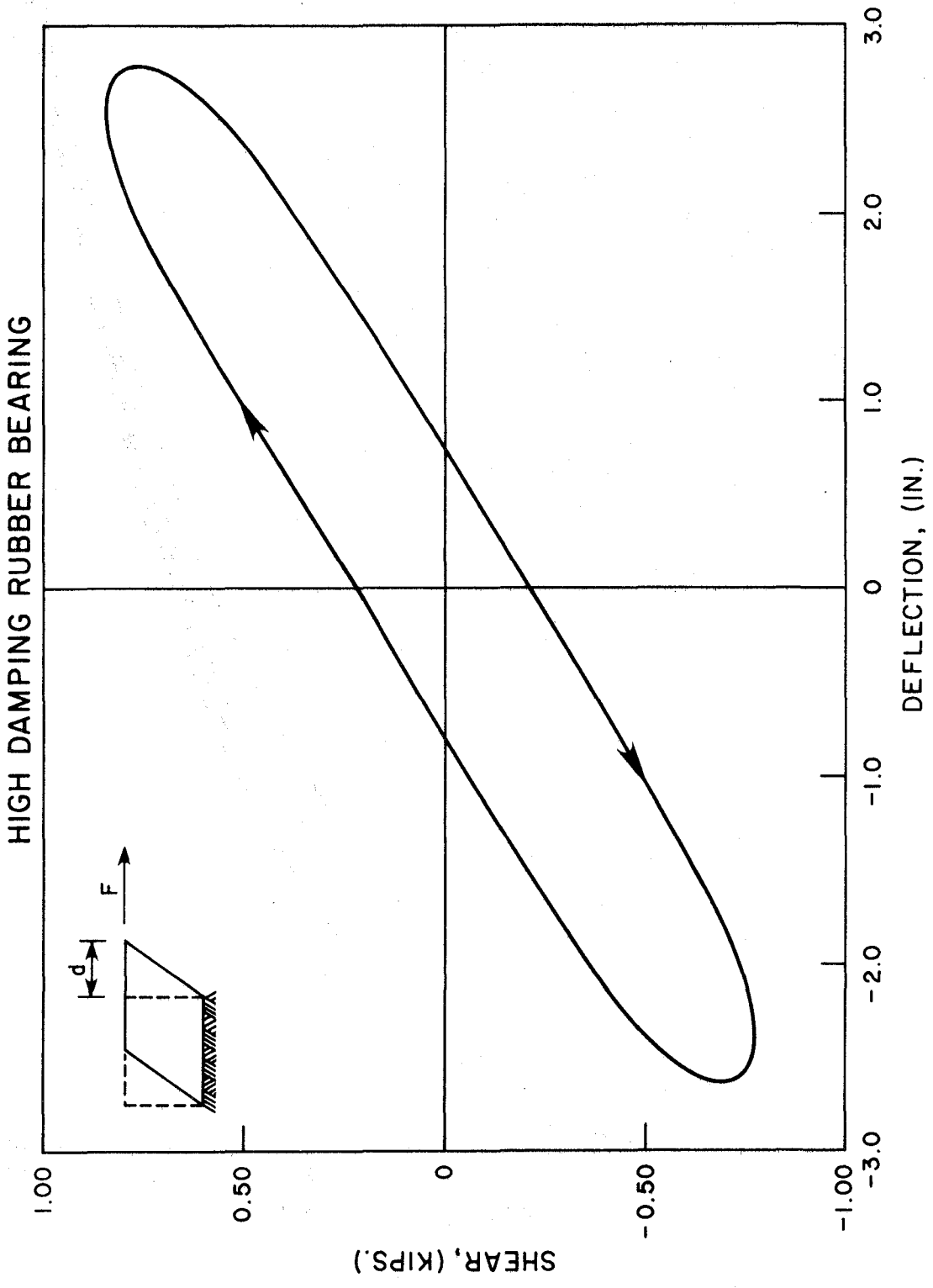


FIGURE 6 HORIZONTAL STIFFNESS OF BEARINGS

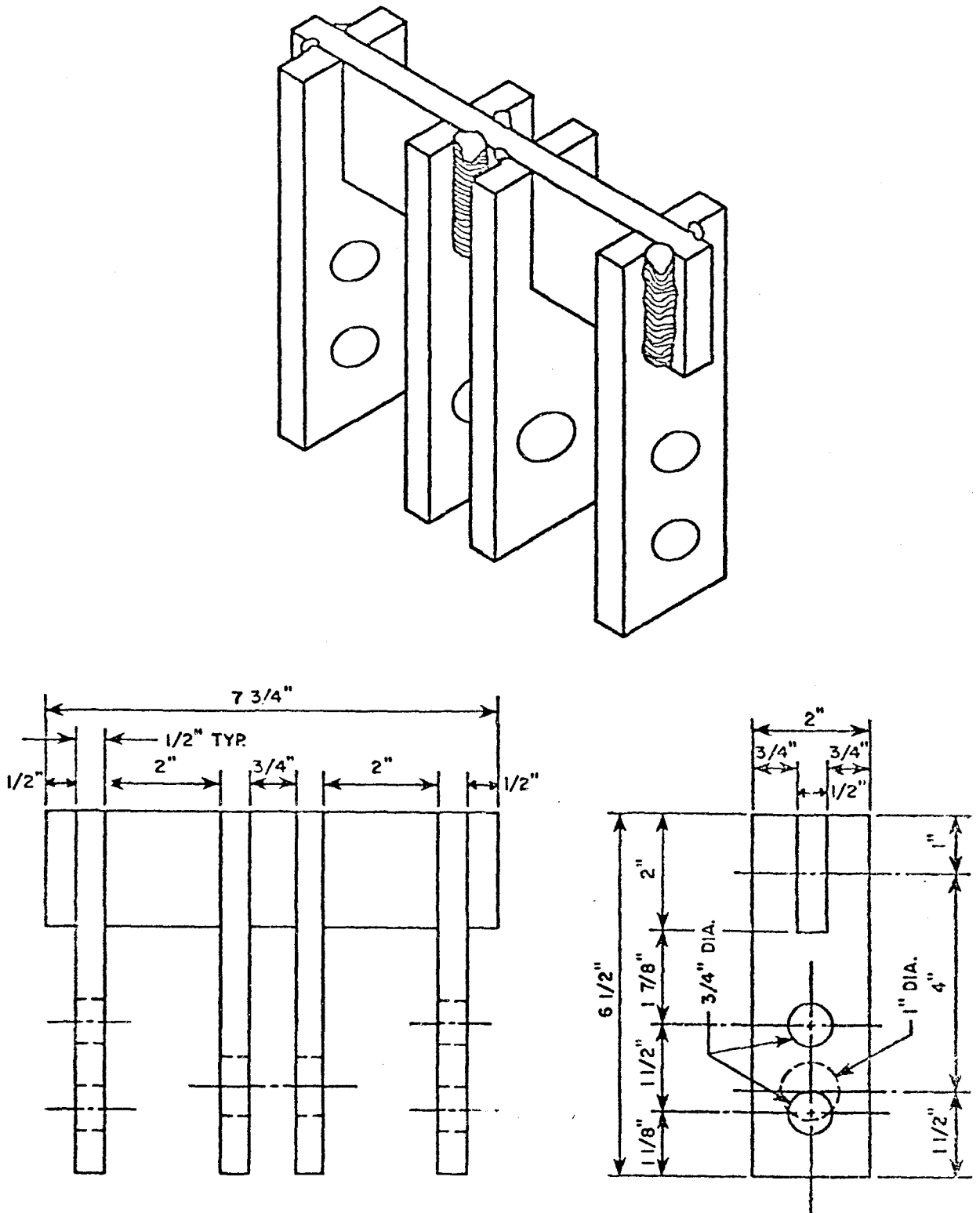


FIGURE 7 DIMENSIONS OF ENERGY ABSORBING DEVICES

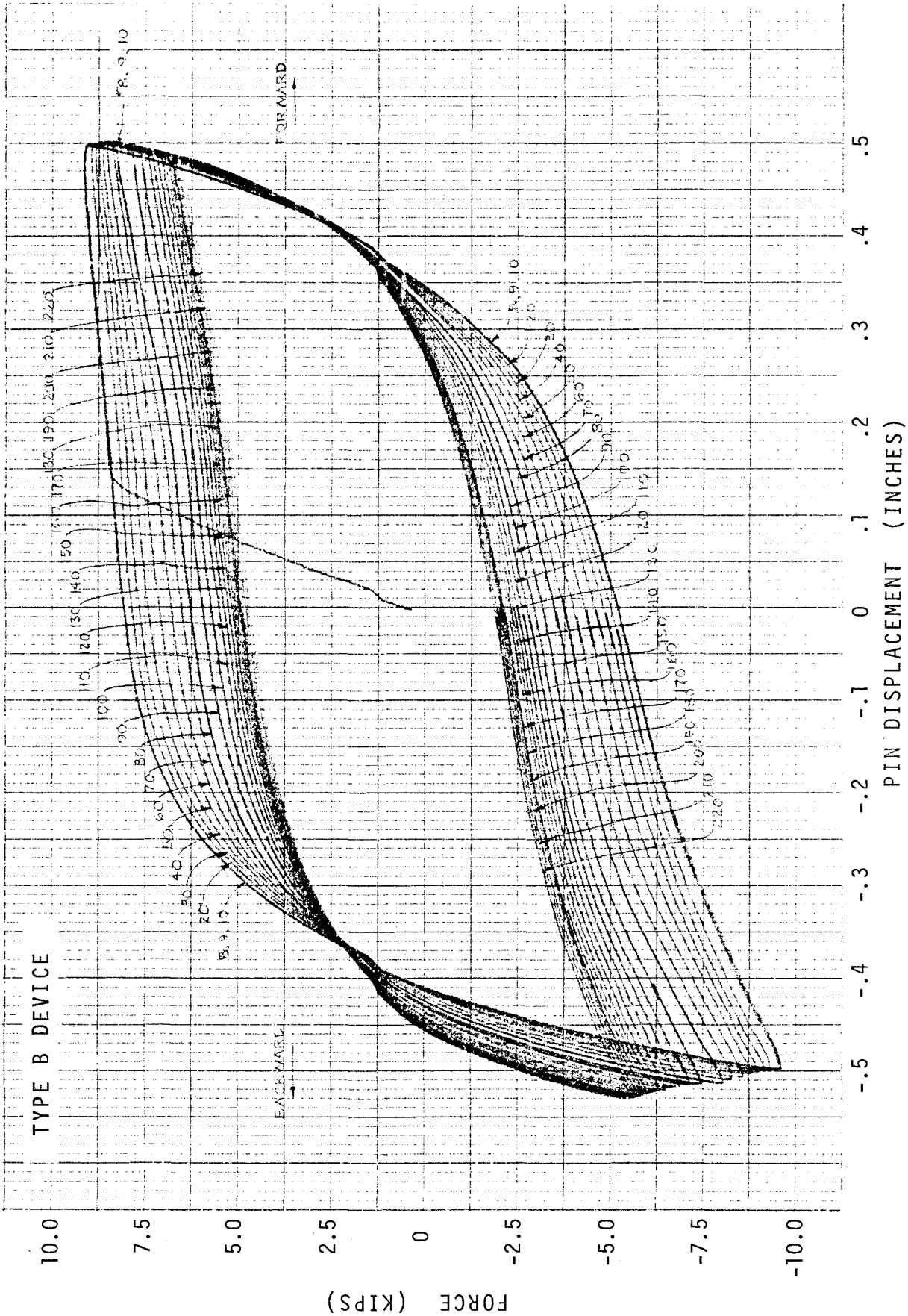


FIGURE 8 HYSTERESIS OF DEVICE UNDER SINUSOIDAL LOADING

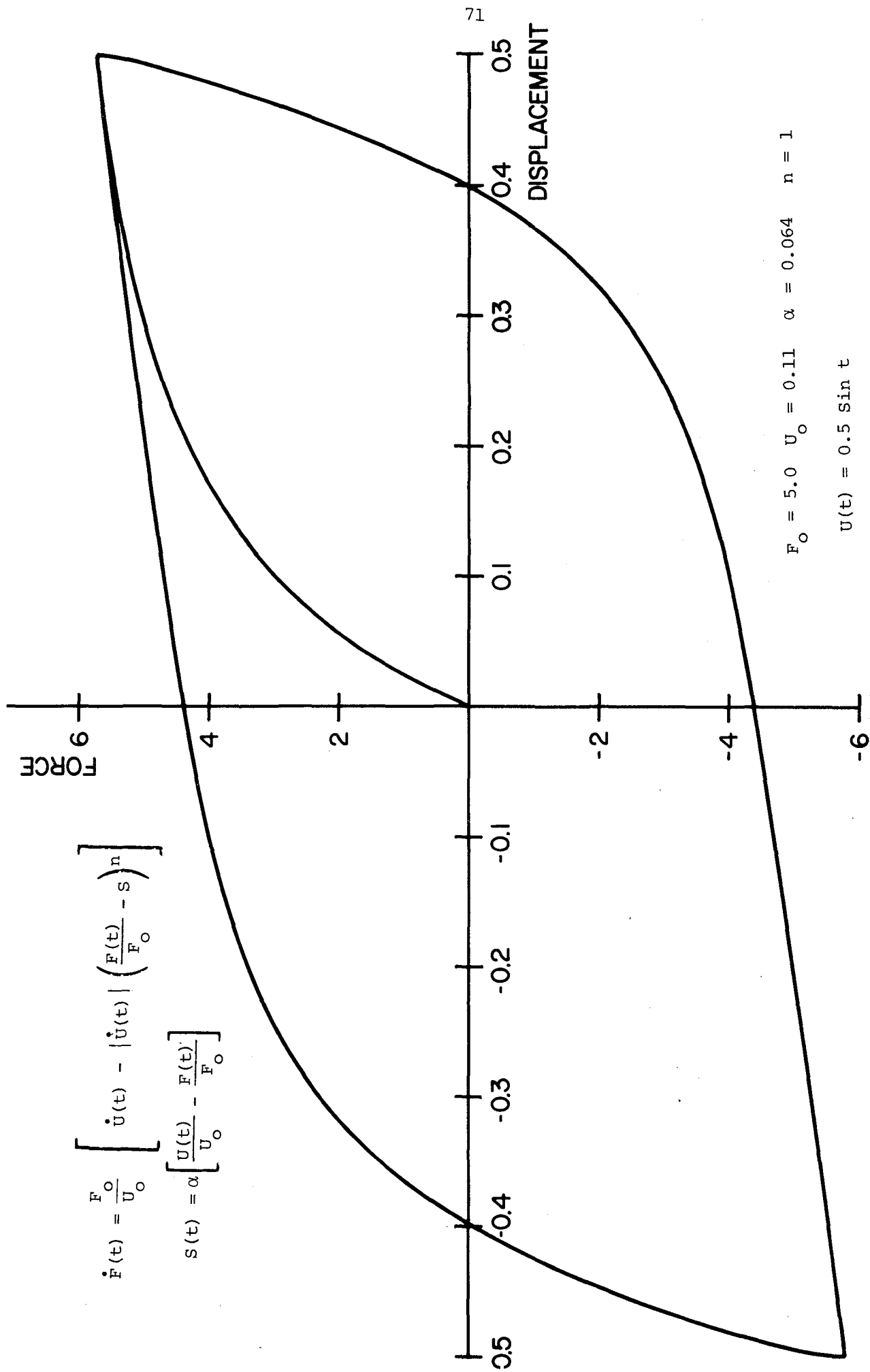
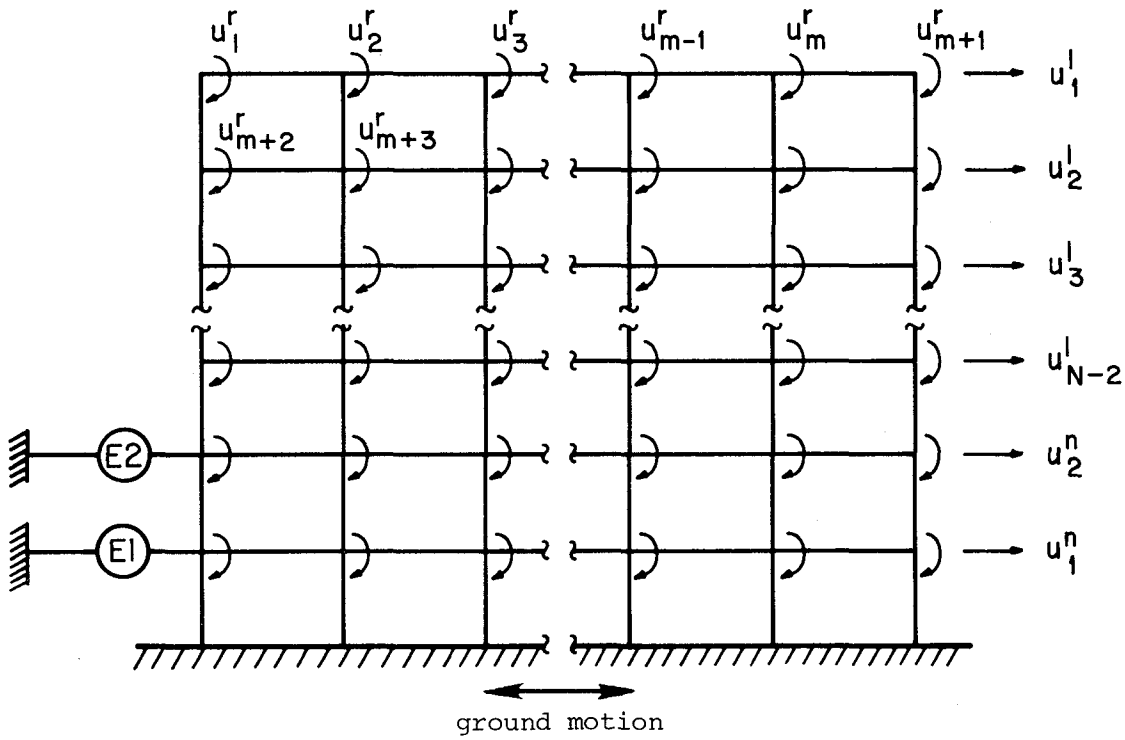


FIG. 9 HYSTERESIS LOOPS GENERATED BY RATE INDEPENDENT HYSTERESIS MODEL UNDER SINUSOIDAL EXCITATION



N STORY - M BAY FRAME

E1, E2 - Non-linear Energy absorbing elements

U^r - Rotational degrees of freedom

U^l - Lateral degrees of freedom

U^n - Lateral degrees of freedom
associated with the non-linear
energy absorbing devices.

Total number of degrees of freedom = $N(M+2)$

FIG. 10 THE STRUCTURAL SYSTEM

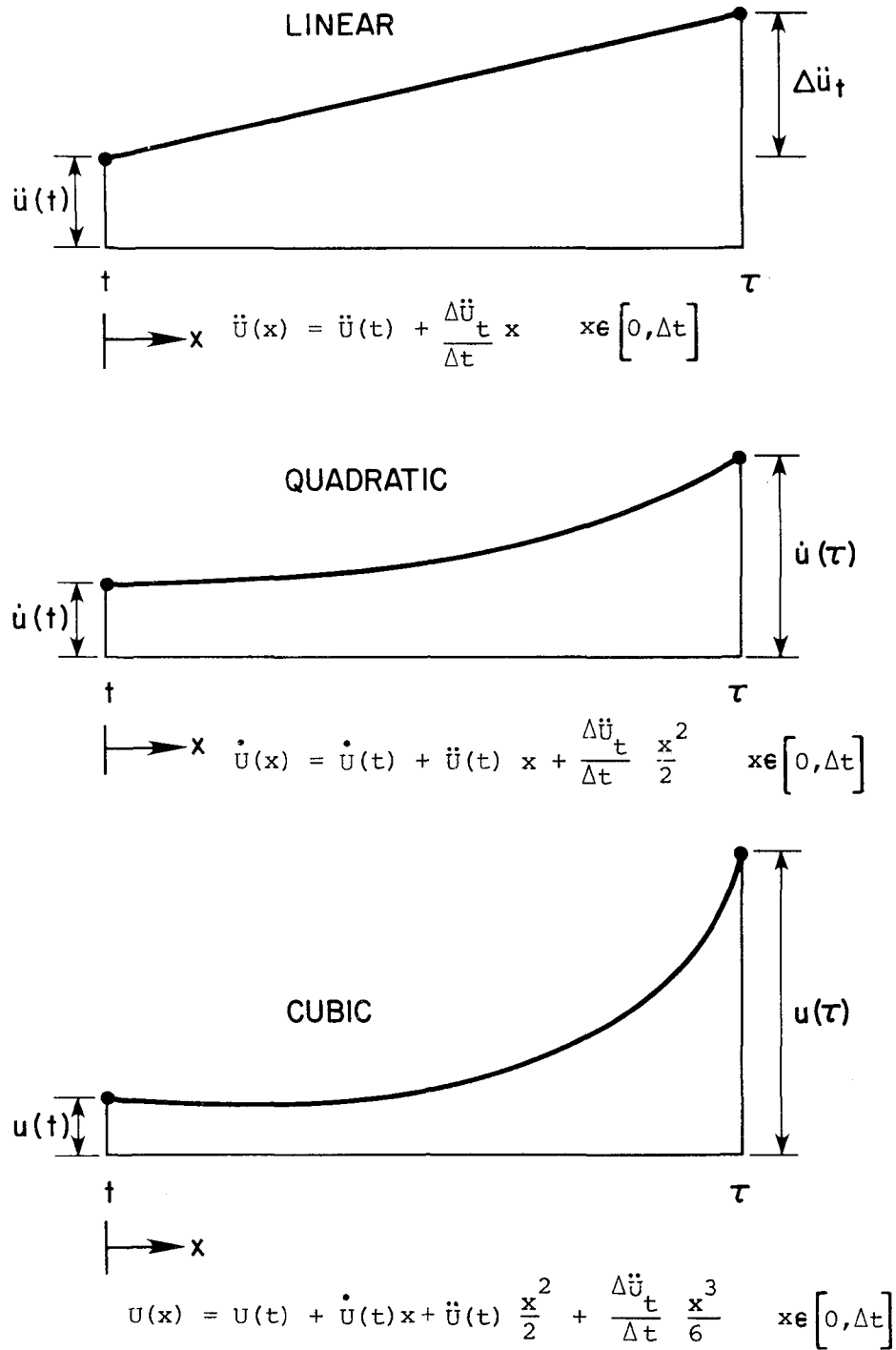


FIG. 11 VARIATIONS IN ACCELERATION, VELOCITY AND DISPLACEMENT DURING TIME INTERVAL $[t, \tau = t + \Delta t]$

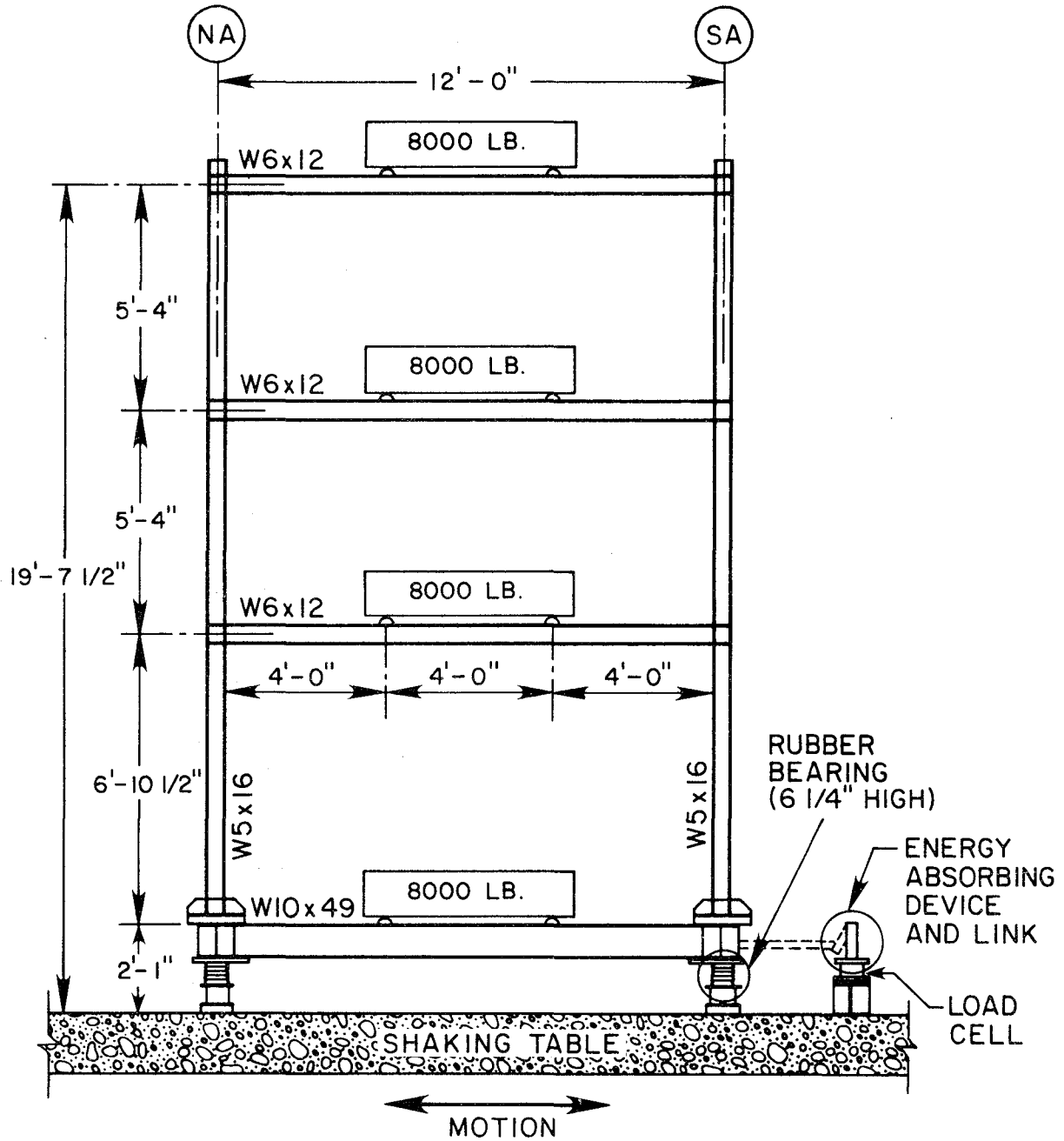
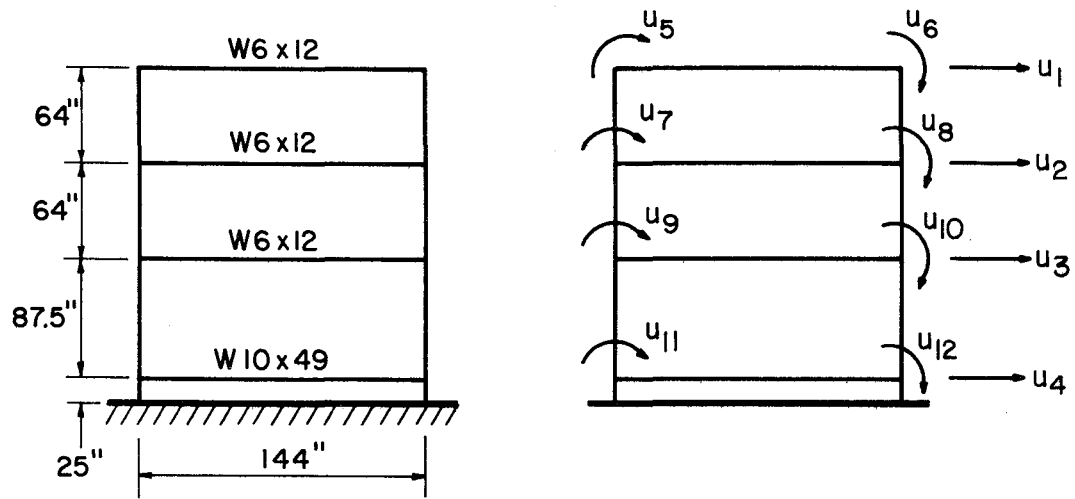


FIGURE 12 DIMENSIONS OF STRUCTURE

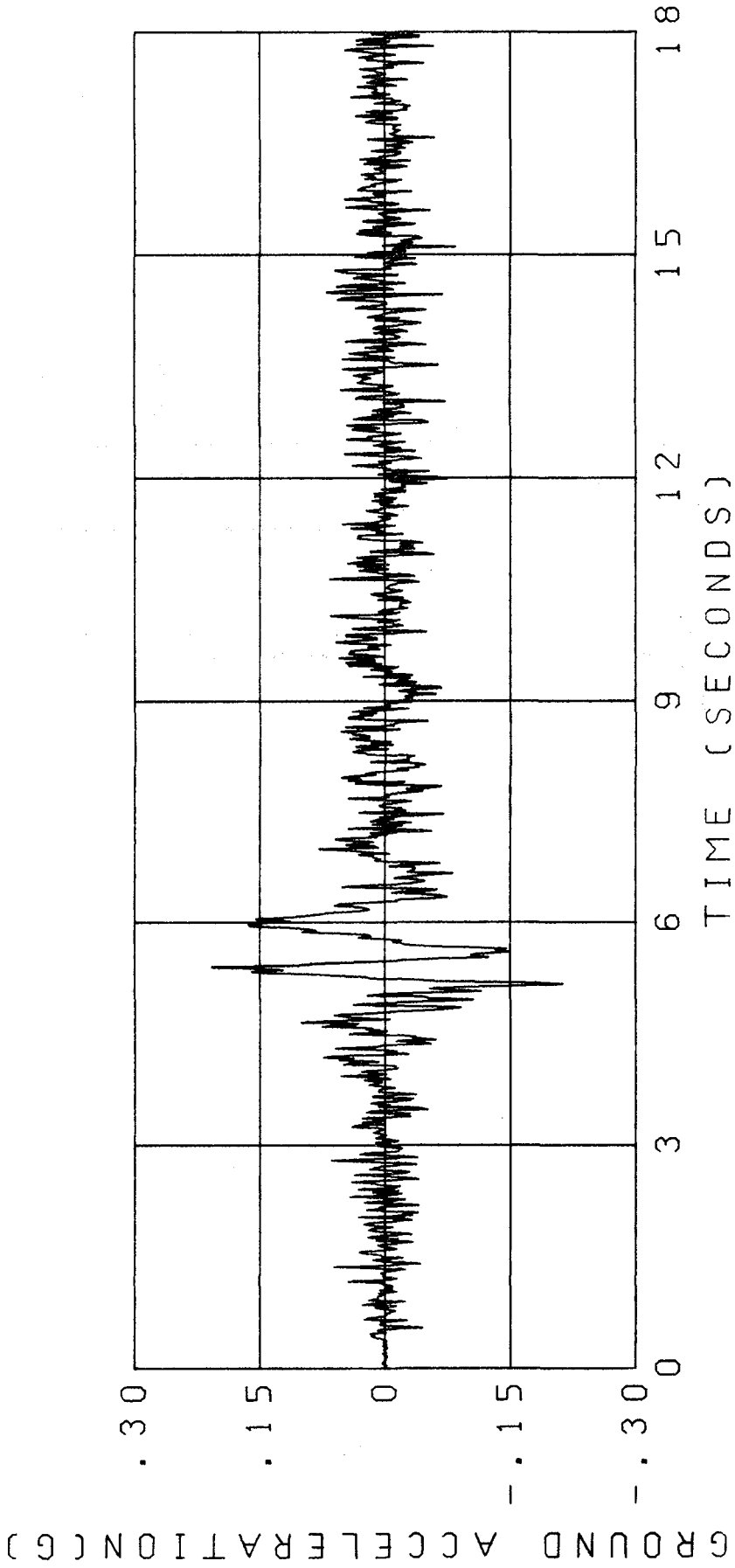


Columns are W5x16

Stiffness of rubber bearings = 1.2 k/in

Section properties:	Area (in ²)	Moment of Inertia (in ⁴)
W6x12	3.54	21.7
W5x16	4.70	21.3
W10x49	14.40	272.9

FIG. 13 STRUCTURAL DATA



PARKFIELD N65E SPAN 500 ACCELEROGRAM

FIGURE 14

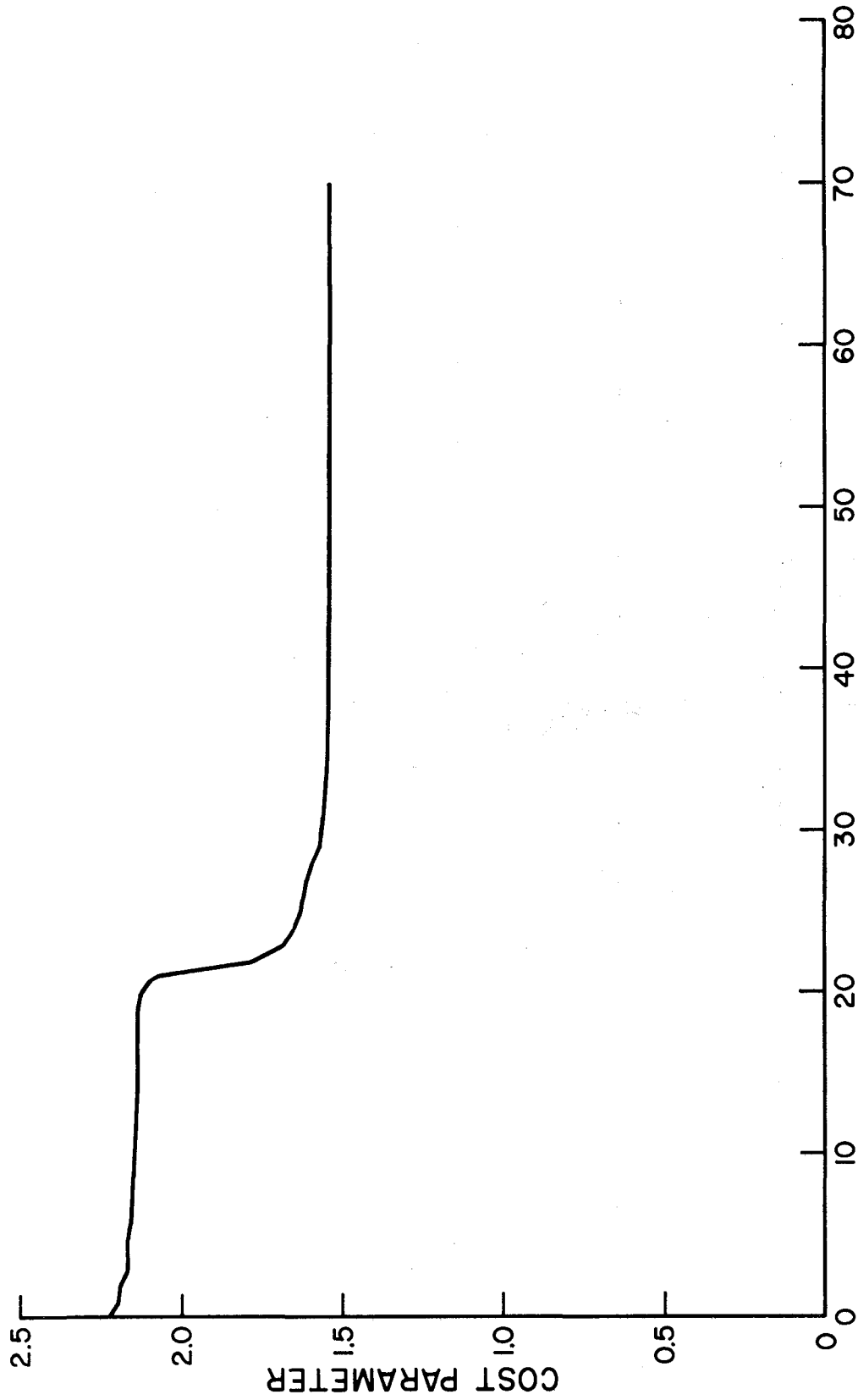


FIGURE 15 COST PARAMETER AND DESIGN ITERATIONS

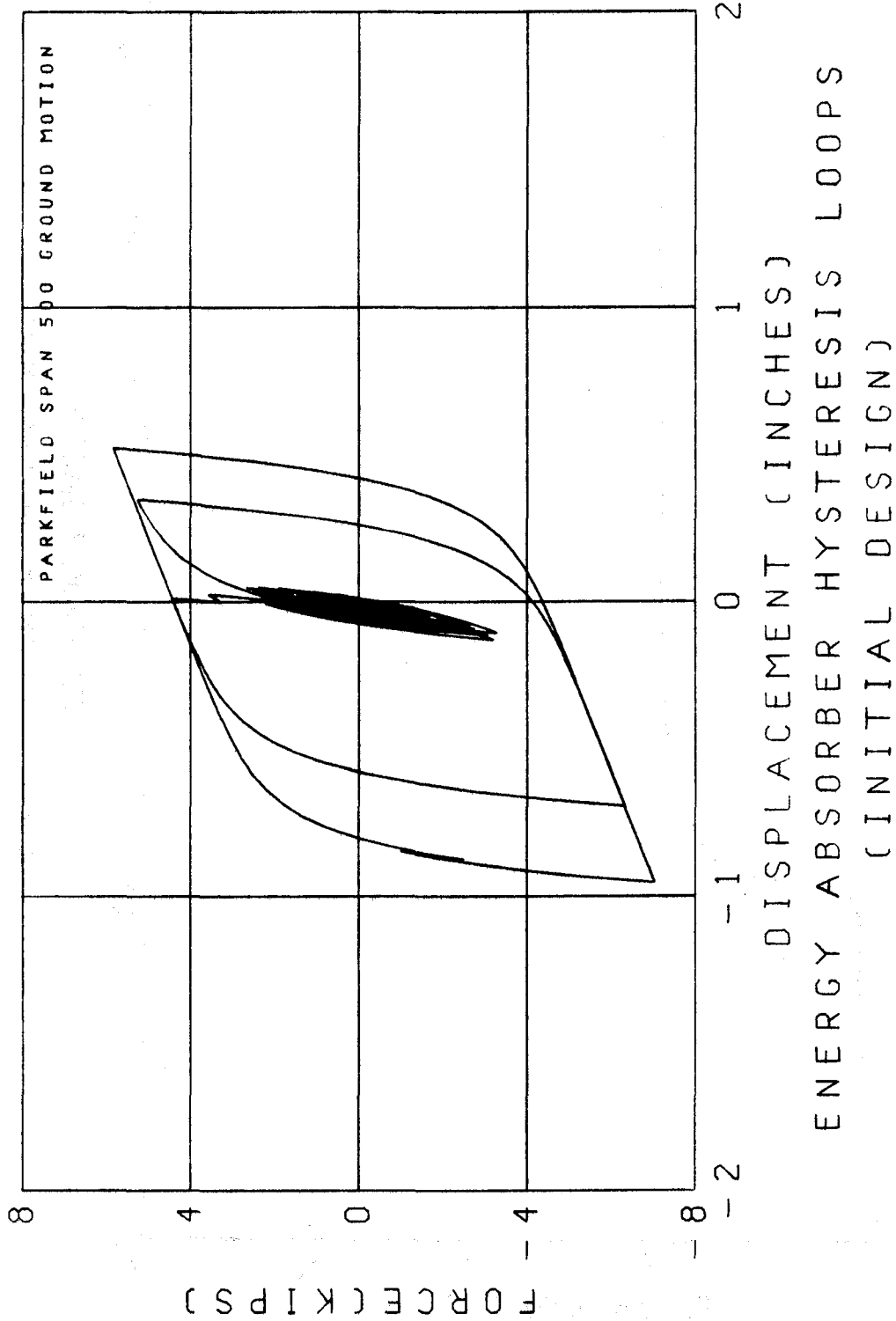


FIGURE 16

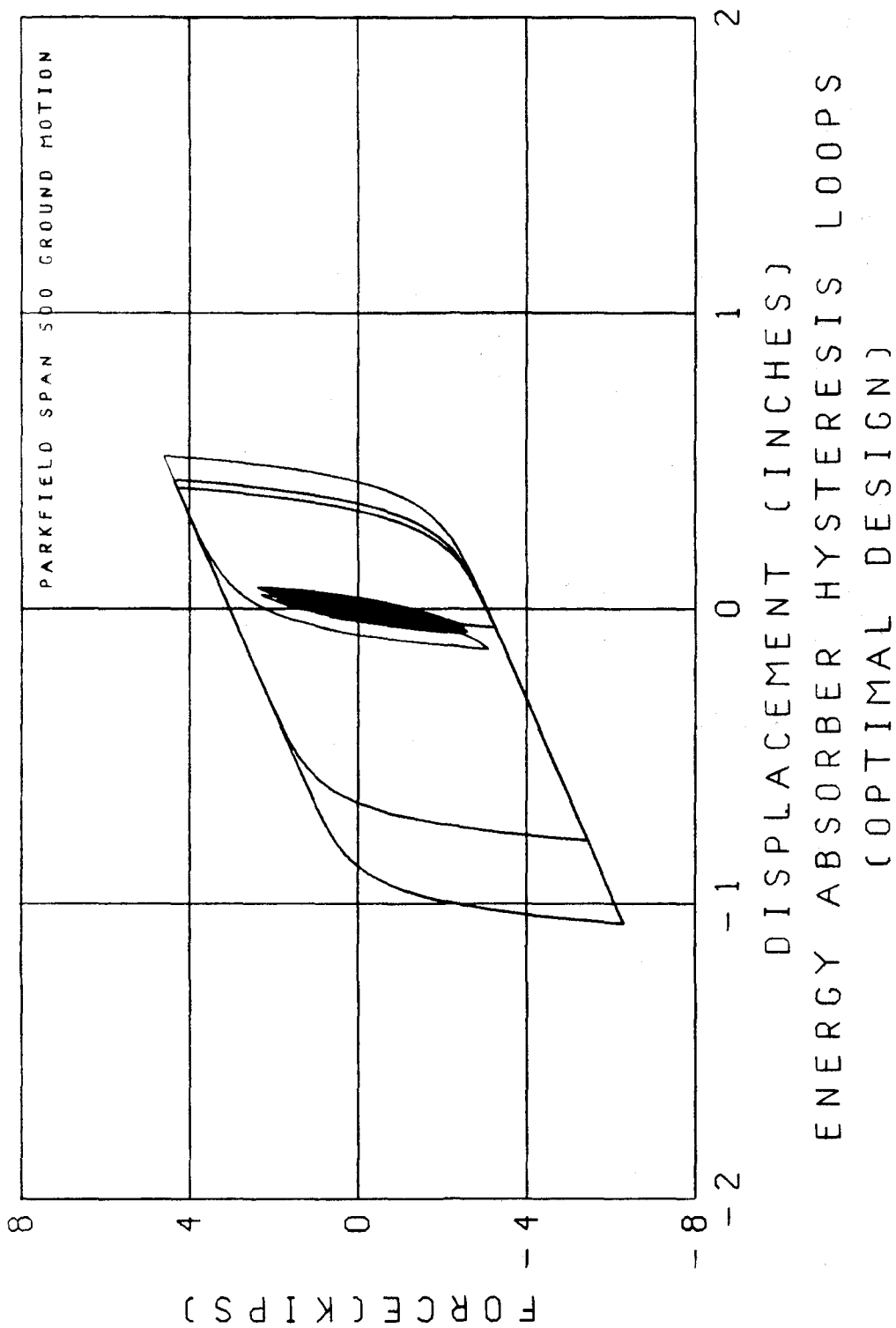


FIGURE 17

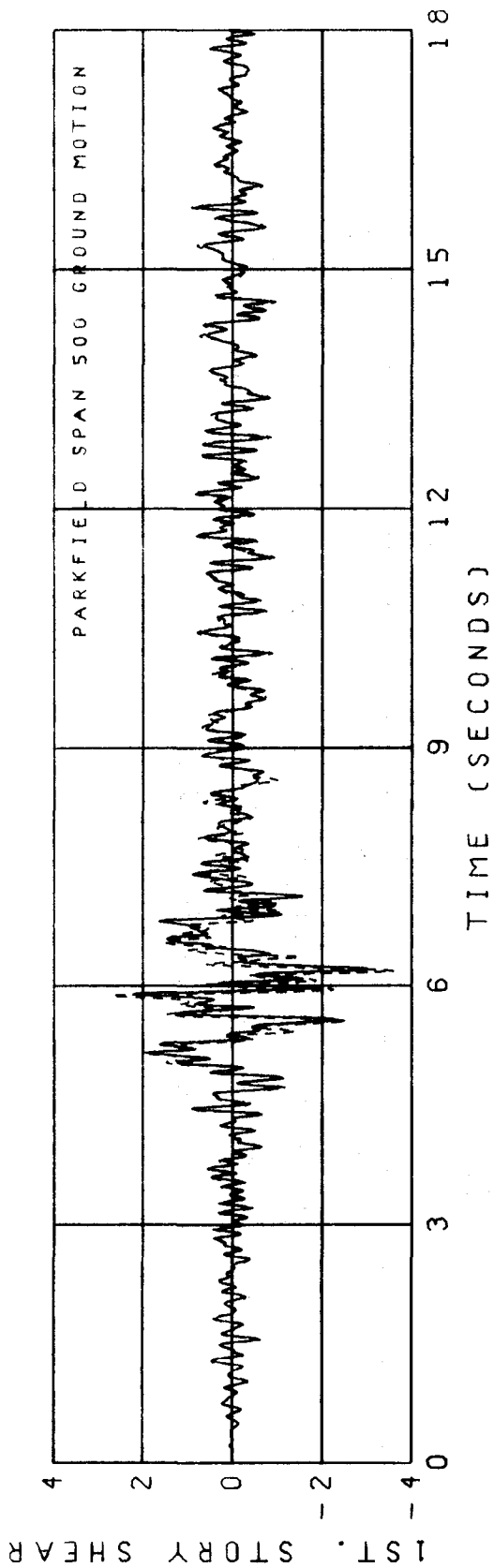


FIGURE 18 FIRST STORY SHEAR TIME HISTORY

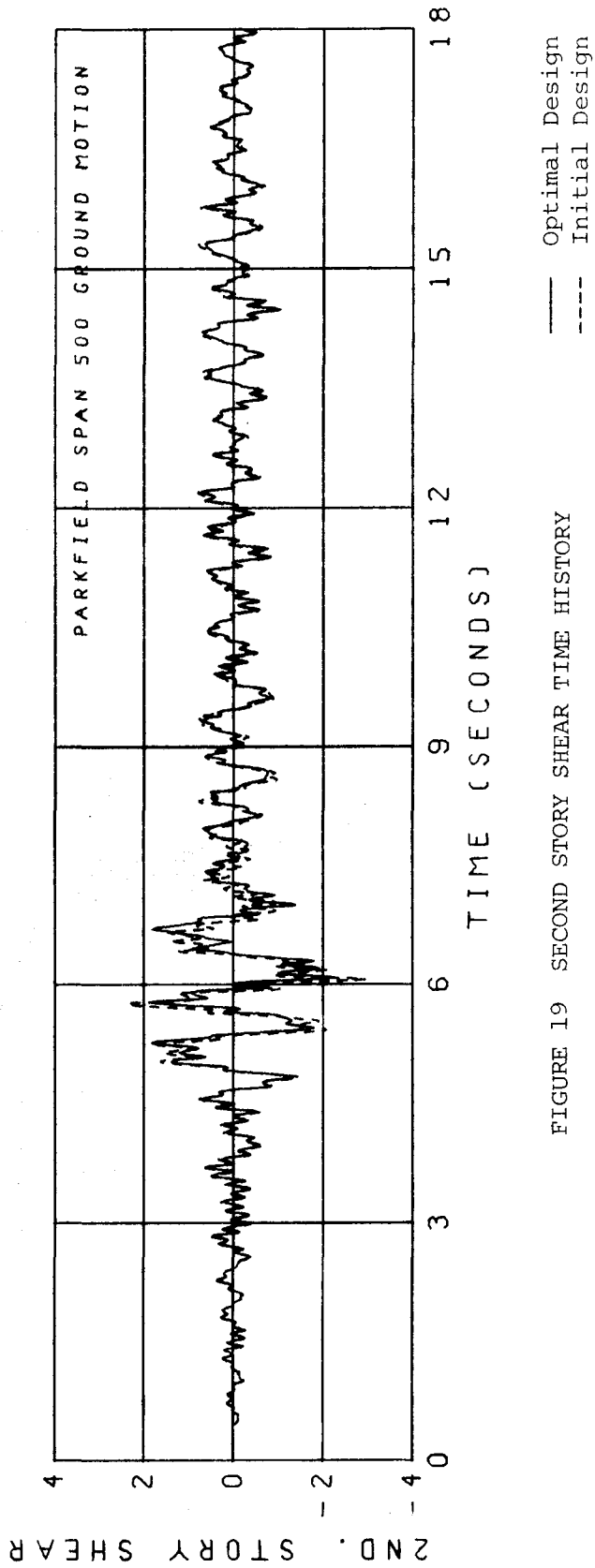


FIGURE 19 SECOND STORY SHEAR TIME HISTORY

— Optimal Design
- - - Initial Design

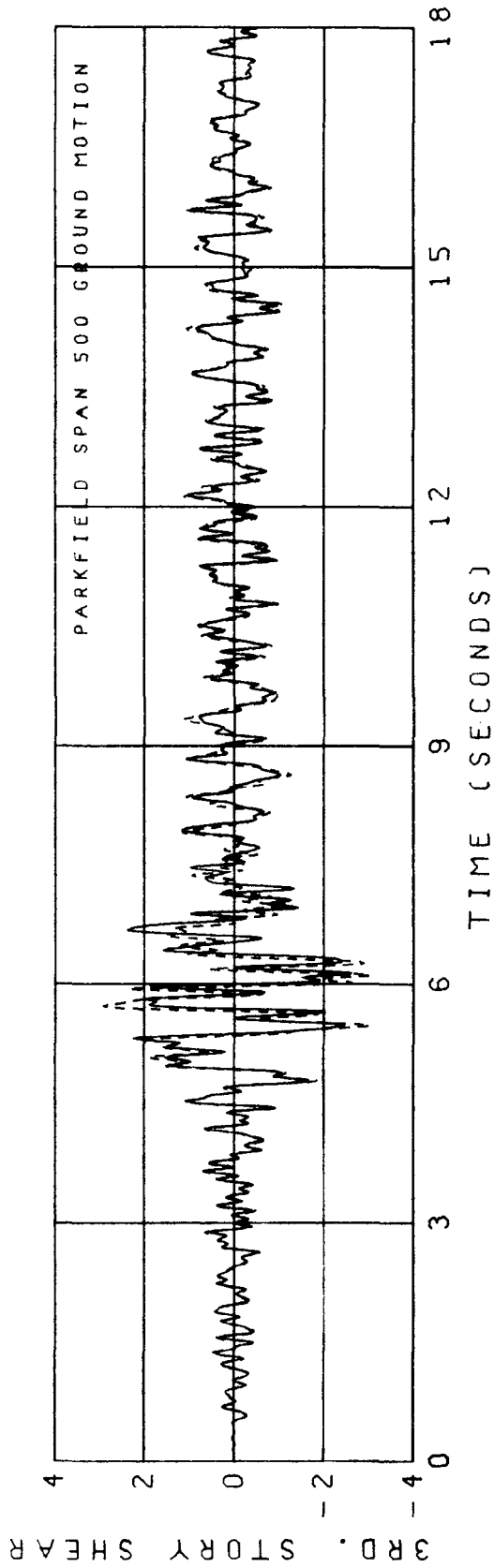


FIGURE 20 THIRD STORY SHEAR TIME HISTORY

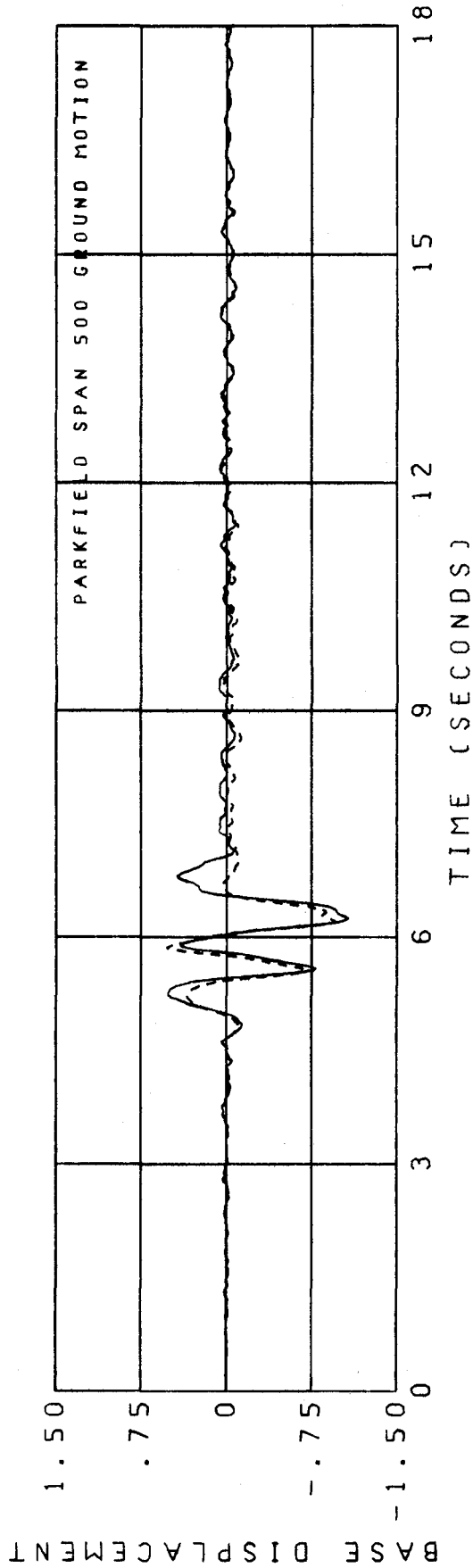
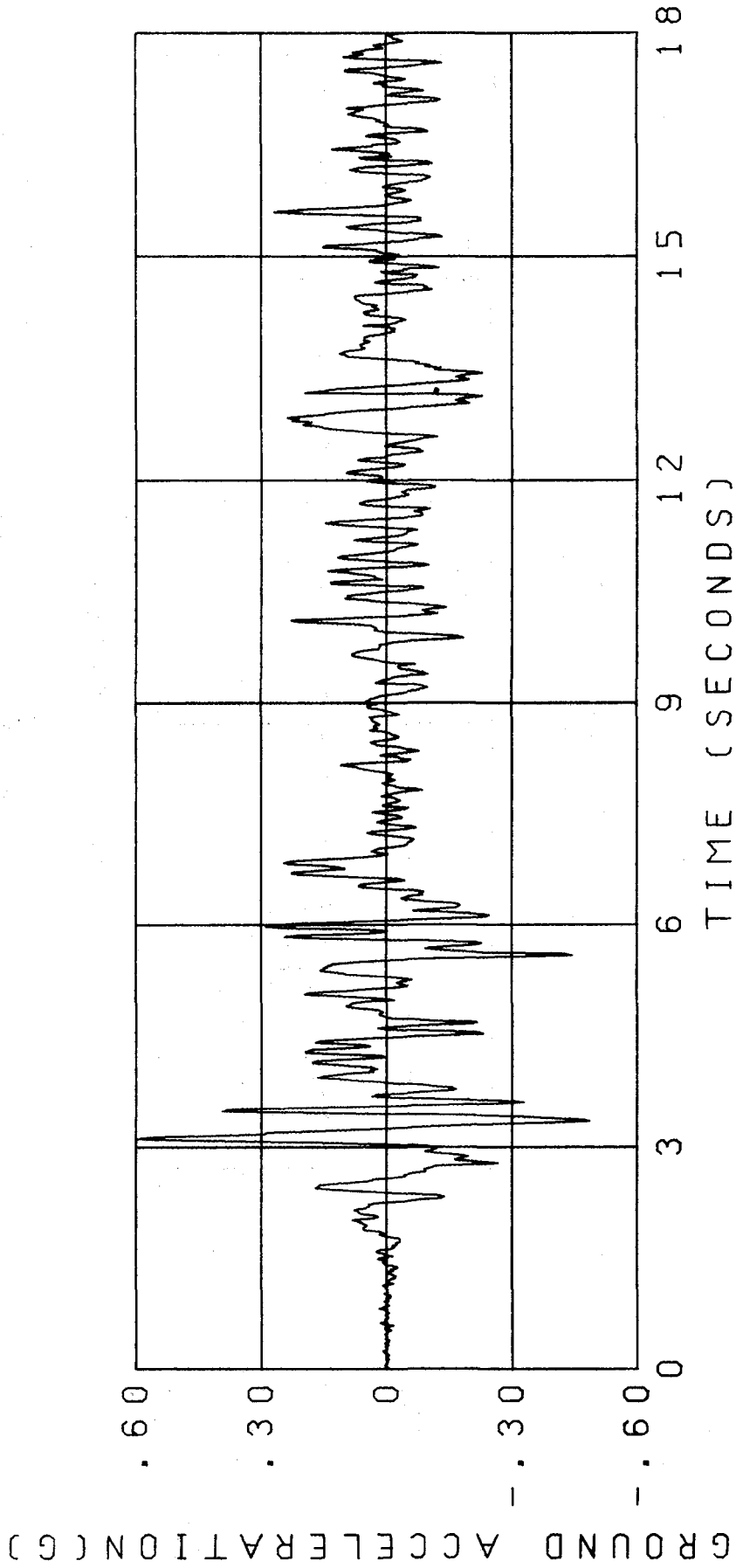


FIGURE 21 BASE DISPLACEMENT TIME HISTORY

— Optimal Design
 - - - Initial Design



EL CENTRO SPAN 750 ACCELEROGRAM

FIGURE 22

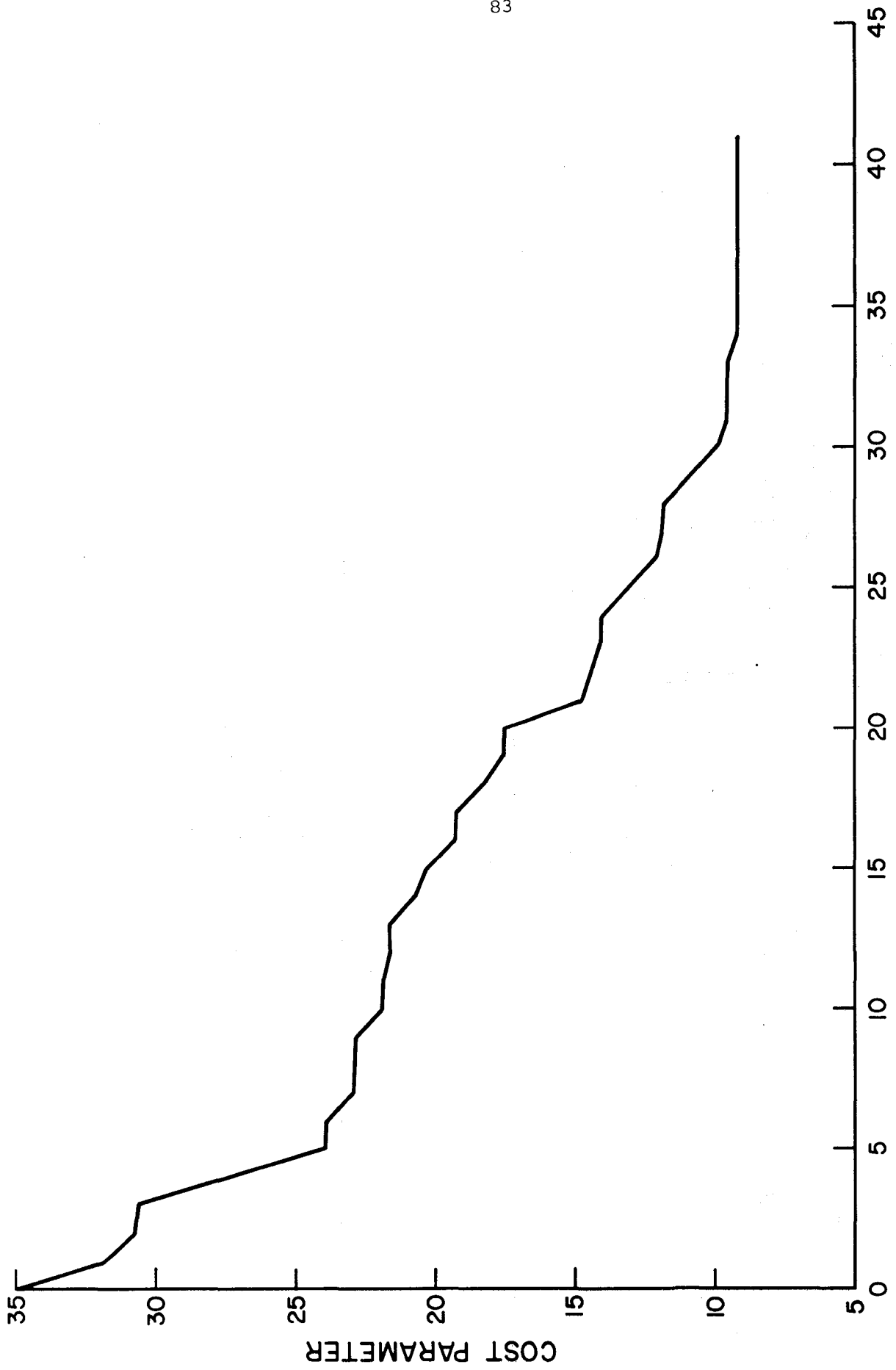


FIGURE 23 COST PARAMETER AND DESIGN ITERATIONS

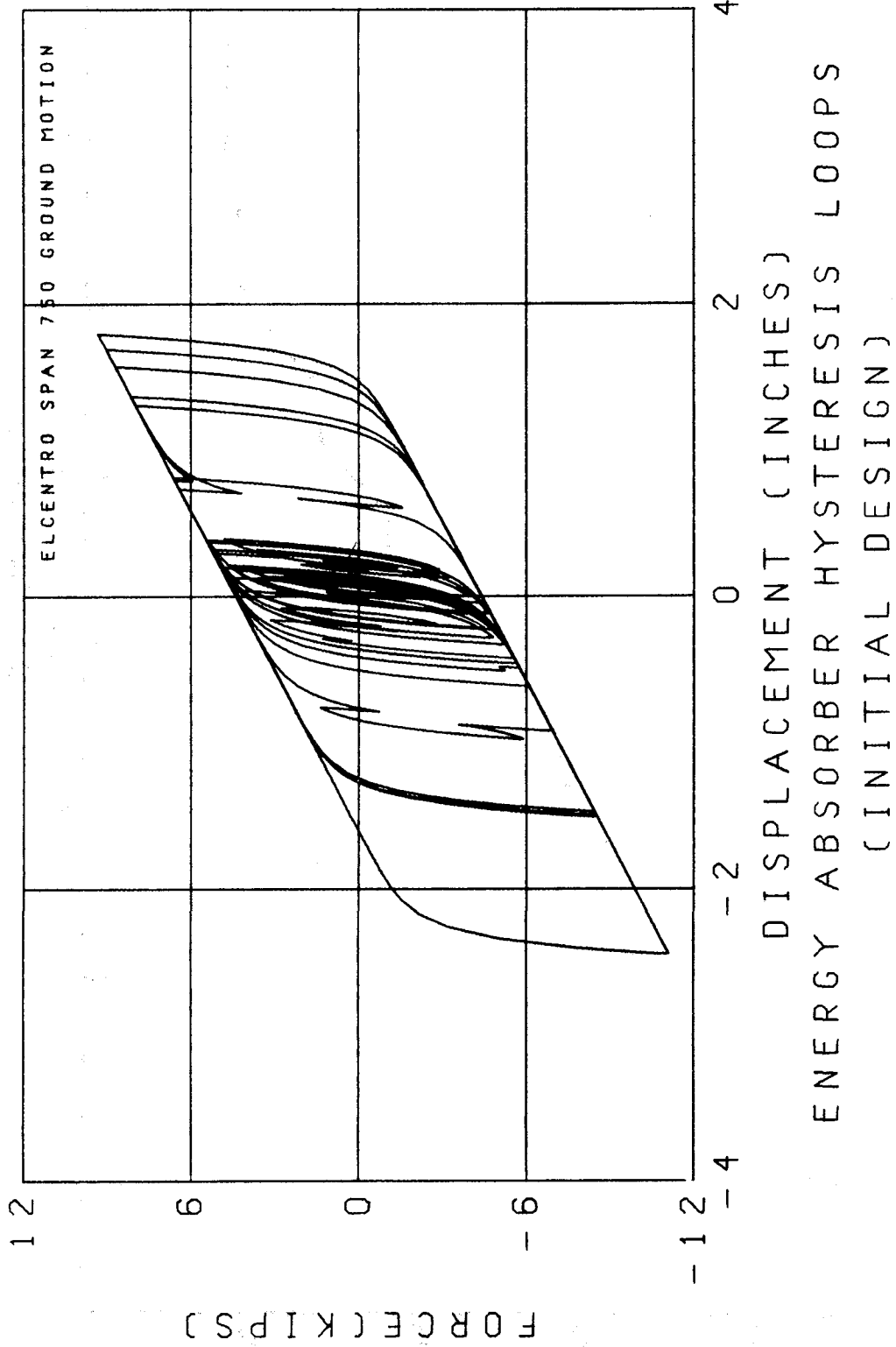


FIGURE 24

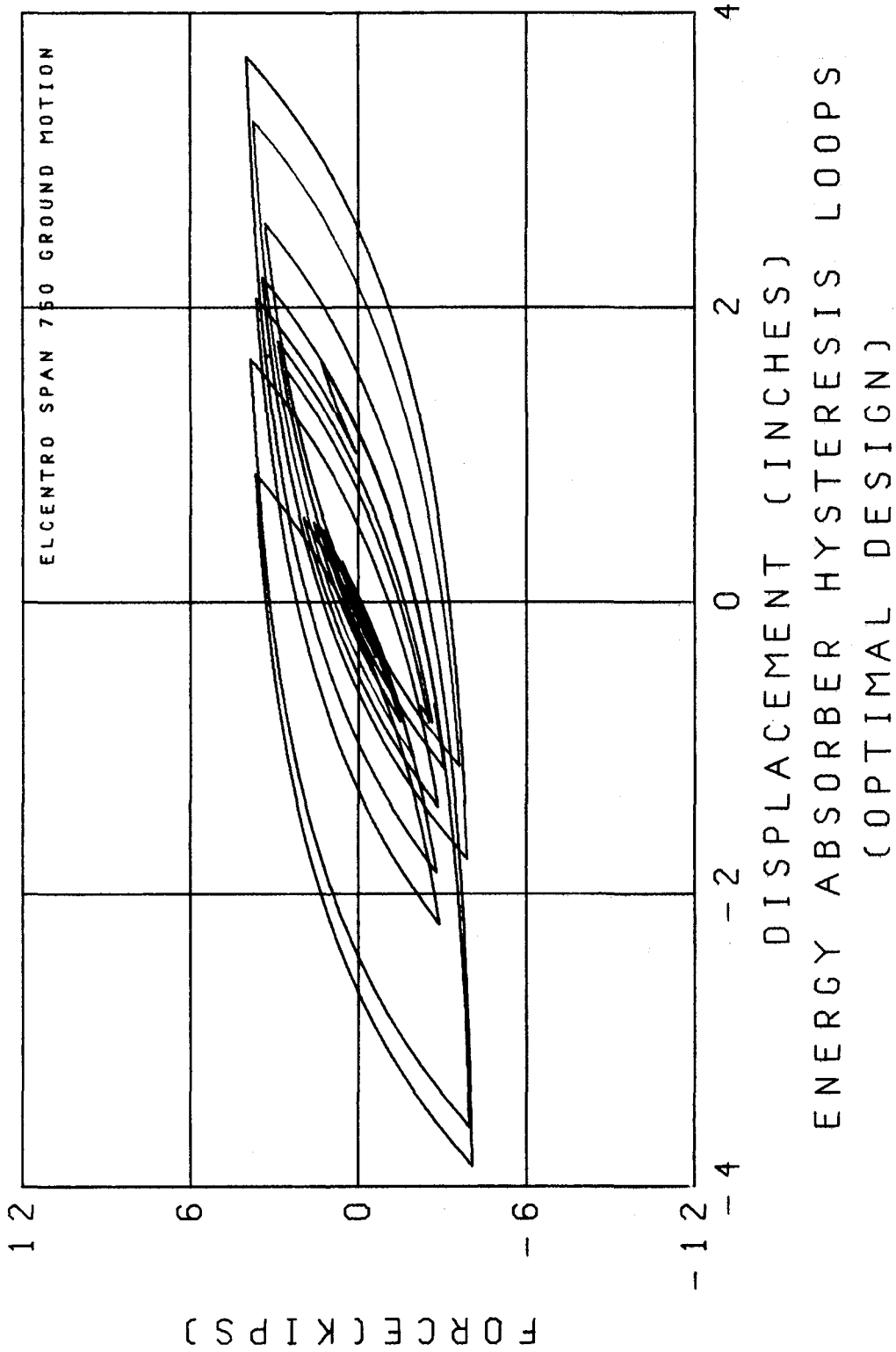


FIGURE 25

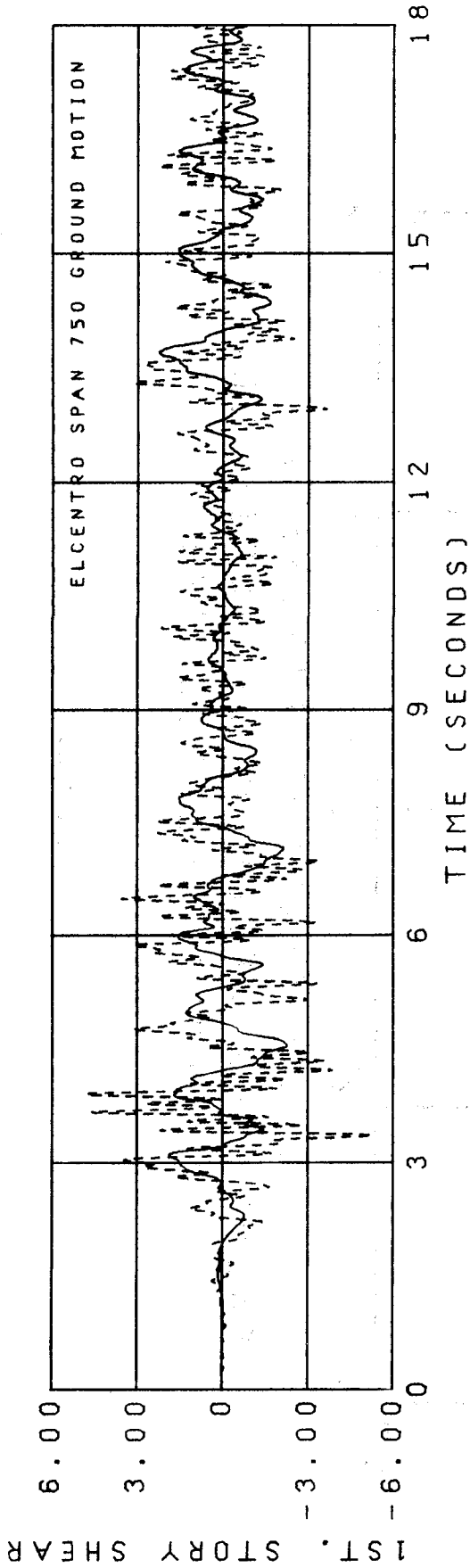


FIGURE 26 FIRST STORY SHEAR TIME HISTORY

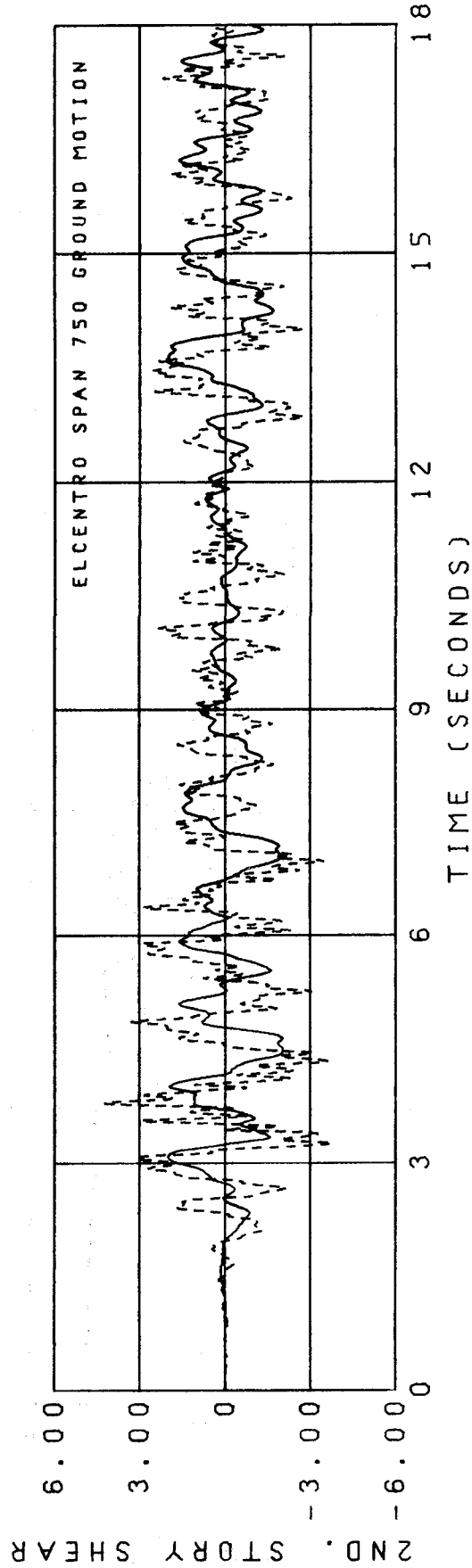


FIGURE 27 SECOND STORY SHEAR TIME HISTORY

— Optimal Design
 ---- Initial Design

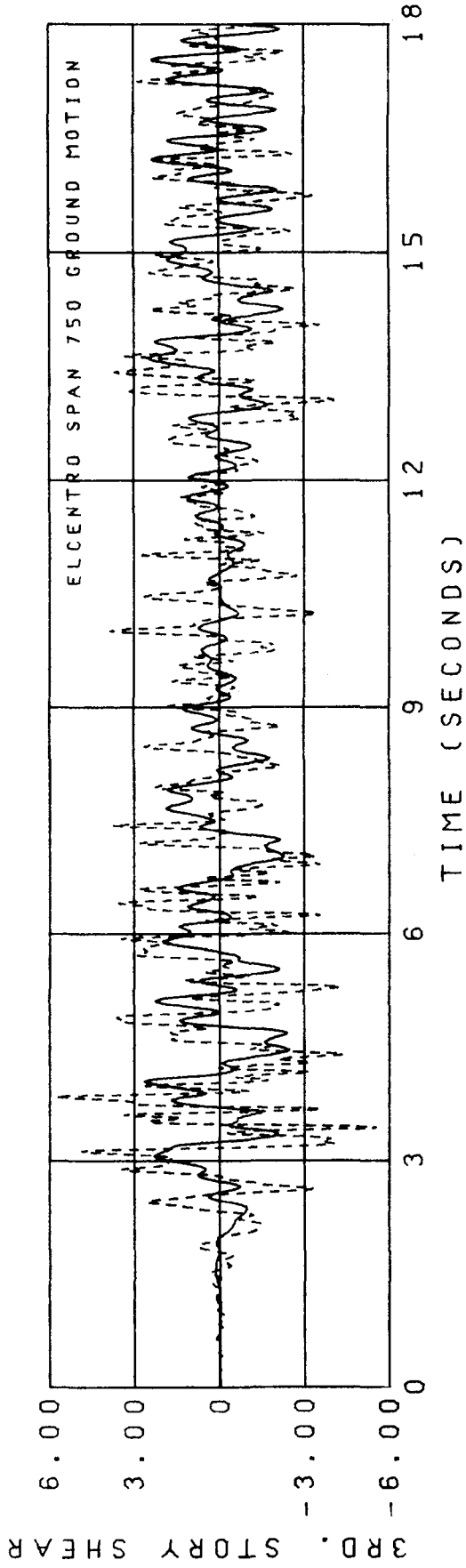


FIGURE 28 THIRD STORY SHEAR TIME HISTORY

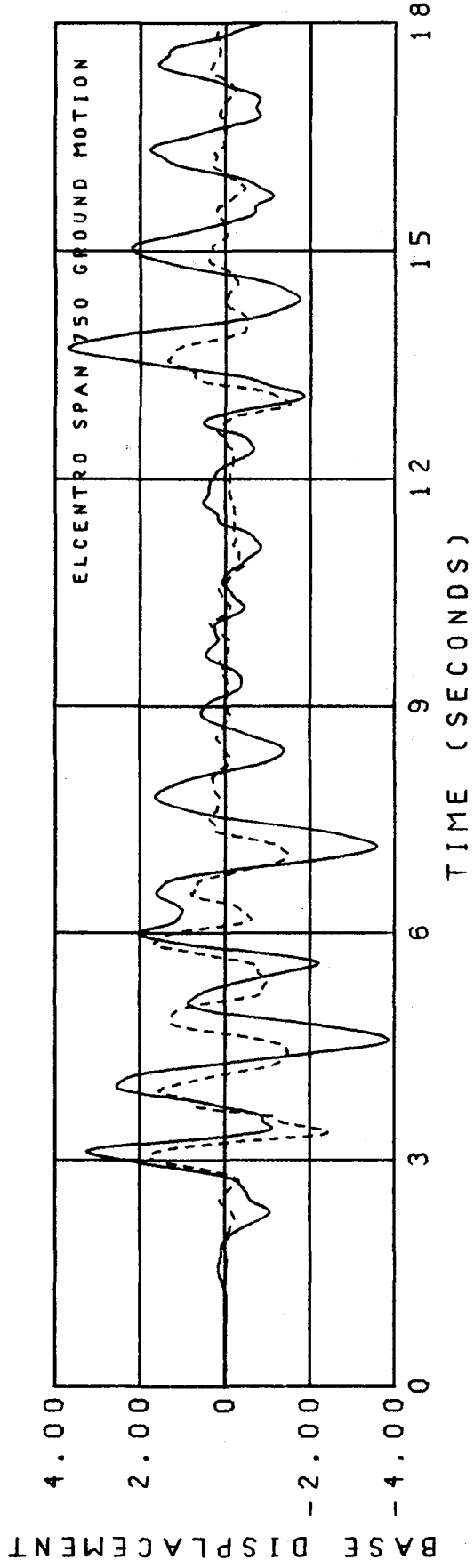
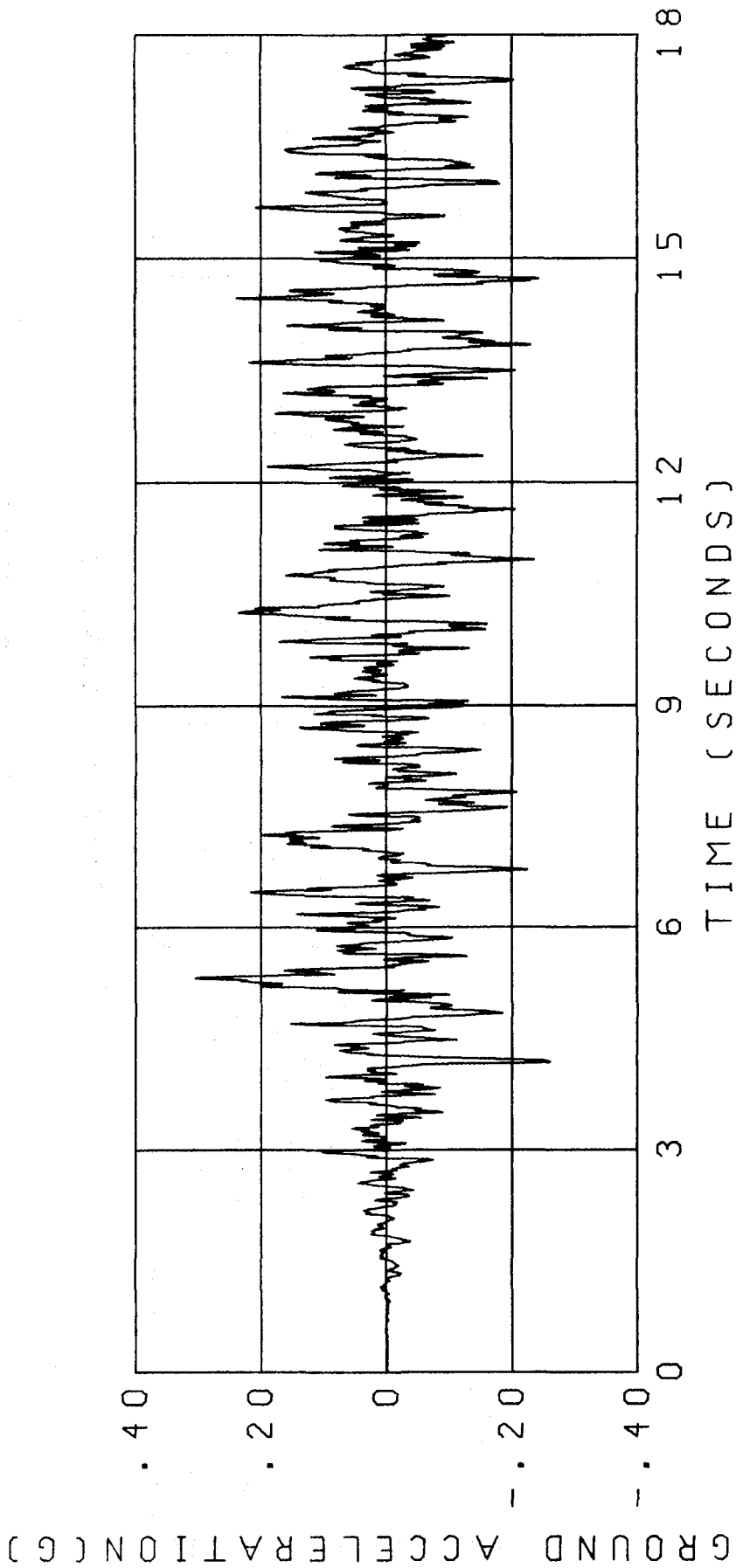


FIGURE 29 BASE DISPLACEMENT TIME HISTORY

— Optimal Design
- - - Initial Design



ARTIFICIAL ACCELEROGRAM NO. 1

FIGURE 30(a)

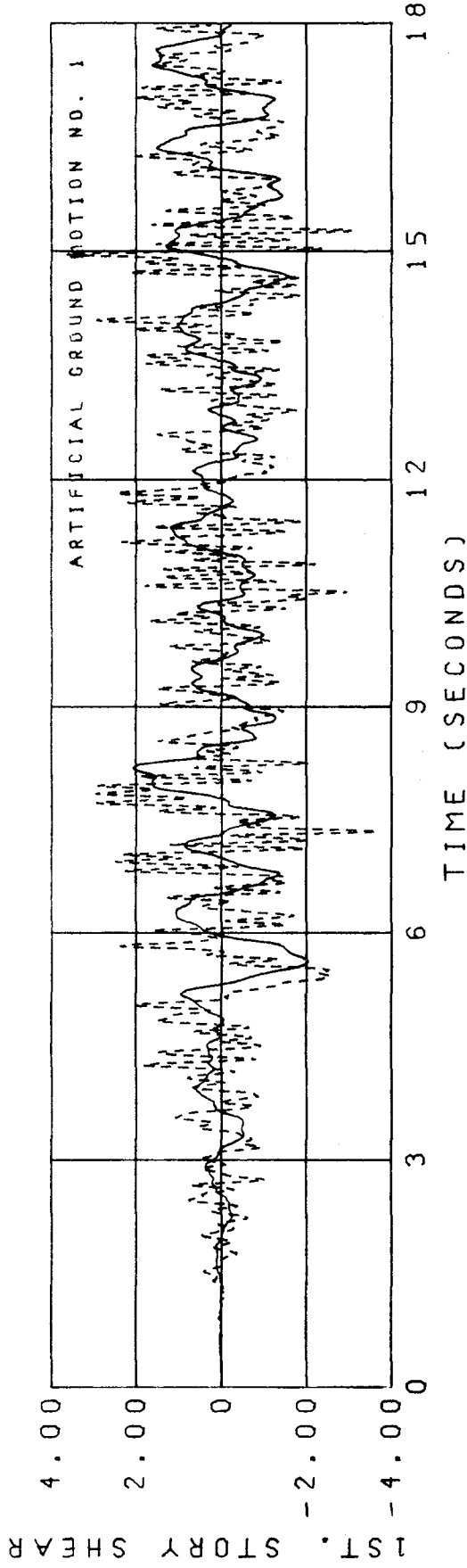


FIGURE 30(b) FIRST STORY SHEAR TIME HISTORY

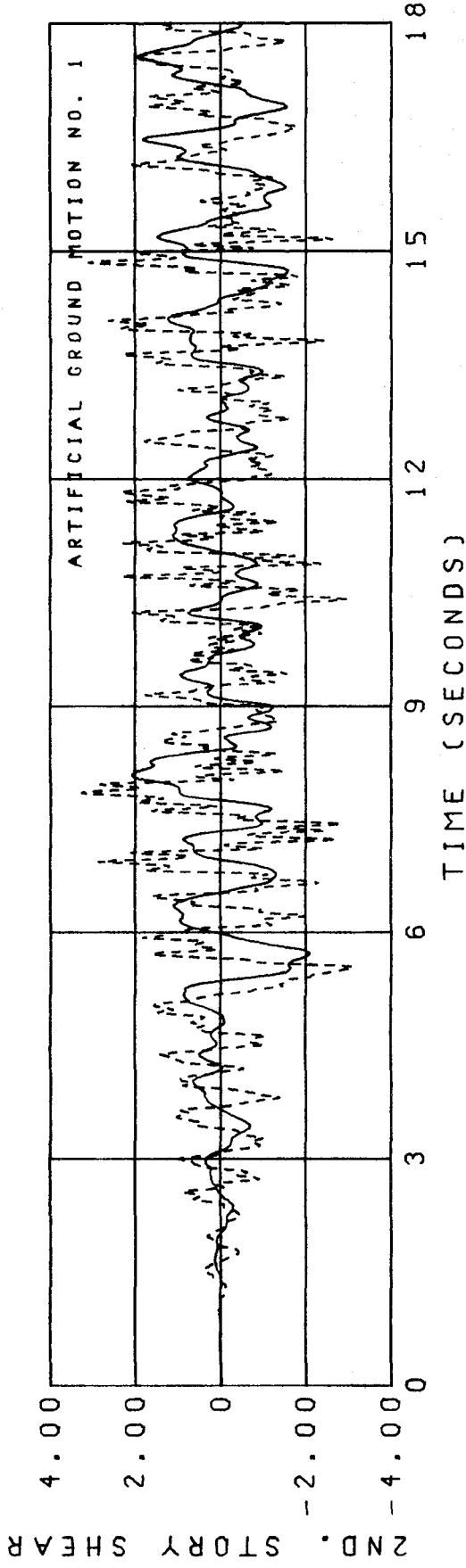


FIGURE 30(c) SECOND STORY SHEAR TIME HISTORY

— Optimal Design
--- Initial Design

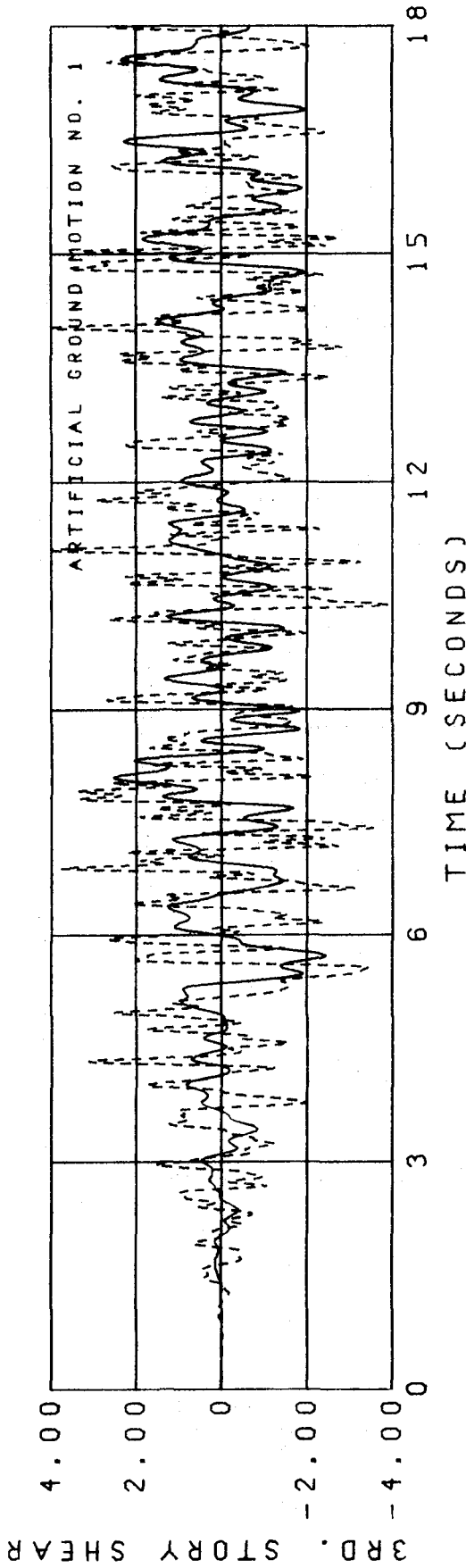


FIGURE 30(d) THIRD STORY SHEAR TIME HISTORY

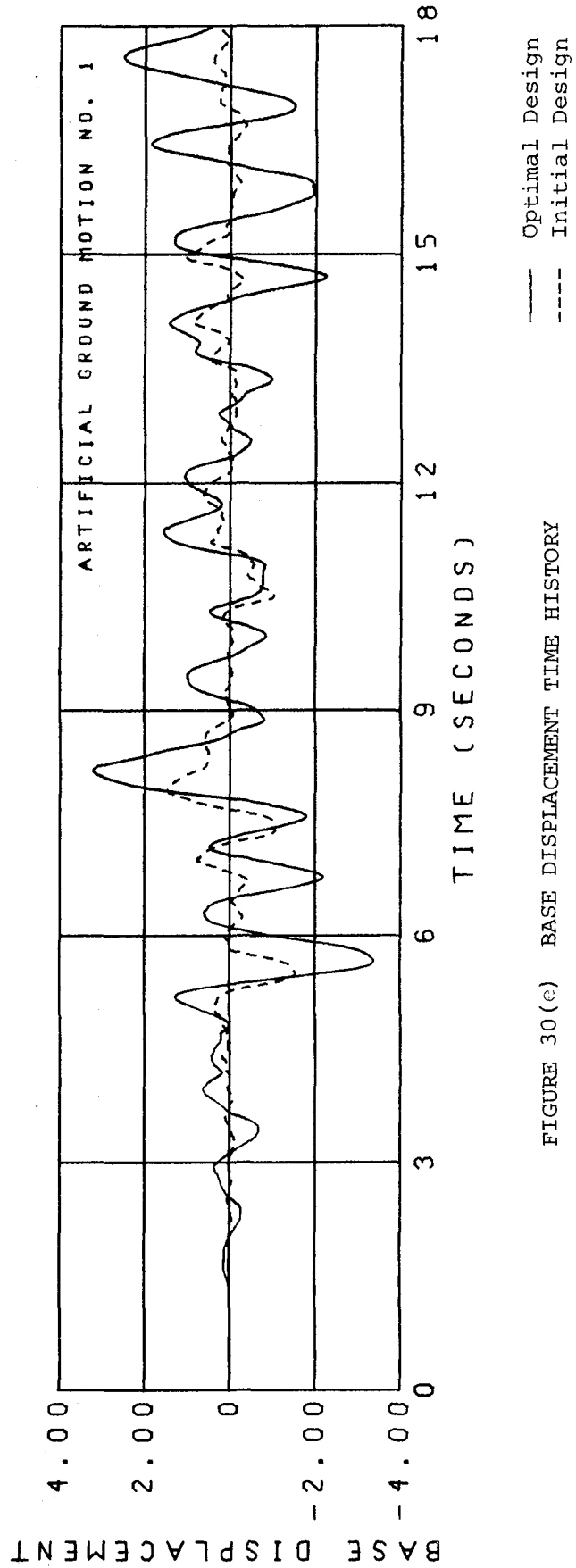
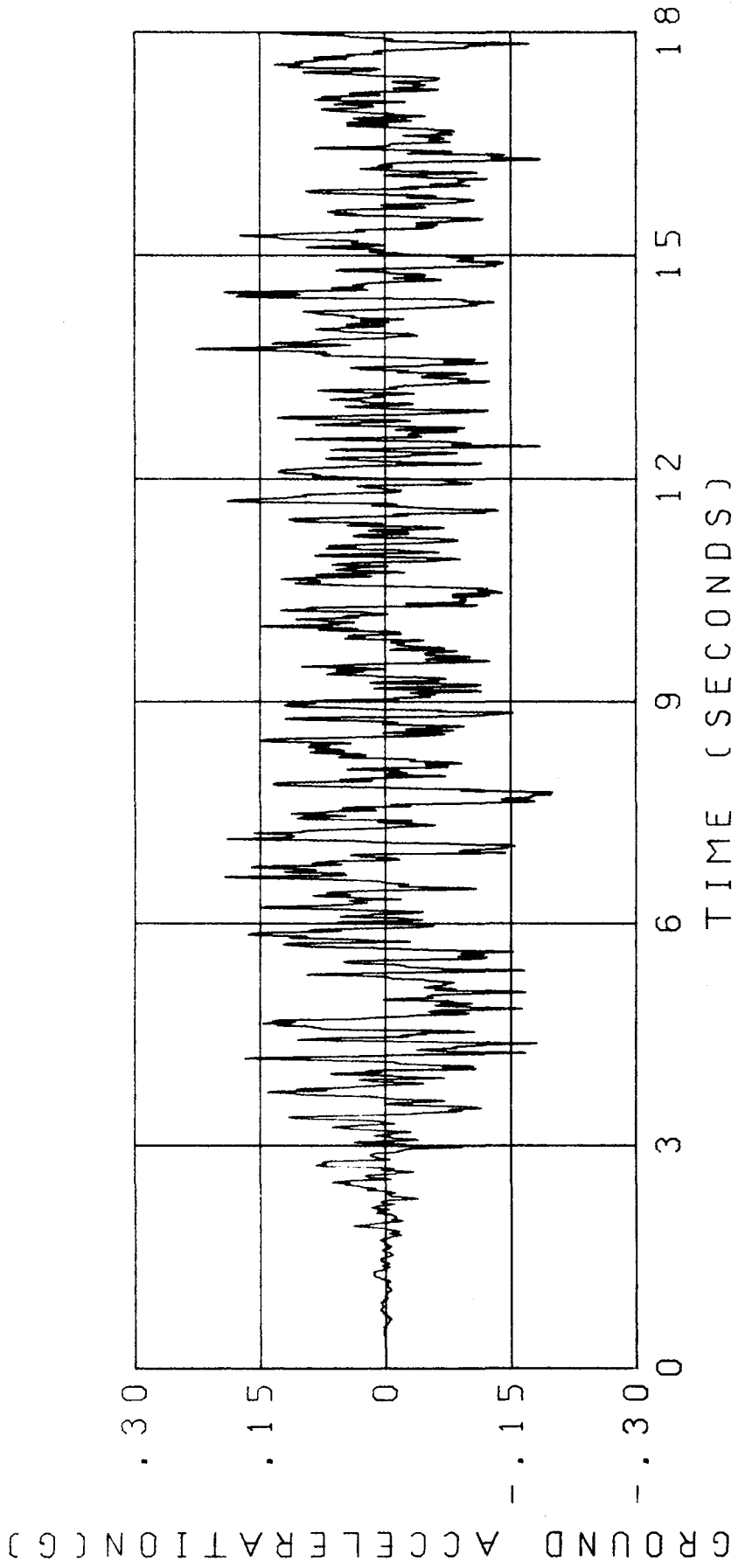


FIGURE 30(e) BASE DISPLACEMENT TIME HISTORY



ARTIFICIAL ACCELEROGRAM NO. 2

FIGURE 31(a)

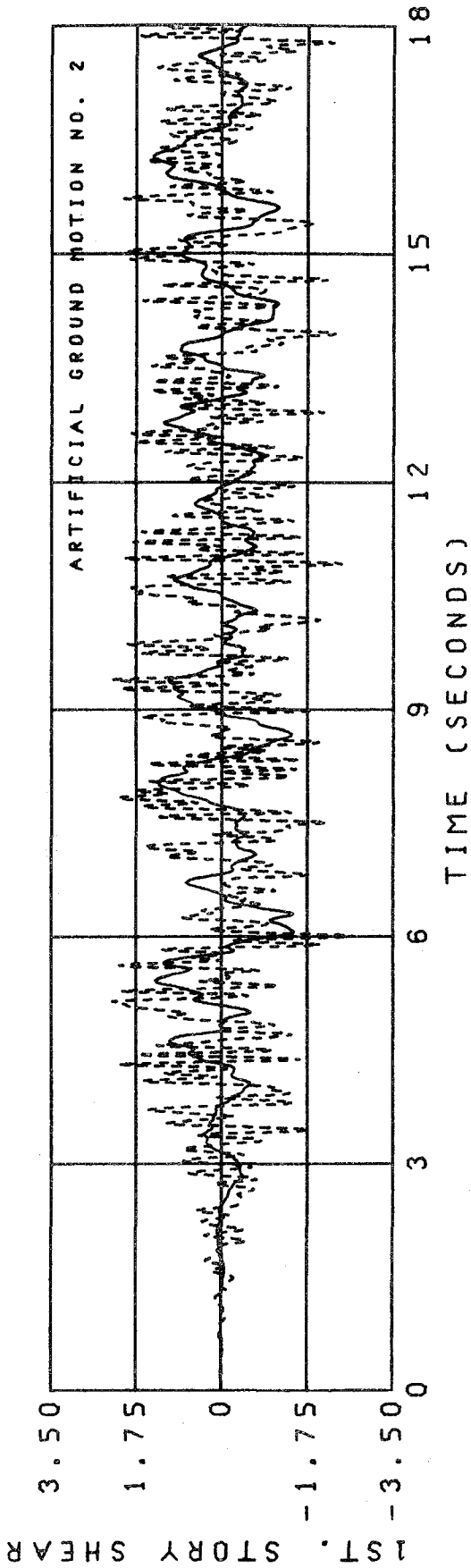


FIGURE 31(b) FIRST STORY SHEAR TIME HISTORY

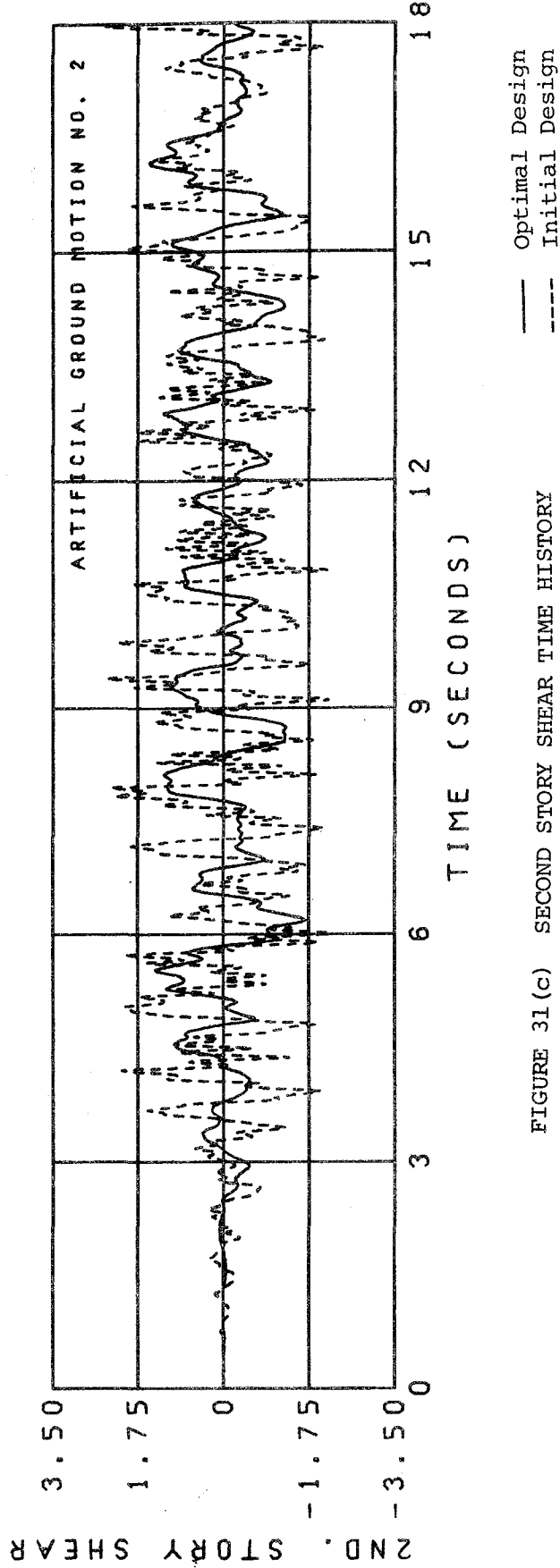


FIGURE 31(c) SECOND STORY SHEAR TIME HISTORY

— Optimal Design
--- Initial Design

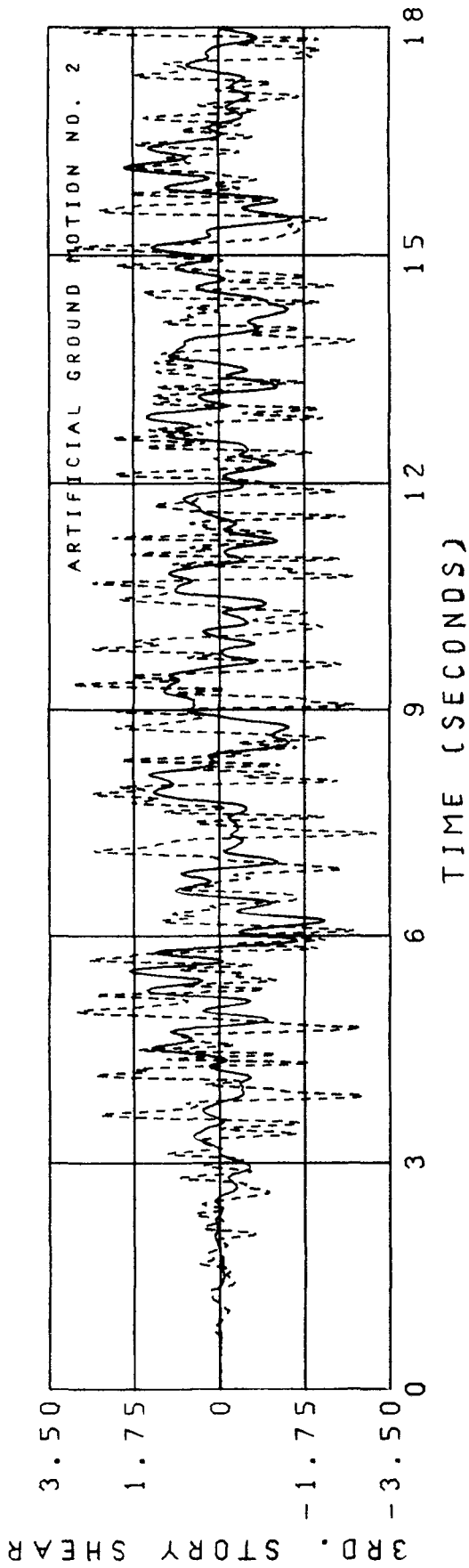


FIGURE 31(d) THIRD STORY SHEAR TIME HISTORY

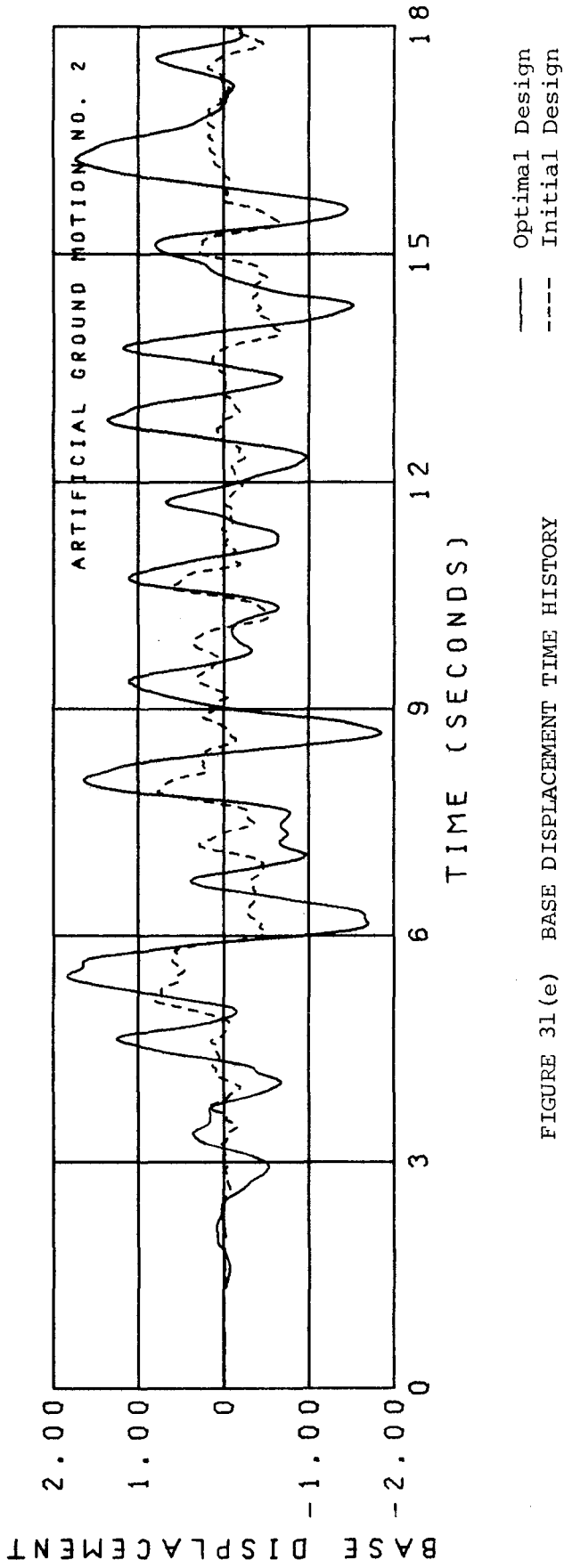
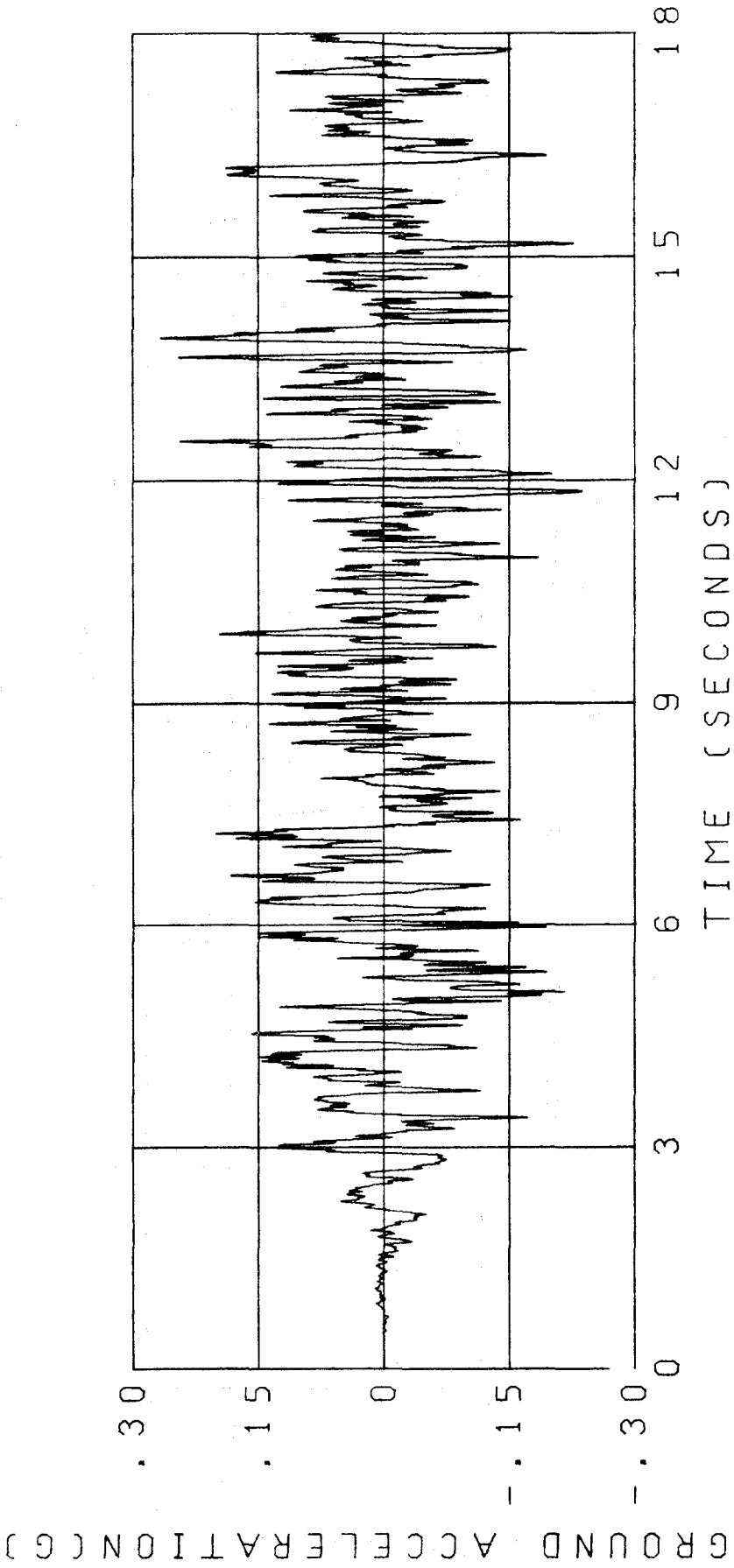


FIGURE 31(e) BASE DISPLACEMENT TIME HISTORY



ARTIFICIAL ACCELEROGRAM NO. 3

FIGURE 32(a)

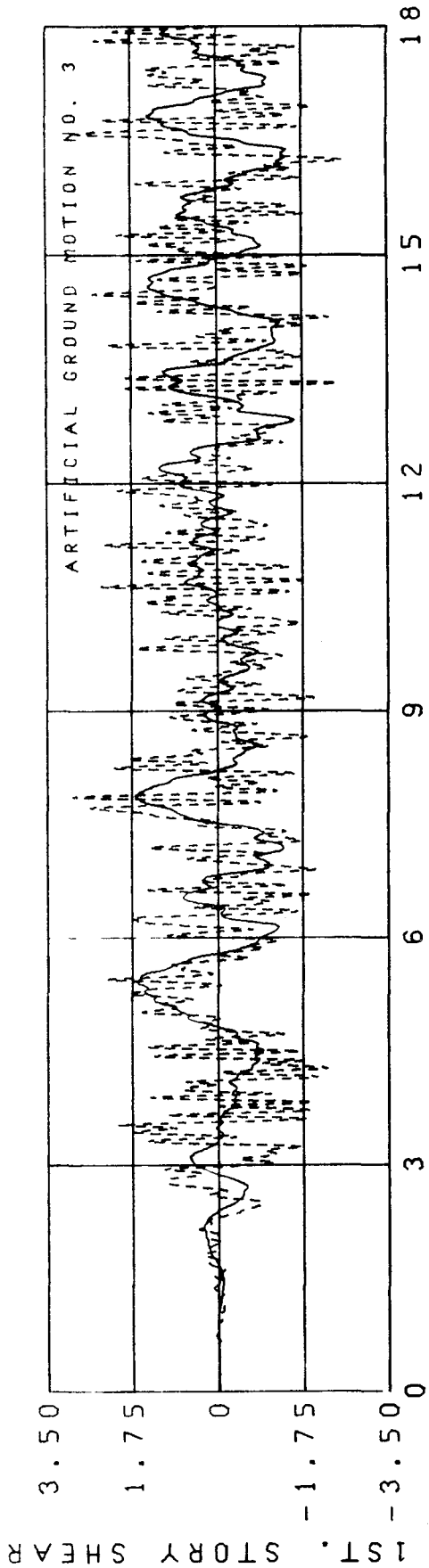


FIGURE 32 (b) FIRST STORY SHEAR TIME HISTORY

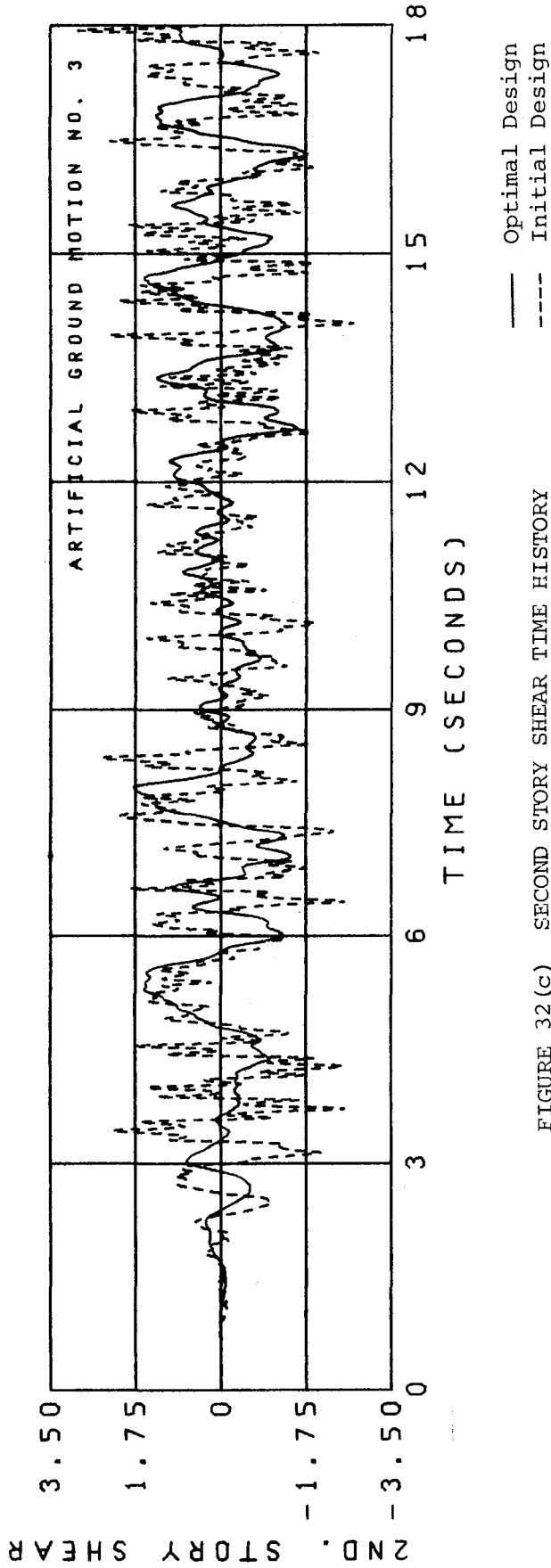


FIGURE 32 (c) SECOND STORY SHEAR TIME HISTORY

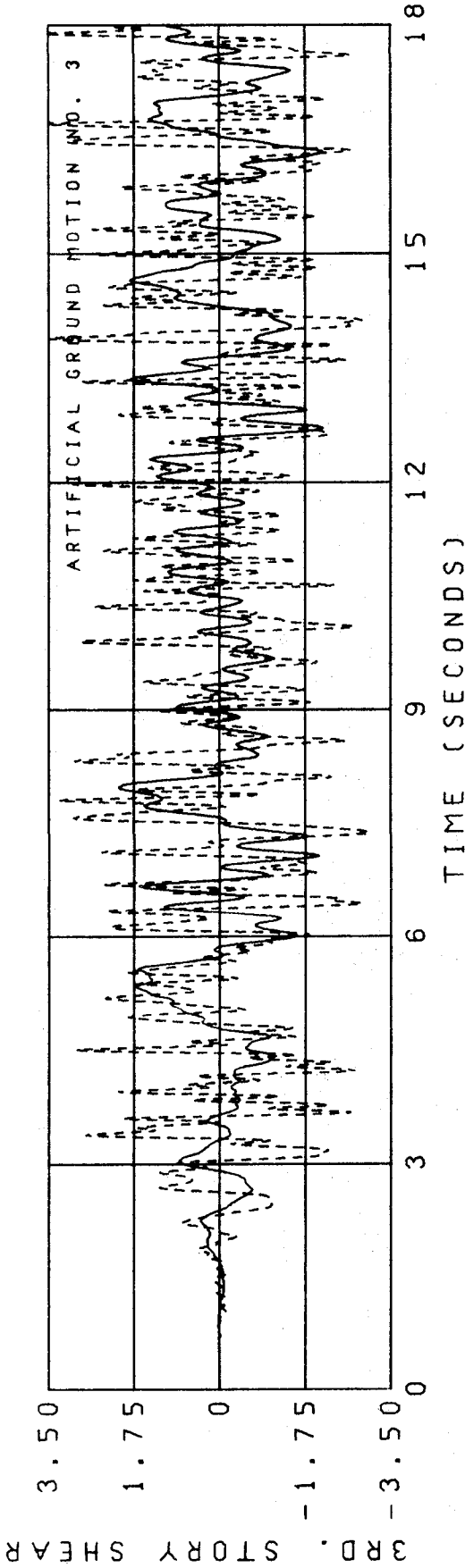


FIGURE 32(d) THIRD STORY SHEAR TIME HISTORY

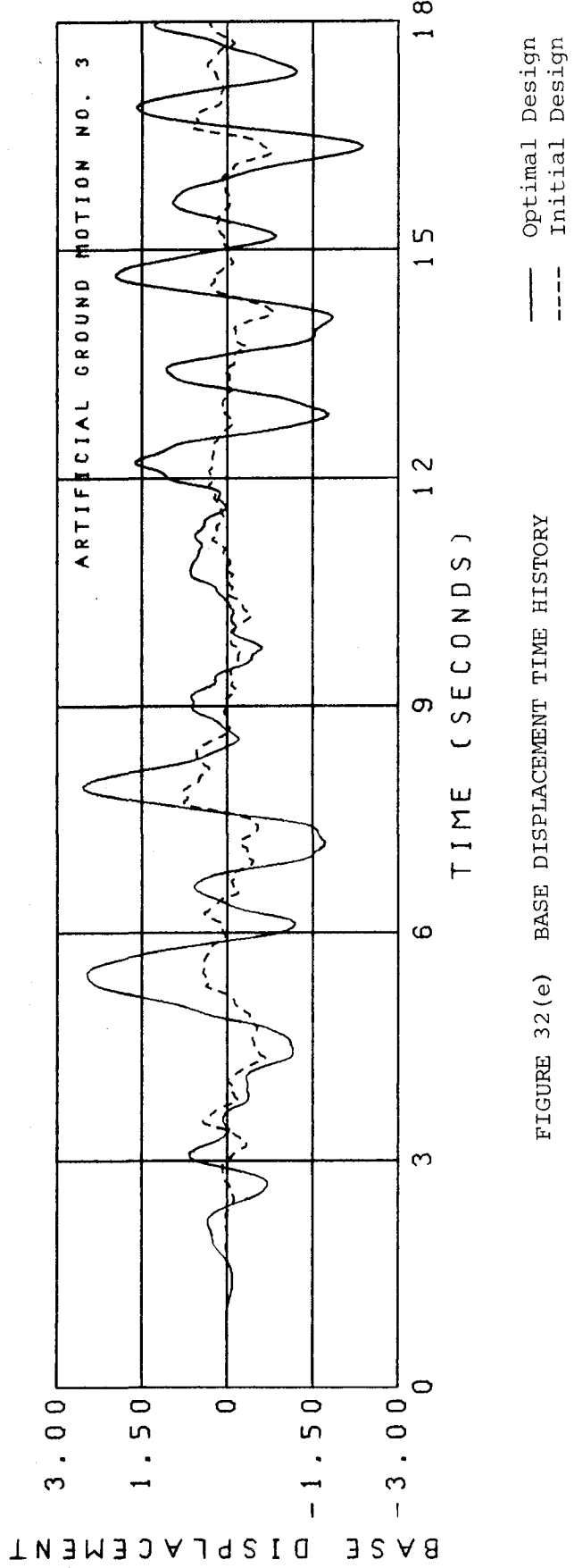
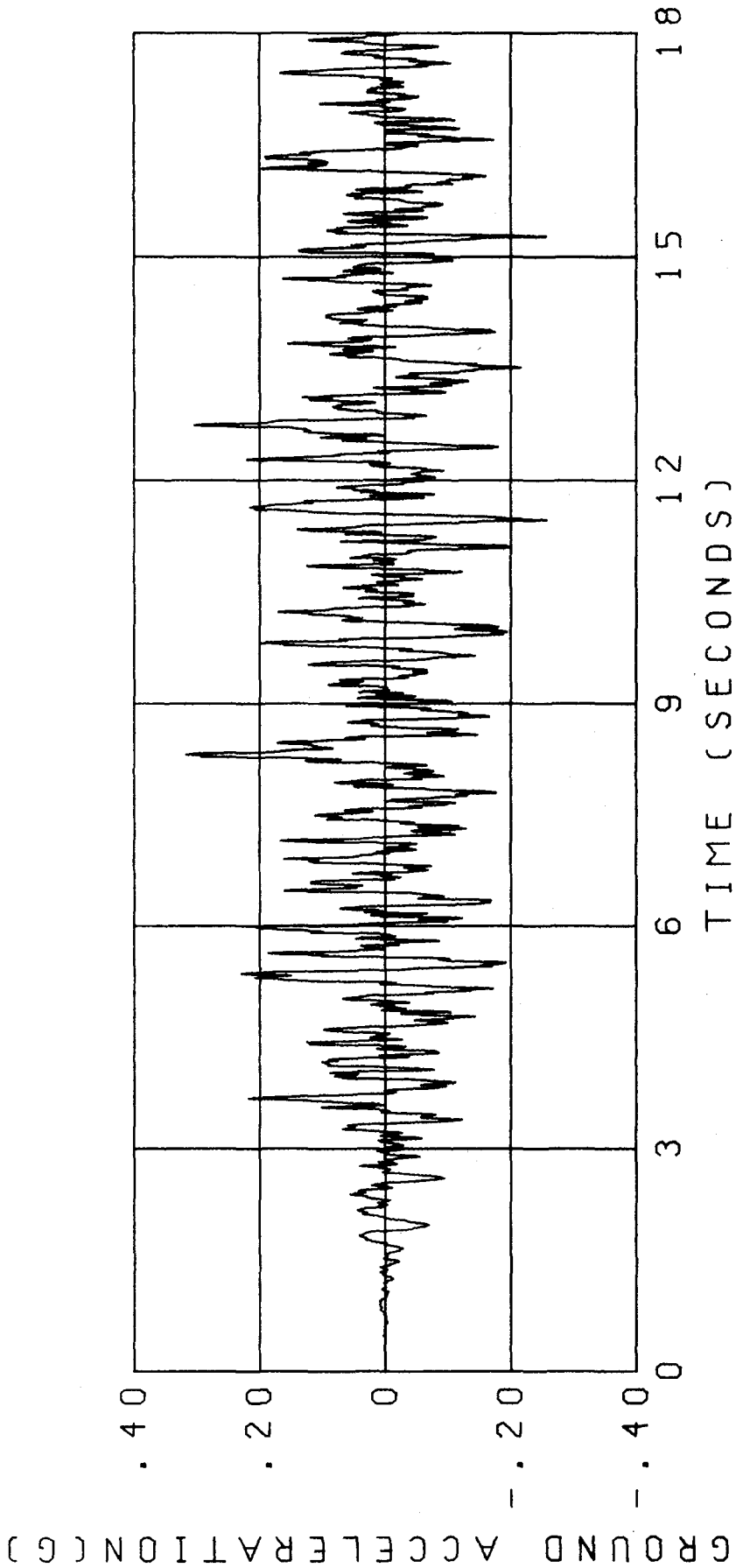


FIGURE 32(e) BASE DISPLACEMENT TIME HISTORY



ARTIFICIAL ACCELEROGRAM NO. 4

FIGURE 33 (a)

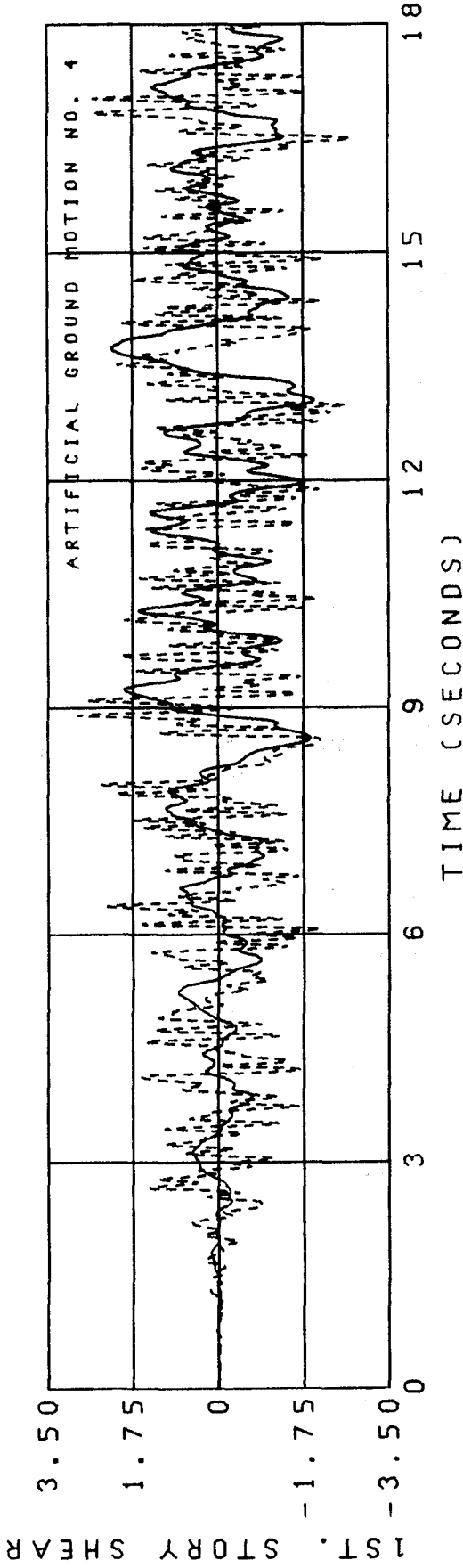


FIGURE 33(b)

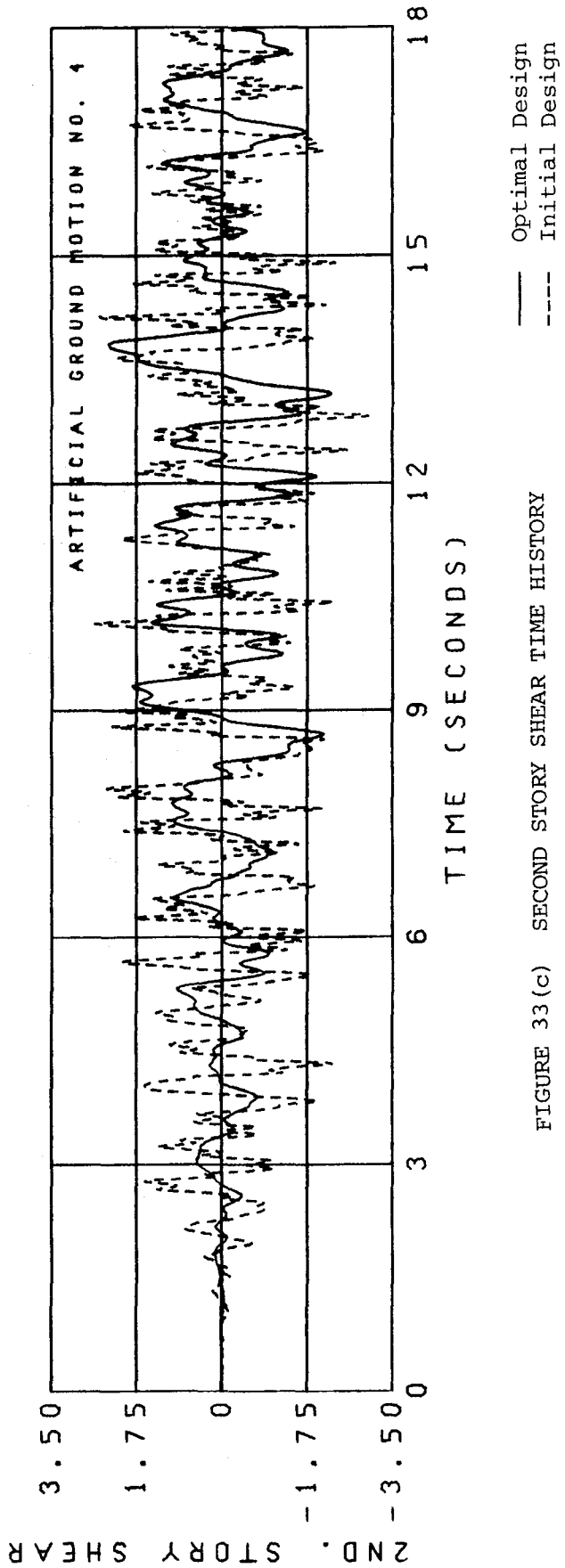


FIGURE 33(c)

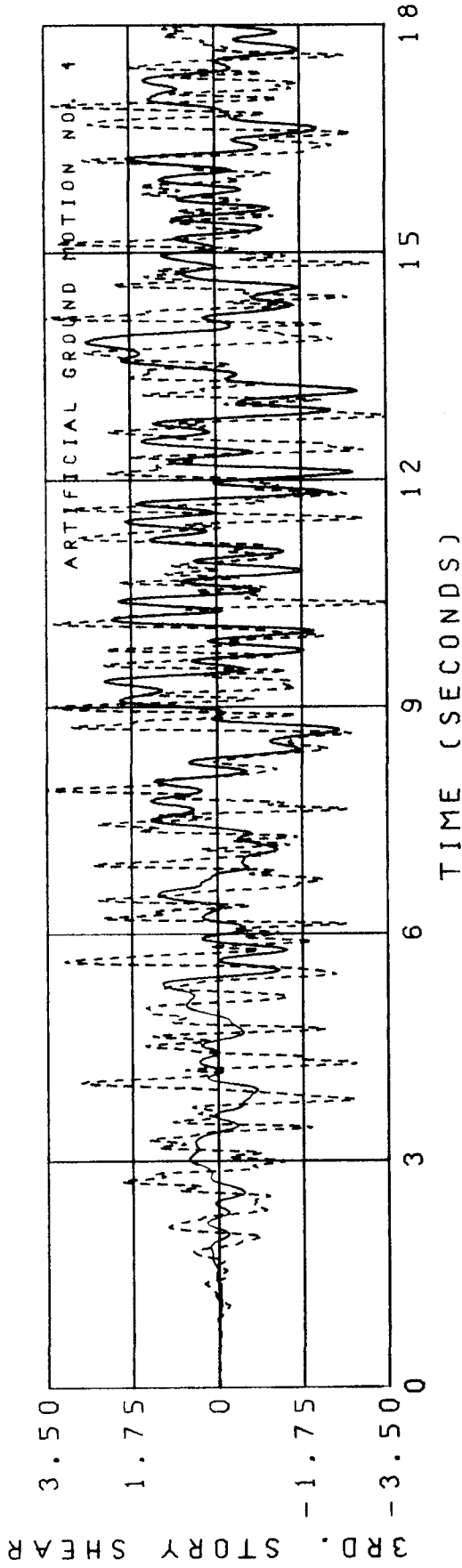


FIGURE 33(d) THIRD STORY SHEAR TIME HISTORY

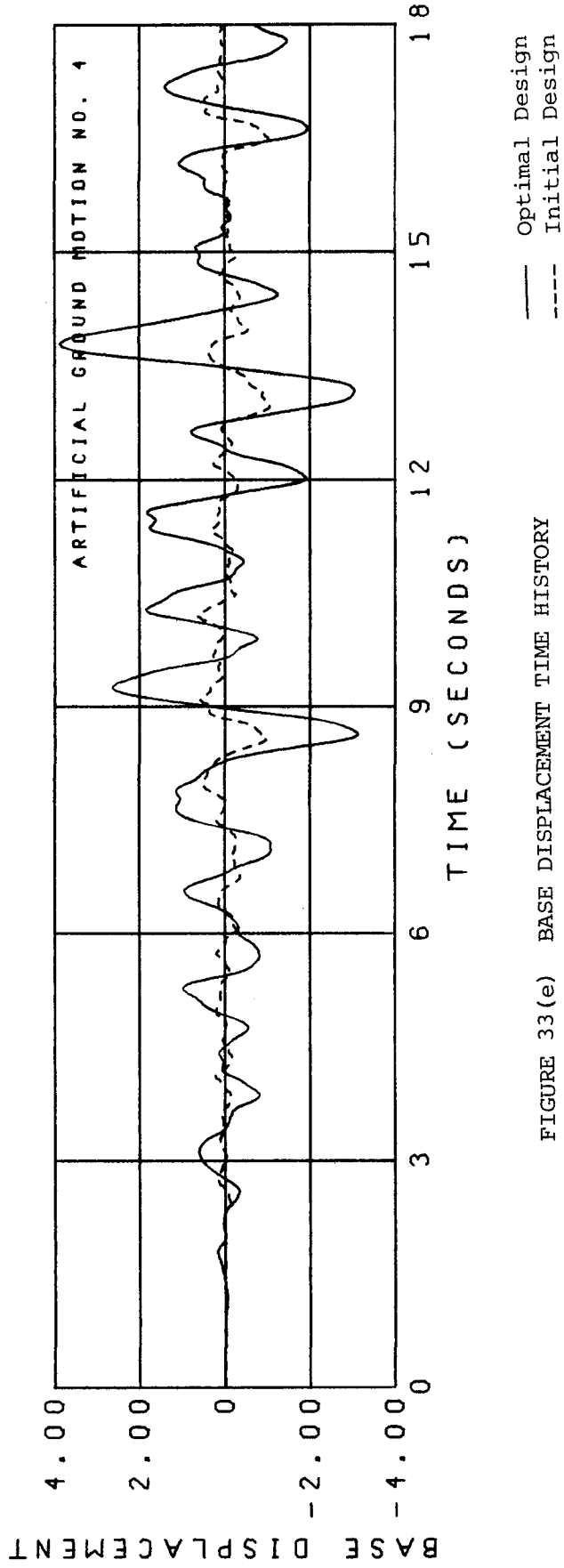
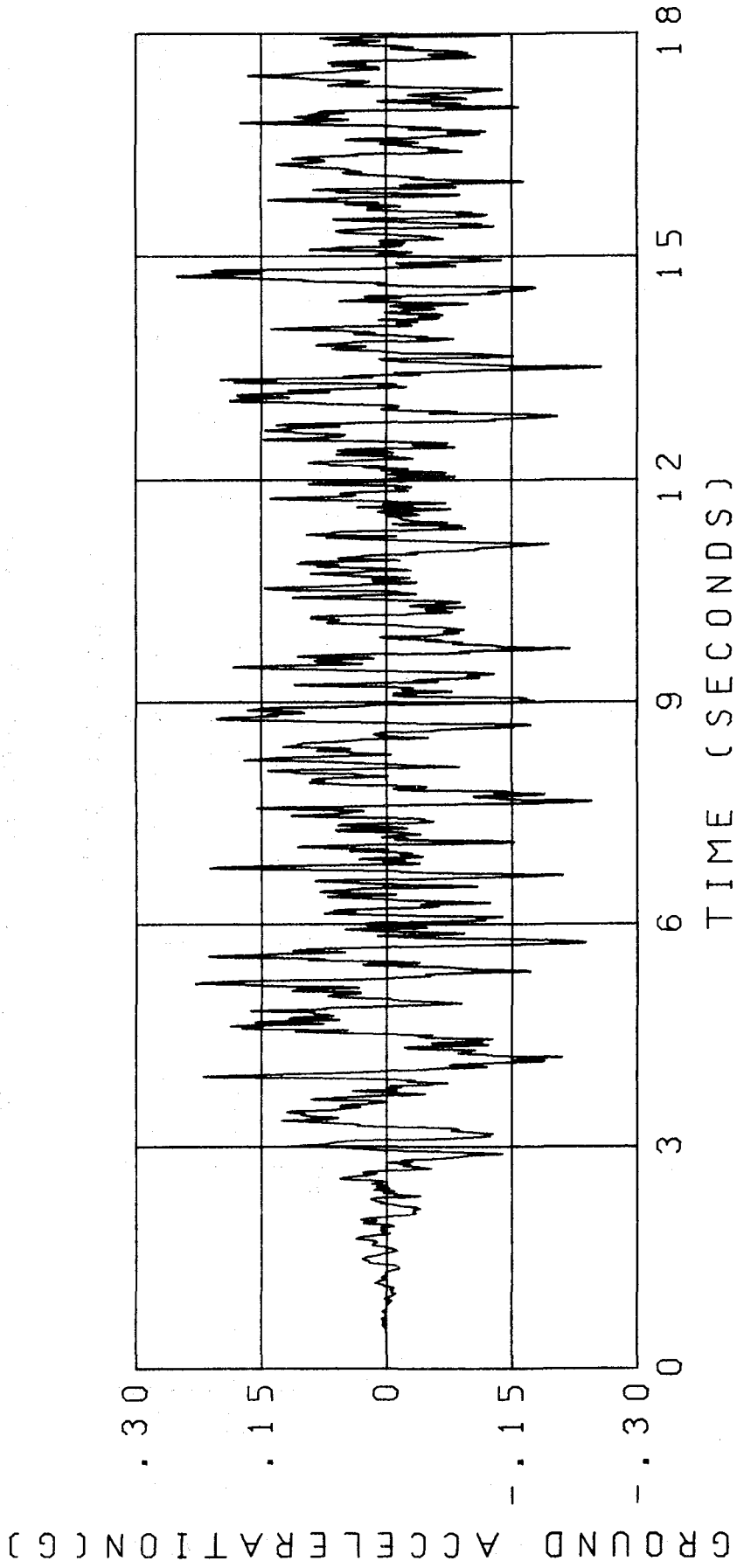


FIGURE 33(e) BASE DISPLACEMENT TIME HISTORY



ARTIFICIAL ACCELEROGRAM NO. 5

FIGURE 34 (a)

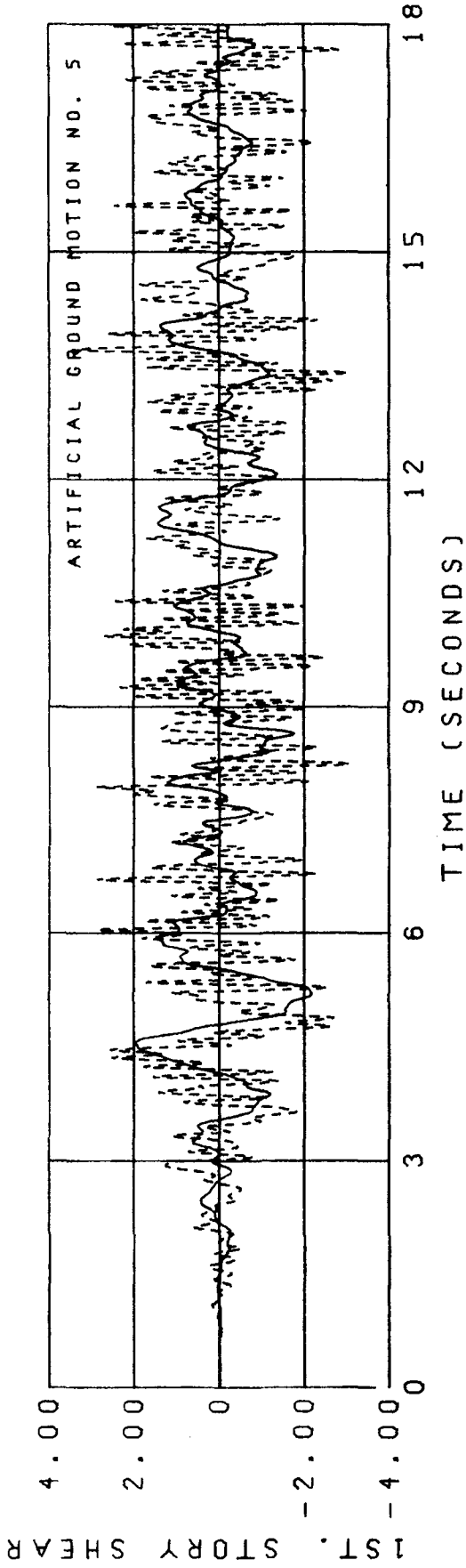


FIGURE 34(b) FIRST STORY SHEAR TIME HISTORY

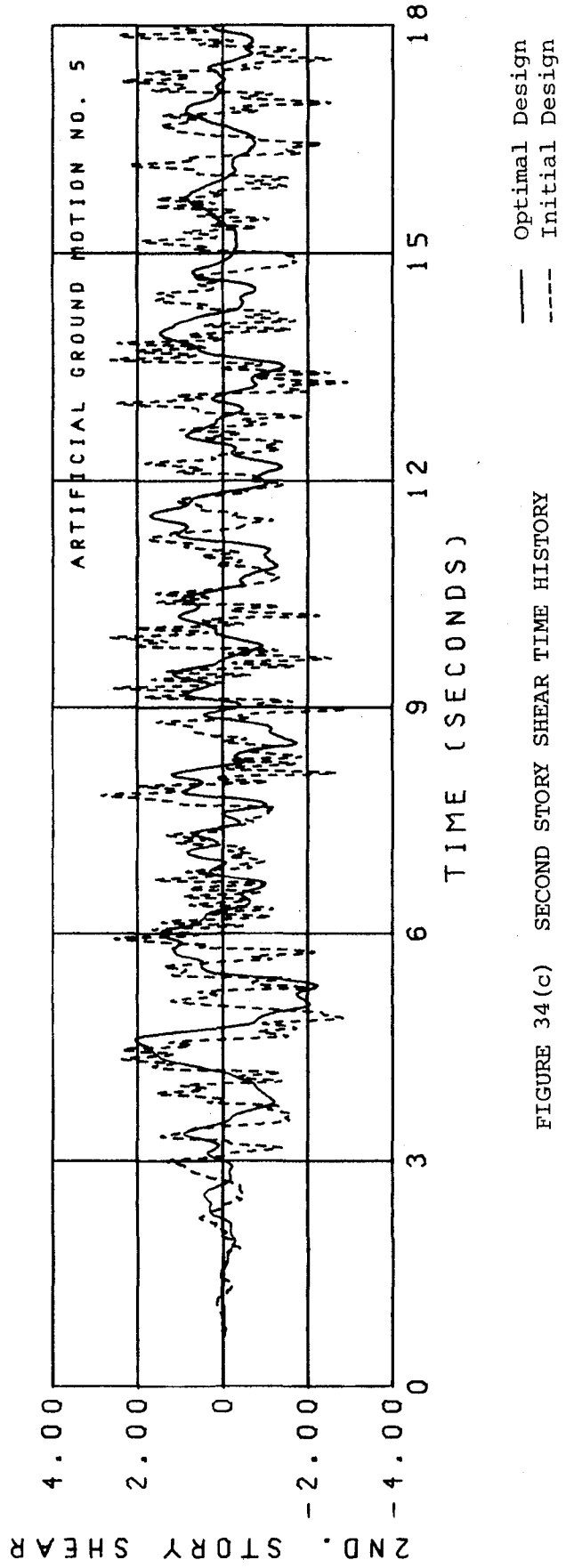


FIGURE 34(c) SECOND STORY SHEAR TIME HISTORY

— Optimal Design
--- Initial Design

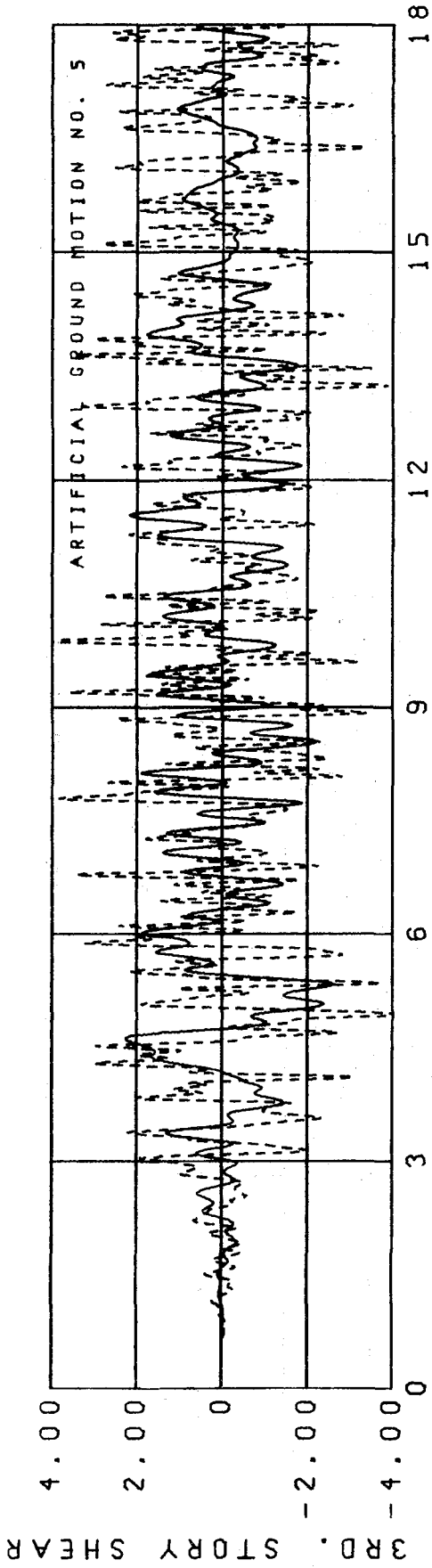


FIGURE 34 (d) THIRD STORY SHEAR TIME HISTORY

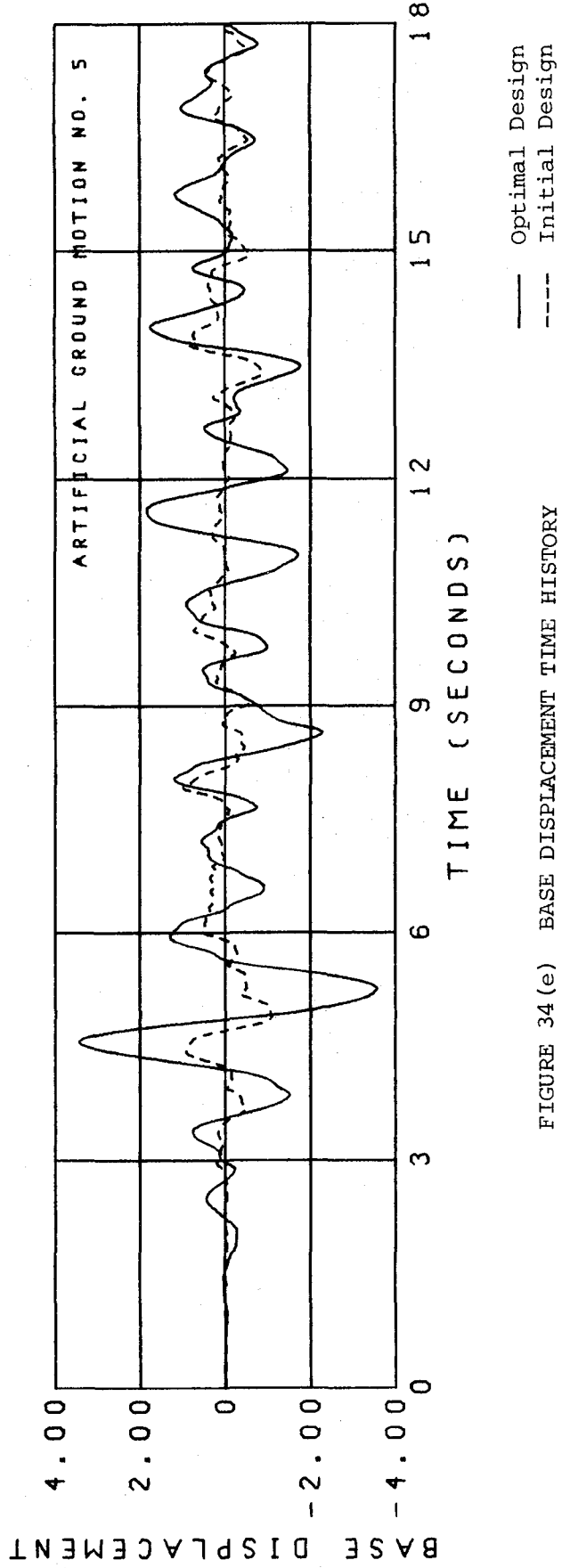


FIGURE 34 (e) BASE DISPLACEMENT TIME HISTORY

— Optimal Design
--- Initial Design

EARTHQUAKE ENGINEERING RESEARCH CENTER REPORTS

NOTE: Numbers in parenthesis are Accession Numbers assigned by the National Technical Information Service; these are followed by a price code. Copies of the reports may be ordered from the National Technical Information Service, 5200 Port Royal Road, Springfield, Virginia, 22161. Accession Numbers should be quoted on orders for reports (PB --- ---) and remittance must accompany each order. Reports without this information were not available at time of printing. Upon request, EERC will mail inquirers this information when it becomes available.

- EERC 67-1 "Feasibility Study Large-Scale Earthquake Simulator Facility," by J. Penzien, J.G. Bouwkamp, R.W. Clough and D. Rea - 1967 (PB 187 905)A07
- EERC 68-1 Unassigned
- EERC 68-2 "Inelastic Behavior of Beam-to-Column Subassemblages Under Repeated Loading," by V.V. Bertero - 1968 (PB 184 888)A05
- EERC 68-3 "A Graphical Method for Solving the Wave Reflection-Refraction Problem," by H.D. McNiven and Y. Mengi - 1968 (PB 187 943)A03
- EERC 68-4 "Dynamic Properties of McKinley School Buildings," by D. Rea, J.G. Bouwkamp and R.W. Clough - 1968 (PB 187 902)A07
- EERC 68-5 "Characteristics of Rock Motions During Earthquakes," by H.B. Seed, I.M. Idriss and F.W. Kiefer - 1968 (PB 188 338)A03
- EERC 69-1 "Earthquake Engineering Research at Berkeley," - 1969 (PB 187 906)A11
- EERC 69-2 "Nonlinear Seismic Response of Earth Structures," by M. Dibaj and J. Penzien - 1969 (PB 187 904)A08
- EERC 69-3 "Probabilistic Study of the Behavior of Structures During Earthquakes," by R. Ruiz and J. Penzien - 1969 (PB 187 886)A06
- EERC 69-4 "Numerical Solution of Boundary Value Problems in Structural Mechanics by Reduction to an Initial Value Formulation," by N. Distefano and J. Schujman - 1969 (PB 187 942)A02
- EERC 69-5 "Dynamic Programming and the Solution of the Biharmonic Equation," by N. Distefano - 1969 (PB 187 941)A03
- EERC 69-6 "Stochastic Analysis of Offshore Tower Structures," by A.K. Malhotra and J. Penzien - 1969 (PB 187 903)A06
- EERC 69-7 "Rock Motion Accelerograms for High Magnitude Earthquakes," by H.B. Seed and I.M. Idriss - 1969 (PB 187 940)A02
- EERC 69-8 "Structural Dynamics Testing Facilities at the University of California, Berkeley," by R.M. Stephen, J.G. Bouwkamp, R.W. Clough and J. Penzien - 1969 (PB 189 111)A04
- EERC 69-9 "Seismic Response of Soil Deposits Underlain by Sloping Rock Boundaries," by H. Dezfulian and H.B. Seed - 1969 (PB 189 114)A03
- EERC 69-10 "Dynamic Stress Analysis of Axisymmetric Structures Under Arbitrary Loading," by S. Ghosh and E.L. Wilson - 1969 (PB 189 026)A10
- EERC 69-11 "Seismic Behavior of Multistory Frames Designed by Different Philosophies," by J.C. Anderson and V. V. Bertero - 1969 (PB 190 662)A10
- EERC 69-12 "Stiffness Degradation of Reinforcing Concrete Members Subjected to Cyclic Flexural Moments," by V.V. Bertero, B. Bresler and H. Ming Liao - 1969 (PB 202 942)A07
- EERC 69-13 "Response of Non-Uniform Soil Deposits to Travelling Seismic Waves," by H. Dezfulian and H.B. Seed - 1969 (PB 191 023)A03
- EERC 69-14 "Damping Capacity of a Model Steel Structure," by D. Rea, R.W. Clough and J.G. Bouwkamp - 1969 (PB 190 663)A06
- EERC 69-15 "Influence of Local Soil Conditions on Building Damage Potential during Earthquakes," by H.B. Seed and I.M. Idriss - 1969 (PB 191 036)A03
- EERC 69-16 "The Behavior of Sands Under Seismic Loading Conditions," by M.L. Silver and H.B. Seed - 1969 (AD 714 982)A07
- EERC 70-1 "Earthquake Response of Gravity Dams," by A.K. Chopra - 1970 (AD 709 640)A03
- EERC 70-2 "Relationships between Soil Conditions and Building Damage in the Caracas Earthquake of July 29, 1967," by H.B. Seed, I.M. Idriss and H. Dezfulian - 1970 (PB 195 762)A05
- EERC 70-3 "Cyclic Loading of Full Size Steel Connections," by E.P. Popov and R.M. Stephen - 1970 (PB 213 545)A04
- EERC 70-4 "Seismic Analysis of the Charaima Building, Caraballeda, Venezuela," by Subcommittee of the SEAONC Research Committee: V.V. Bertero, P.F. Fratessa, S.A. Mahin, J.H. Sexton, A.C. Scordelis, E.L. Wilson, L.A. Wyllie, H.B. Seed and J. Penzien, Chairman - 1970 (PB 201 455)A06



- EERC 70-5 "A Computer Program for Earthquake Analysis of Dams," by A.K. Chopra and P. Chakrabarti - 1970 (AD 723 994)A05
- EERC 70-6 "The Propagation of Love Waves Across Non-Horizontally Layered Structures," by J. Lysmer and L.A. Drake 1970 (PB 197 896)A03
- EERC 70-7 "Influence of Base Rock Characteristics on Ground Response," by J. Lysmer, H.B. Seed and P.B. Schnabel 1970 (PB 197 897)A03
- EERC 70-8 "Applicability of Laboratory Test Procedures for Measuring Soil Liquefaction Characteristics under Cyclic Loading," by H.B. Seed and W.H. Peacock - 1970 (PB 198 016)A03
- EERC 70-9 "A Simplified Procedure for Evaluating Soil Liquefaction Potential," by H.B. Seed and I.M. Idriss - 1970 (PB 198 009)A03
- EERC 70-10 "Soil Moduli and Damping Factors for Dynamic Response Analysis," by H.B. Seed and I.M. Idriss - 1970 (PB 197 869)A03
- EERC 71-1 "Koyna Earthquake of December 11, 1967 and the Performance of Koyna Dam," by A.K. Chopra and P. Chakrabarti 1971 (AD 731 496)A06
- EERC 71-2 "Preliminary In-Situ Measurements of Anelastic Absorption in Soils Using a Prototype Earthquake Simulator," by R.D. Borcherdt and P.W. Rodgers - 1971 (PB 201 454)A03
- EERC 71-3 "Static and Dynamic Analysis of Inelastic Frame Structures," by F.L. Porter and G.H. Powell - 1971 (PB 210 135)A06
- EERC 71-4 "Research Needs in Limit Design of Reinforced Concrete Structures," by V.V. Bertero - 1971 (PB 202 943)A04
- EERC 71-5 "Dynamic Behavior of a High-Rise Diagonally Braced Steel Building," by D. Rea, A.A. Shah and J.G. Bouwhuis 1971 (PB 203 584)A06
- EERC 71-6 "Dynamic Stress Analysis of Porous Elastic Solids Saturated with Compressible Fluids," by J. Ghaboussi and E. L. Wilson - 1971 (PB 211 396)A06
- EERC 71-7 "Inelastic Behavior of Steel Beam-to-Column Subassemblages," by H. Krawinkler, V.V. Bertero and E.P. Popov 1971 (PB 211 335)A14
- EERC 71-8 "Modification of Seismograph Records for Effects of Local Soil Conditions," by P. Schnabel, H.B. Seed and J. Lysmer - 1971 (PB 214 450)A03
- EERC 72-1 "Static and Earthquake Analysis of Three Dimensional Frame and Shear Wall Buildings," by E.L. Wilson and H.H. Dovey - 1972 (PB 212 904)A05
- EERC 72-2 "Accelerations in Rock for Earthquakes in the Western United States," by P.B. Schnabel and H.B. Seed - 1972 (PB 213 100)A03
- EERC 72-3 "Elastic-Plastic Earthquake Response of Soil-Building Systems," by T. Minami - 1972 (PB 214 868)A08
- EERC 72-4 "Stochastic Inelastic Response of Offshore Towers to Strong Motion Earthquakes," by M.K. Kaul - 1972 (PB 215 713)A05
- EERC 72-5 "Cyclic Behavior of Three Reinforced Concrete Flexural Members with High Shear," by E.P. Popov, V.V. Bertero and H. Krawinkler - 1972 (PB 214 555)A05
- EERC 72-6 "Earthquake Response of Gravity Dams Including Reservoir Interaction Effects," by P. Chakrabarti and A.K. Chopra - 1972 (AD 762 330)A08
- EERC 72-7 "Dynamic Properties of Pine Flat Dam," by D. Rea, C.Y. Liaw and A.K. Chopra - 1972 (AD 763 928)A05
- EERC 72-8 "Three Dimensional Analysis of Building Systems," by E.L. Wilson and H.H. Dovey - 1972 (PB 222 438)A06
- EERC 72-9 "Rate of Loading Effects on Uncracked and Repaired Reinforced Concrete Members," by S. Mahin, V.V. Bertero, D. Rea and M. Atalay - 1972 (PB 224 520)A08
- EERC 72-10 "Computer Program for Static and Dynamic Analysis of Linear Structural Systems," by E.L. Wilson, K.-J. Bathe, J.E. Peterson and H.H. Dovey - 1972 (PB 220 437)A04
- EERC 72-11 "Literature Survey - Seismic Effects on Highway Bridges," by T. Iwasaki, J. Penzien and R.W. Clough - 1972 (PB 215 613)A19
- EERC 72-12 "SHAKE-A Computer Program for Earthquake Response Analysis of Horizontally Layered Sites," by P.B. Schnabel and J. Lysmer - 1972 (PB 220 207)A06
- EERC 73-1 "Optimal Seismic Design of Multistory Frames," by V.V. Bertero and H. Kamil - 1973
- EERC 73-2 "Analysis of the Slides in the San Fernando Dams During the Earthquake of February 9, 1971," by H.B. Seed, K.L. Lee, I.M. Idriss and F. Makdisi - 1973 (PB 223 402)A14

- EERC 73-3 "Computer Aided Ultimate Load Design of Unbraced Multistory Steel Frames," by M.B. El-Hafez and G.H. Powell 1973 (PB 248 315)A09
- EERC 73-4 "Experimental Investigation into the Seismic Behavior of Critical Regions of Reinforced Concrete Components as Influenced by Moment and Shear," by M. Celebi and J. Penzien - 1973 (PB 215 884)A09
- EERC 73-5 "Hysteretic Behavior of Epoxy-Repaired Reinforced Concrete Beams," by M. Celebi and J. Penzien - 1973 (PB 239 568)A03
- EERC 73-6 "General Purpose Computer Program for Inelastic Dynamic Response of Plane Structures," by A. Kanaan and G.H. Powell - 1973 (PB 221 260)A08
- EERC 73-7 "A Computer Program for Earthquake Analysis of Gravity Dams Including Reservoir Interaction," by P. Chakrabarti and A.K. Chopra - 1973 (AD 766 271)A04
- EERC 73-8 "Behavior of Reinforced Concrete Deep Beam-Column Subassemblages Under Cyclic Loads," by O. Küstü and J.G. Bouwkamp - 1973 (PB 246 117)A12
- EERC 73-9 "Earthquake Analysis of Structure-Foundation Systems," by A.K. Vaish and A.K. Chopra - 1973 (AD 766 272)A07
- EERC 73-10 "Deconvolution of Seismic Response for Linear Systems," by R.B. Reimer - 1973 (PB 227 179)A08
- EERC 73-11 "SAP IV: A Structural Analysis Program for Static and Dynamic Response of Linear Systems," by K.-J. Bathe, E.L. Wilson and F.E. Peterson - 1973 (PB 221 967)A09
- EERC 73-12 "Analytical Investigations of the Seismic Response of Long, Multiple Span Highway Bridges," by W.S. Tseng and J. Penzien - 1973 (PB 227 816)A10
- EERC 73-13 "Earthquake Analysis of Multi-Story Buildings Including Foundation Interaction," by A.K. Chopra and J.A. Gutierrez - 1973 (PB 222 970)A03
- EERC 73-14 "ADAP: A Computer Program for Static and Dynamic Analysis of Arch Dams," by R.W. Clough, J.M. Raphael and S. Mojtahedi - 1973 (PB 223 763)A09
- EERC 73-15 "Cyclic Plastic Analysis of Structural Steel Joints," by R.B. Pinkney and R.W. Clough - 1973 (PB 226 843)A08
- EERC 73-16 "QUAD-4: A Computer Program for Evaluating the Seismic Response of Soil Structures by Variable Damping Finite Element Procedures," by I.M. Idriss, J. Lysmer, R. Hwang and H.B. Seed - 1973 (PB 229 424)A05
- EERC 73-17 "Dynamic Behavior of a Multi-Story Pyramid Shaped Building," by R.M. Stephen, J.P. Hollings and J.G. Bouwkamp - 1973 (PB 240 718)A06
- EERC 73-18 "Effect of Different Types of Reinforcing on Seismic Behavior of Short Concrete Columns," by V.V. Bertero, J. Hollings, O. Küstü, R.M. Stephen and J.G. Bouwkamp - 1973
- EERC 73-19 "Olive View Medical Center Materials Studies, Phase I," by B. Bresler and V.V. Bertero - 1973 (PB 235 986)A06
- EERC 73-20 "Linear and Nonlinear Seismic Analysis Computer Programs for Long Multiple-Span Highway Bridges," by W.S. Tseng and J. Penzien - 1973
- EERC 73-21 "Constitutive Models for Cyclic Plastic Deformation of Engineering Materials," by J.M. Kelly and P.P. Gillis 1973 (PB 226 024)A03
- EERC 73-22 "DRAIN - 2D User's Guide," by G.H. Powell - 1973 (PB 227 016)A05
- EERC 73-23 "Earthquake Engineering at Berkeley - 1973," (PB 226 033)A11
- EERC 73-24 Unassigned
- EERC 73-25 "Earthquake Response of Axisymmetric Tower Structures Surrounded by Water," by C.Y. Liaw and A.K. Chopra 1973 (AD 773 052)A09
- EERC 73-26 "Investigation of the Failures of the Olive View Stairtowers During the San Fernando Earthquake and Their Implications on Seismic Design," by V.V. Bertero and R.G. Collins - 1973 (PB 235 106)A13
- EERC 73-27 "Further Studies on Seismic Behavior of Steel Beam-Column Subassemblages," by V.V. Bertero, H. Krawinkler and E.P. Popov - 1973 (PB 234 172)A06
- EERC 74-1 "Seismic Risk Analysis," by C.S. Oliveira - 1974 (PB 235 920)A06
- EERC 74-2 "Settlement and Liquefaction of Sands Under Multi-Directional Shaking," by R. Pyke, C.K. Chan and H.B. Seed 1974
- EERC 74-3 "Optimum Design of Earthquake Resistant Shear Buildings," by D. Ray, K.S. Pister and A.K. Chopra - 1974 (PB 231 172)A06
- EERC 74-4 "LUSH - A Computer Program for Complex Response Analysis of Soil-Structure Systems," by J. Lysmer, T. Udaka, H.B. Seed and R. Hwang - 1974 (PB 236 796)A05

- EERC 74-5 "Sensitivity Analysis for Hysteretic Dynamic Systems: Applications to Earthquake Engineering," by D. Ray 1974 (PB 233 213)A06
- EERC 74-6 "Soil Structure Interaction Analyses for Evaluating Seismic Response," by H.B. Seed, J. Lysmer and R. Hwang 1974 (PB 236 519)A04
- EERC 74-7 Unassigned
- EERC 74-8 "Shaking Table Tests of a Steel Frame - A Progress Report," by R.W. Clough and D. Tang - 1974 (PB 240 869)A03
- EERC 74-9 "Hysteretic Behavior of Reinforced Concrete Flexural Members with Special Web Reinforcement," by V.V. Bertero, E.P. Popov and T.Y. Wang - 1974 (PB 236 797)A07
- EERC 74-10 "Applications of Reliability-Based, Global Cost Optimization to Design of Earthquake Resistant Structures," by E. Vitiello and K.S. Pister - 1974 (PB 237 231)A06
- EERC 74-11 "Liquefaction of Gravelly Soils Under Cyclic Loading Conditions," by R.T. Wong, H.B. Seed and C.K. Chan 1974 (PB 242 042)A03
- EERC 74-12 "Site-Dependent Spectra for Earthquake-Resistant Design," by H.B. Seed, C. Ugas and J. Lysmer - 1974 (PB 240 953)A03
- EERC 74-13 "Earthquake Simulator Study of a Reinforced Concrete Frame," by P. Hidalgo and R.W. Clough - 1974 (PB 241 944)A13
- EERC 74-14 "Nonlinear Earthquake Response of Concrete Gravity Dams," by N. Pal - 1974 (AD/A 006 583)A06
- EERC 74-15 "Modeling and Identification in Nonlinear Structural Dynamics - I. One Degree of Freedom Models," by N. Distefano and A. Rath - 1974 (PB 241 548)A06
- EERC 75-1 "Determination of Seismic Design Criteria for the Dumbarton Bridge Replacement Structure, Vol. I: Description, Theory and Analytical Modeling of Bridge and Parameters," by F. Baron and S.-H. Pang - 1975 (PB 259 407)A15
- EERC 75-2 "Determination of Seismic Design Criteria for the Dumbarton Bridge Replacement Structure, Vol. II: Numerical Studies and Establishment of Seismic Design Criteria," by F. Baron and S.-H. Pang - 1975 (PB 259 408)A11 (For set of EERC 75-1 and 75-2 (PB 259 406))
- EERC 75-3 "Seismic Risk Analysis for a Site and a Metropolitan Area," by C.S. Oliveira - 1975 (PB 248 134)A09
- EERC 75-4 "Analytical Investigations of Seismic Response of Short, Single or Multiple-Span Highway Bridges," by M.-C. Chen and J. Penzien - 1975 (PB 241 454)A09
- EERC 75-5 "An Evaluation of Some Methods for Predicting Seismic Behavior of Reinforced Concrete Buildings," by S.A. Mahin and V.V. Bertero - 1975 (PB 246 306)A16
- EERC 75-6 "Earthquake Simulator Study of a Steel Frame Structure, Vol. I: Experimental Results," by R.W. Clough and D.T. Tang - 1975 (PB 243 981)A13
- EERC 75-7 "Dynamic Properties of San Bernardino Intake Tower," by D. Rea, C.-Y. Liaw and A.K. Chopra - 1975 (AD/A008 406)A05
- EERC 75-8 "Seismic Studies of the Articulation for the Dumbarton Bridge Replacement Structure, Vol. I: Description, Theory and Analytical Modeling of Bridge Components," by F. Baron and R.E. Hamati - 1975 (PB 251 539)A07
- EERC 75-9 "Seismic Studies of the Articulation for the Dumbarton Bridge Replacement Structure, Vol. 2: Numerical Studies of Steel and Concrete Girder Alternates," by F. Baron and R.E. Hamati - 1975 (PB 251 540)A10
- EERC 75-10 "Static and Dynamic Analysis of Nonlinear Structures," by D.P. Mondkar and G.H. Powell - 1975 (PB 242 434)A08
- EERC 75-11 "Hysteretic Behavior of Steel Columns," by E.P. Popov, V.V. Bertero and S. Chandramouli - 1975 (PB 252 365)A11
- EERC 75-12 "Earthquake Engineering Research Center Library Printed Catalog," - 1975 (PB 243 711)A26
- EERC 75-13 "Three Dimensional Analysis of Building Systems (Extended Version)," by E.L. Wilson, J.P. Hollings and H.H. Dovey - 1975 (PB 243 989)A07
- EERC 75-14 "Determination of Soil Liquefaction Characteristics by Large-Scale Laboratory Tests," by P. De Alba, C.K. Chan and H.B. Seed - 1975 (NUREG 0027)A08
- EERC 75-15 "A Literature Survey - Compressive, Tensile, Bond and Shear Strength of Masonry," by R.L. Mayes and R.W. Clough - 1975 (PB 246 292)A10
- EERC 75-16 "Hysteretic Behavior of Ductile Moment Resisting Reinforced Concrete Frame Components," by V.V. Bertero and E.P. Popov - 1975 (PB 246 388)A05
- EERC 75-17 "Relationships Between Maximum Acceleration, Maximum Velocity, Distance from Source, Local Site Conditions for Moderately Strong Earthquakes," by H.B. Seed, R. Murarka, J. Lysmer and I.M. Idriss - 1975 (PB 248 172)A03
- EERC 75-18 "The Effects of Method of Sample Preparation on the Cyclic Stress-Strain Behavior of Sands," by J. Mulilis, C.K. Chan and H.B. Seed - 1975 (Summarized in EERC 75-28)

- EERC 75-19 "The Seismic Behavior of Critical Regions of Reinforced Concrete Components as Influenced by Moment, Shear and Axial Force," by M.B. Atalay and J. Penzien - 1975 (PB 258 842)A11
- EERC 75-20 "Dynamic Properties of an Eleven Story Masonry Building," by R.M. Stephen, J.P. Hollings, J.G. Bouwkamp and D. Jurukovski - 1975 (PB 246 945)A04
- EERC 75-21 "State-of-the-Art in Seismic Strength of Masonry - An Evaluation and Review," by R.L. Mayes and R.W. Clough - 1975 (PB 249 040)A07
- EERC 75-22 "Frequency Dependent Stiffness Matrices for Viscoelastic Half-Plane Foundations," by A.K. Chopra, P. Chakrabarti and G. Dasgupta - 1975 (PB 248 121)A07
- EERC 75-23 "Hysteretic Behavior of Reinforced Concrete Framed Walls," by T.Y. Wong, V.V. Bertero and E.P. Popov - 1975
- EERC 75-24 "Testing Facility for Subassemblages of Frame-Wall Structural Systems," by V.V. Bertero, E.P. Popov and T. Endo - 1975
- EERC 75-25 "Influence of Seismic History on the Liquefaction Characteristics of Sands," by H.B. Seed, K. Mori and C.K. Chan - 1975 (Summarized in EERC 75-28)
- EERC 75-26 "The Generation and Dissipation of Pore Water Pressures during Soil Liquefaction," by H.B. Seed, P.P. Martin and J. Lysmer - 1975 (PB 252 648)A03
- EERC 75-27 "Identification of Research Needs for Improving Aseismic Design of Building Structures," by V.V. Bertero - 1975 (PB 248 136)A05
- EERC 75-28 "Evaluation of Soil Liquefaction Potential during Earthquakes," by H.B. Seed, I. Arango and C.K. Chan - 1975 (NUREG 0026)A13
- EERC 75-29 "Representation of Irregular Stress Time Histories by Equivalent Uniform Stress Series in Liquefaction Analyses," by H.B. Seed, I.M. Idriss, F. Makdisi and N. Banerjee - 1975 (PB 252 635)A03
- EERC 75-30 "FLUSH - A Computer Program for Approximate 3-D Analysis of Soil-Structure Interaction Problems," by J. Lysmer, T. Udaka, C.-F. Tsai and H.B. Seed - 1975 (PB 259 332)A07
- EERC 75-31 "ALUSH - A Computer Program for Seismic Response Analysis of Axisymmetric Soil-Structure Systems," by E. Berger, J. Lysmer and H.B. Seed - 1975
- EERC 75-32 "TRIP and TRAVEL - Computer Programs for Soil-Structure Interaction Analysis with Horizontally Travelling Waves," by T. Udaka, J. Lysmer and H.B. Seed - 1975
- EERC 75-33 "Predicting the Performance of Structures in Regions of High Seismicity," by J. Penzien - 1975 (PB 248 130)A03
- EERC 75-34 "Efficient Finite Element Analysis of Seismic Structure - Soil - Direction," by J. Lysmer, H.B. Seed, T. Udaka, R.N. Hwang and C.-F. Tsai - 1975 (PB 253 570)A03
- EERC 75-35 "The Dynamic Behavior of a First Story Girder of a Three-Story Steel Frame Subjected to Earthquake Loading," by R.W. Clough and L.-Y. Li - 1975 (PB 248 841)A05
- EERC 75-36 "Earthquake Simulator Study of a Steel Frame Structure, Volume II - Analytical Results," by D.T. Tang - 1975 (PB 252 926)A10
- EERC 75-37 "ANSR-I General Purpose Computer Program for Analysis of Non-Linear Structural Response," by D.P. Mondkar and G.H. Powell - 1975 (PB 252 386)A08
- EERC 75-38 "Nonlinear Response Spectra for Probabilistic Seismic Design and Damage Assessment of Reinforced Concrete Structures," by M. Murakami and J. Penzien - 1975 (PB 259 530)A05
- EERC 75-39 "Study of a Method of Feasible Directions for Optimal Elastic Design of Frame Structures Subjected to Earthquake Loading," by N.D. Walker and K.S. Pister - 1975 (PB 257 781)A06
- EERC 75-40 "An Alternative Representation of the Elastic-Viscoelastic Analogy," by G. Dasgupta and J.L. Sackman - 1975 (PB 252 173)A03
- EERC 75-41 "Effect of Multi-Directional Shaking on Liquefaction of Sands," by H.B. Seed, R. Pyke and G.R. Martin - 1975 (PB 258 781)A03
- EERC 76-1 "Strength and Ductility Evaluation of Existing Low-Rise Reinforced Concrete Buildings - Screening Method," by T. Okada and B. Bresler - 1976 (PB 257 906)A11
- EERC 76-2 "Experimental and Analytical Studies on the Hysteretic Behavior of Reinforced Concrete Rectangular and T-Beams," by S.-Y.M. Ma, E.P. Popov and V.V. Bertero - 1976 (PB 260 843)A12
- EERC 76-3 "Dynamic Behavior of a Multistory Triangular-Shaped Building," by J. Petrovski, R.M. Stephen, E. Gartenbaum and J.G. Bouwkamp - 1976
- EERC 76-4 "Earthquake Induced Deformations of Earth Dams," by N. Serff and H.B. Seed - 1976

- EERC 76-5 "Analysis and Design of Tube-Type Tall Building Structures," by H. de Clercq and G.H. Powell - 1976 (PB 252 220) A10
- EERC 76-6 "Time and Frequency Domain Analysis of Three-Dimensional Ground Motions, San Fernando Earthquake," by T. Kubo and J. Penzien (PB 260 556)A11
- EERC 76-7 "Expected Performance of Uniform Building Code Design Masonry Structures," by R.L. Mayes, Y. Omote, S.W. Chen and R.W. Clough - 1976
- EERC 76-8 "Cyclic Shear Tests on Concrete Masonry Piers," Part I - Test Results," by R.L. Mayes, Y. Omote and R.W. Clough - 1976 (PB 264 424)A06
- EERC 76-9 "A Substructure Method for Earthquake Analysis of Structure - Soil Interaction," by J.A. Gutierrez and A.K. Chopra - 1976 (PB 257 783)A08
- EERC 76-10 "Stabilization of Potentially Liquefiable Sand Deposits using Gravel Drain Systems," by H.B. Seed and J.R. Booker - 1976 (PB 258 820)A04
- EERC 76-11 "Influence of Design and Analysis Assumptions on Computed Inelastic Response of Moderately Tall Frames," by G.H. Powell and D.G. Row - 1976
- EERC 76-12 "Sensitivity Analysis for Hysteretic Dynamic Systems: Theory and Applications," by D. Ray, K.S. Pister and E. Polak - 1976 (PB 262 859)A04
- EERC 76-13 "Coupled Lateral Torsional Response of Buildings to Ground Shaking," by C.L. Kan and A.K. Chopra - 1976 (PB 257 907)A09
- EERC 76-14 "Seismic Analyses of the Banco de America," by V.V. Bertero, S.A. Mahin and J.A. Hollings - 1976
- EERC 76-15 "Reinforced Concrete Frame 2: Seismic Testing and Analytical Correlation," by R.W. Clough and J. Gidwani - 1976 (PB 261 323)A08
- EERC 76-16 "Cyclic Shear Tests on Masonry Piers, Part II - Analysis of Test Results," by R.L. Mayes, Y. Omote and R.W. Clough - 1976
- EERC 76-17 "Structural Steel Bracing Systems: Behavior Under Cyclic Loading," by E.P. Popov, K. Takanashi and C.W. Roeder - 1976 (PB 260 715)A05
- EERC 76-18 "Experimental Model Studies on Seismic Response of High Curved Overcrossings," by D. Williams and W.G. Godden - 1976
- EERC 76-19 "Effects of Non-Uniform Seismic Disturbances on the Dumbarton Bridge Replacement Structure," by F. Baron and R.E. Hamati - 1976
- EERC 76-20 "Investigation of the Inelastic Characteristics of a Single Story Steel Structure Using System Identification and Shaking Table Experiments," by V.C. Matzen and H.D. McNiven - 1976 (PB 258 453)A07
- EERC 76-21 "Capacity of Columns with Splice Imperfections," by E.P. Popov, R.M. Stephen and R. Philbrick - 1976 (PB 260 378)A04
- EERC 76-22 "Response of the Olive View Hospital Main Building during the San Fernando Earthquake," by S. A. Mahin, R. Collins, A.K. Chopra and V.V. Bertero - 1976
- EERC 76-23 "A Study on the Major Factors Influencing the Strength of Masonry Prisms," by N.M. Mostaghel, R.L. Mayes, R. W. Clough and S.W. Chen - 1976
- EERC 76-24 "GADFLEA - A Computer Program for the Analysis of Pore Pressure Generation and Dissipation during Cyclic or Earthquake Loading," by J.R. Booker, M.S. Rahman and H.B. Seed - 1976 (PB 263 947)A04
- EERC 76-25 "Rehabilitation of an Existing Building: A Case Study," by B. Bresler and J. Axley - 1976
- EERC 76-26 "Correlative Investigations on Theoretical and Experimental dynamic Behavior of a Model Bridge Structure," by K. Kawashima and J. Penzien - 1976 (PB 263 388)A11
- EERC 76-27 "Earthquake Response of Coupled Shear Wall Buildings," by T. Srichatrapimuk - 1976 (PB 265 157)A07
- EERC 76-28 "Tensile Capacity of Partial Penetration Welds," by E.P. Popov and R.M. Stephen - 1976 (PB 262 899)A03
- EERC 76-29 "Analysis and Design of Numerical Integration Methods in Structural Dynamics," by H.M. Hilber - 1976 (PB 264 410)A06
- EERC 76-30 "Contribution of a Floor System to the Dynamic Characteristics of Reinforced Concrete Buildings," by L.J. Edgar and V.V. Bertero - 1976
- EERC 76-31 "The Effects of Seismic Disturbances on the Golden Gate Bridge," by F. Baron, M. Arikan and R.E. Hamati - 1976
- EERC 76-32 "Infilled Frames in Earthquake Resistant Construction," by R.E. Klingner and V.V. Bertero - 1976 (PB 265 892)A13



- UCB/EERC-77/01 "PLUS - A Computer Program for Probabilistic Finite Element Analysis of Seismic Soil-Structure Interaction," by M.P. Romo Organista, J. Lysmer and H.B. Seed - 1977
- UCB/EERC-77/02 "Soil-Structure Interaction Effects at the Humboldt Bay Power Plant in the Ferndale Earthquake of June 7, 1975," by J.E. Valera, H.B. Seed, C.F. Tsai and J. Lysmer - 1977 (PB 265 795)A04
- UCB/EERC-77/03 "Influence of Sample Disturbance on Sand Response to Cyclic Loading," by K. Mori, H.B. Seed and C.K. Chan - 1977 (PB 267 352)A04
- UCB/EERC-77/04 "Seismological Studies of Strong Motion Records," by J. Shoja-Taheri - 1977 (PB 269 655)A10
- UCB/EERC-77/05 "Testing Facility for Coupled-Shear Walls," by L. Li-Hyung, V.V. Bertero and E.P. Popov - 1977
- UCB/EERC-77/06 "Developing Methodologies for Evaluating the Earthquake Safety of Existing Buildings," by No. 1 - B. Bresler; No. 2 - B. Bresler, T. Okada and D. Zisling; No. 3 - T. Okada and B. Bresler; No. 4 - V.V. Bertero and B. Bresler - 1977 (PB 267 354)A08
- UCB/EERC-77/07 "A Literature Survey - Transverse Strength of Masonry Walls," by Y. Omote, R.L. Mayes, S.W. Chen and R.W. Clough - 1977 (PB 277 933)A07
- UCB/EERC-77/08 "DRAIN-TABS: A Computer Program for Inelastic Earthquake Response of Three Dimensional Buildings," by R. Guendelman-Israel and G.H. Powell - 1977 (PB 270 693)A07
- UCB/EERC-77/09 "SUBWALL: A Special Purpose Finite Element Computer Program for Practical Elastic Analysis and Design of Structural Walls with Substructure Option," by D.Q. Le, H. Peterson and E.P. Popov - 1977 (PB 270 567)A05
- UCB/EERC-77/10 "Experimental Evaluation of Seismic Design Methods for Broad Cylindrical Tanks," by D.P. Clough (PB 272 280)A13
- UCB/EERC-77/11 "Earthquake Engineering Research at Berkeley - 1976," - 1977 (PB 273 507)A09
- UCB/EERC-77/12 "Automated Design of Earthquake Resistant Multistory Steel Building Frames," by N.D. Walker, Jr. - 1977 (PB 276 526)A09
- UCB/EERC-77/13 "Concrete Confined by Rectangular Hoops Subjected to Axial Loads," by J. Vallenias, V.V. Bertero and E.P. Popov - 1977 (PB 275 165)A06
- UCB/EERC-77/14 "Seismic Strain Induced in the Ground During Earthquakes," by Y. Sugimura - 1977 (PB 284 201)A04
- UCB/EERC-77/15 "Bond Deterioration under Generalized Loading," by V.V. Bertero, E.P. Popov and S. Viathanatepa - 1977
- UCB/EERC-77/16 "Computer Aided Optimum Design of Ductile Reinforced Concrete Moment Resisting Frames," by S.W. Zagajeski and V.V. Bertero - 1977 (PB 280 137)A07
- UCB/EERC-77/17 "Earthquake Simulation Testing of a Stepping Frame with Energy-Absorbing Devices," by J.M. Kelly and D.F. Tsztoo - 1977 (PB 273 506)A04
- UCB/EERC-77/18 "Inelastic Behavior of Eccentrically Braced Steel Frames under Cyclic Loadings," by C.W. Roeder and E.P. Popov - 1977 (PB 275 526)A15
- UCB/EERC-77/19 "A Symplified Procedure for Estimating Earthquake-Induced Deformations in Dams and Embankments," by F.I. Makdisi and H.B. Seed - 1977 (PB 276 820) A04
- UCB/EERC-77/20 "The Performance of Earth Dams during Earthquakes," by H.B. Seed, F.I. Makdisi and P. de Alba - 1977 (PB 276 821)A04
- UCB/EERC-77/21 "Dynamic Plastic Analysis Using Stress Resultant Finite Element Formulation," by P. Lukkunapvasit and J.M. Kelly - 1977 (PB 275 453)A04
- UCB/EERC-77/22 "Preliminary Experimental Study of Seismic Uplift of a Steel Frame," by R.W. Clough and A.A. Huckelbridge 1977 (PB 278 769)A08
- UCB/EERC-77/23 "Earthquake Simulator Tests of a Nine-Story Steel Frame with Columns Allowed to Uplift," by A.A. Huckelbridge - 1977 (PB 277 944)A09
- UCB/EERC-77/24 "Nonlinear Soil-Structure Interaction of Skew Highway Bridges," by M.-C. Chen and J. Penzien - 1977 (PB 276 176)A07
- UCB/EERC-77/25 "Seismic Analysis of an Offshore Structure Supported on Pile Foundations," by D.D.-N. Liou and J. Penzien 1977 (PB 283 180)A06
- UCB/EERC-77/26 "Dynamic Stiffness Matrices for Homogeneous Viscoelastic Half-Planes," by G. Dasgupta and A.K. Chopra - 1977 (PB 279 654)A06
- UCB/EERC-77/27 "A Practical Soft Story Earthquake Isolation System," by J.M. Kelly and J.M. Eidingner - 1977 (PB 276 814)A07
- UCB/EERC-77/28 "Seismic Safety of Existing Buildings and Incentives for Hazard Mitigation in San Francisco: An Exploratory Study," by A.J. Meltsner - 1977 (PB 281 970)A05
- UCB/EERC-77/29 "Dynamic Analysis of Electrohydraulic Shaking Tables," by D. Rea, S. Abedi-Hayati and Y. Takahashi 1977 (PB 282 569)A04
- UCB/EERC-77/30 "An Approach for Improving Seismic - Resistant Behavior of Reinforced Concrete Interior Joints," by

- UCB/EERC-78/01 "The Development of Energy-Absorbing Devices for Aseismic Base Isolation Systems," by J.M. Kelly and D.F. Tsztoo 1978 (PB 284 978)A04
- UCB/EERC-78/02 "Effect of Tensile Prestrain on the Cyclic Response of Structural Steel Connections," by J.G. Bouwkamp and A. Mukhopadhyay - 1978
- UCB/EERC-78/03 "Experimental Results of an Earthquake Isolation System using Natural Rubber Bearings," by J.M. Eidingler and J.M. Kelly - 1978
- UCB/EERC-78/04 "Seismic Behavior of Tall Liquid Storage Tanks," by A. Niwa 1978
- UCB/EERC-78/05 "Hysteretic Behavior of Reinforced Concrete Columns Subjected to High Axial and Cyclic Shear Forces," by S.W. Zagajeski, V.V. Bertero and J.G. Bouwkamp - 1978
- UCB/EERC-78/06 "Inelastic Beam-Column Elements for the ANSR-I Program," by A. Riahi, D.G. Row and G.H. Powell - 1978
- UCB/EERC-78/07 "Studies of Structural Response to Earthquake Ground Motion," by O.A. Lopez and A.K. Chopra - 1978
- UCB/EERC-78/08 "A Laboratory Study of the Fluid-Structure Interaction of Submerged Tanks and Caissons in Earthquakes," by R.C. Byrd - 1978 (PB 284 957)A08
- UCB/EERC-78/09 "Models for Evaluating Damageability of Structures," by I. Sakamoto and B. Bresler - 1978
- UCB/EERC-78/10 "Seismic Performance of Secondary Structural Elements," by I. Sakamoto - 1978
- UCB/EERC-78/11 Case Study--Seismic Safety Evaluation of a Reinforced Concrete School Building," by J. Axley and B. Bresler 1978
- UCB/EERC-78/12 "Potential Damageability in Existing Buildings," by T. Blejwas and B. Bresler - 1978
- UCB/EERC-78/13 "Dynamic Behavior of a Pedestal Base Multistory Building," by R. M. Stephen, E. L. Wilson, J. G. Bouwkamp and M. Button - 1978
- UCB/EERC-78/14 "Seismic Response of Bridges - Case Studies," by R.A. Imbsen, V. Nutt and J. Penzien - 1978
- UCB/EERC-78/15 "A Substructure Technique for Nonlinear Static and Dynamic Analysis," by D.G. Row and G.H. Powell - 1978
- UCB/EERC-78/16 "Seismic Performance of Nonstructural and Secondary Structural Elements," by Isao Sakamoto - 1978

BIBLIOGRAPHIC DATA SHEET		1. Report No. NSF/RA-780544	2.	3. Key Reports Accession No. PB294735
4. Title and Subtitle Optimal Design of an Earthquake Isolation System			5. Report Date October 1978	
7. Author(s) M.A. Bhatti, K.S. Pister and E. Polak			8. Performing Organization Rept. No. UCB/EERC-78/22	
9. Performing Organization Name and Address Earthquake Engineering Research Center University of California, Richmond Field Station 47th and Hoffman Blvd Richmond, California 94804			10. Project/Task/Work Unit No.	
12. Sponsoring Organization Name and Address National Science Foundation 1800 G. Street, N.W. Washington, D.C. 20550			11. Contract/Grant No. ENV76-04264	
			13. Type of Report & Period Covered	
15. Supplementary Notes			14.	
16. Abstracts Optimal design of an earthquake isolation system, consisting of natural rubber bearings and special nonlinear energy absorbing devices, is presented. An algorithm for efficient analysis of structural response, based upon the Newmark and Runge-Kutta methods with optional Newton-Raphson iteration, is given. The optimal design problem, incorporating this simulation algorithm, is formulated as a mathematical programming problem with time-dependent constraints and is solved using a feasible directions algorithm. Several numerical examples are presented, in which it is demonstrated that a properly designed isolation system can substantially reduce structural damage for a class of potential earthquakes.				
17b. Identifiers/Open-Ended Terms				
17c. COSATI Field/Group				
18. Availability Statement Release Unlimited			19. Security Class (This Report) UNCLASSIFIED	21. No. of Pages 120
			20. Security Class (This Page) UNCLASSIFIED	22. Price A06-A01

